A MASS SPECTROMETRIC EXAMINATION OF SOME CARBOHYDRATES

BY

JOHN M. PELTIER, B.Sc.

A Thesis

Submitted to the School of Graduate Studies

in Partial Fulfilment of the Requirements

for the Degree

Doctor of Philosophy

McMaster University

1992

A MASS SPECTROMETRIC EXAMINATION

OF SOME CARBOHYDRATES

DOCTOR OF PHILOSOPHY (1992) McMaster Univerity

(Chemistry) Hamilton, Ontario

TITLE: A Mass Spectrometric Examination of Some Carbohydrates.

AUTHOR: John Marcel Peltier, B.Sc. (McMaster University)

SUPERVISOR: Professor D.B. MacLean

NUMBER OF PAGES: xiv, 193

Abstract

Many carbohydrates have useful biological properties, which has generated interest in the structural elucidation of this class of compounds. One technique that has been applied successfully to the structural elucidation of carbohydrates and carbohydrate derivatives is mass spectrometry (MS). In this research a number of peracetylated and pertrideuteroacetylated mono- and disaccharides were examined by ammonia desorption chemical ionization (NH_3-DCI) in order to gain insight into the fragmentation processes and to assess the structural information available in the NH_3-DCI mass spectra. As a result of these studies a new method has been developed to determine the position of linkage in peracetylated disaccharides comprised of hexopyranose (glucose or mannose) units by use of mass-analyzed ion kinetic energy (MIKE) scans.

The second part of this thesis deals with the structural elucidation of the core portion (core) of the lipopolysaccharides (LPS) derived from two mutants (AK1012 and AK1401) of the bacterium Pseudomonas aeruginosa, a ubiquitous opportunistic pathogen, which is resistant to antibiotic therapy. Since LPS are the principal antigenic determinants of this bacterium a knowledge of the structure of the LPS is important in the development of synthetic vaccines. In this work mass spectrometry, in conjunction with a number of chemical and chromatographic techniques, was applied to the structural elucidation of the AK1012 core and AK1401 core. The combination of methods applied to this problem resulted in the

elucidation of many of the structural features of these carbohydrates; however, some aspects of the structure remain unknown.

Acknowledgements

I would like to express my gratitude and appreciation to Professor D.B. MacLean for his patience, guidance and support during the course of this project. I would like to thank Professors W.A. Szarek and A.M. Kropinski for the samples they contributed for this study.

Special thanks are due Dr. Richard Smith for his assistance and advice regarding many of the mass spectrometric experiments that were conducted during this investigation and Mr. F. Ramelan for the technical assistance that he provided. Todd Arsenault is gratefully acknowledged for all those occasions when we could test ideas on each other before wasting time trying them in the lab. Dr. Henrianna Pang is greatfully acknowledged for her assistance in obtaining the FAB spectra of the core oligosaccharides.

I would like to express my gratitude to my parents for the many years of support that they have given me. Lastly, but most of all, I would like to thank my wife, Susan, who assisted me as my gopher, typist, proofreader and too many other things to list here. Without her support and assistance this thesis might never have been completed.

TABLE OF CONTENTS

LIST OF TABLES

LIST OF FIGURES

CHAPTER 1

INTRODUCTION

1.1 General Introduction

Carbohydrates are widely distributed in nature and exhibit an enormous structural diversity. New compounds are constantly being isolated and many are found to have useful biological properties. The growing pool of biologically active carbohydrates provides a continuing challenge for those researchers interested in their structural elucidation.

Many groups have examined carbohydrates and carbohydrate derivatives by mass spectrometry and research in this area has been reviewed a number of times.[1-7] One area that has received relatively little attention, is the study of peracetylated carbohydrates by ammonia chemical ionization mass spectrometry (CI-MS). In this thesis a number of peracetylated carbohydrates have been examined by ammonia CI-MS in order to gain insight into the fragmentation processes and to assess the structural information available in the NH_3-CI mass spectra.

The second part of the thesis is concerned with an investigation of the structure of the core portion (core oligosaccharides) of the cell surface lipopolysaccharides (LPS) derived from two mutants (AK1401 and AK1012) of the bacterium, Pseudomonas aeruginosa strain PAO1. LPS are the principal antigenic determinants of bacteria.[8] Therefore, the determination of the structure of these

molecules is a vital step in the process of developing synthetic vaccines. This phase of the work involved the application of CI-MS, fast atom bombardment MS, and a number of other mass spectrometric techniques in conjunction with classical chemical methods, to the structure elucidation of the core oligosaccharides.

The thesis has been organized as follows. Chapter 1 discusses carbohydrate structure, the general principles of mass spectrometry and the mass spectrometric techniques used in this study, as well as the application of these techniques to the analysis of peracetylated carbohydrates. The second part of Chapter 1 discusses the occurrence and structure of LPS and the techniques which are used to determine the structure of carbohydrates. A description of the source of materials, and the techniques and procedures used in this study is found in Chapter 2. Chapters 3 and 4 discuss the results obtained from the mass spectrometric study of the peracetylated carbohydrates and the core oligosaccharides, respectively. Finally, Chapter 5 summarizes the results obtained in this study.

1.2 Carbohydrate Structure

Monosaccharides, the simplest carbohydrates, consist of a group of substances which are polyhydroxyaldehydes, the aldoses, or polyhydroxyketones, the ketoses (see Fig. 1). In nature the most common monosaccharides are those which have 5 or 6 carbon atoms. They are referred to as pentoses or hexoses, respectively. Thus, in the case of the aldoses in Figure 1, if n=3 then the

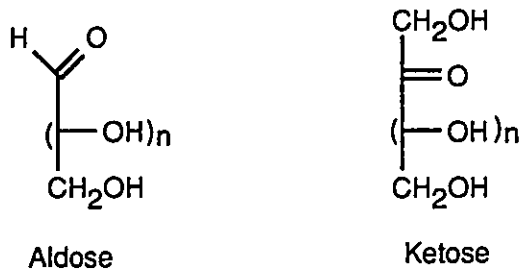

Figure 1. General monosaccharide structures.

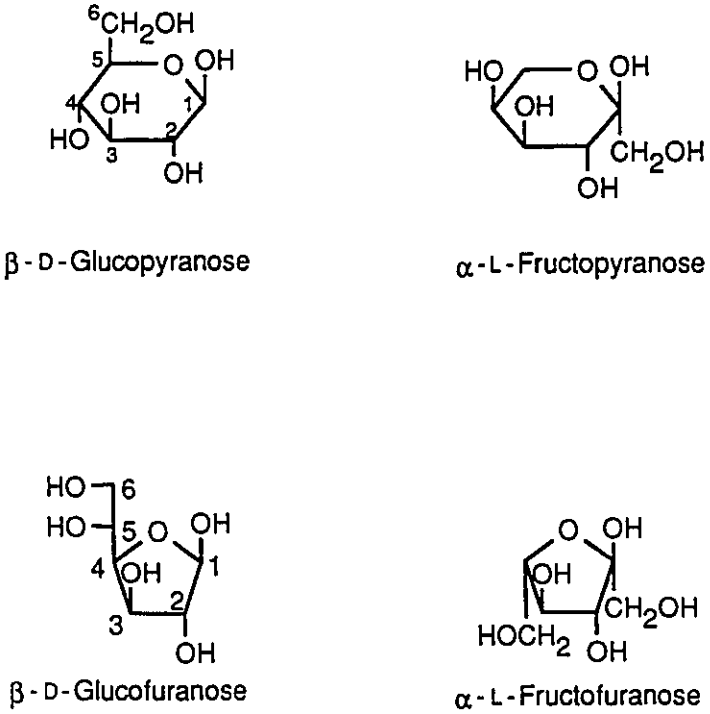

Figure 2. Some cyclic aldoses and ketoses.

monosaccharide is an aldopentose and if n=4 then it is an aldohexose. Similarly, the ketose in Figure 1 is a ketopentose if n=2 and a ketohexose if n=3.

Aldohexoses (in the linear form, as in Fig. 1) have four chiral centres resulting in 16 aldohexose isomers. These 16 isomers exist as 8 pairs of enantiomers, with each pair of enantiomers sharing a common name. Each enantiomer in a pair is assigned to a D-series or an L-series based on the configuration of the penultimate carbon in the chain.

The monosaccharides with 5 or more carbon atoms exist almost exclusively in a cyclic form in which the ring may be five-membered (the less common furanose form) or six-membered (the more common pyranose form), as shown in Figure 2. The formation of a ring creates a new chiral centre (the anomeric centre) at C-1 of an aldose or at C-2 of a ketose. The relative configuration of the anomeric centre is designated as either α or β. When a D-series sugar is oriented as shown in Figure 2 (carbon atom numbers increasing in the clockwise direction) and the anomeric hydroxyl is oriented above the plane of the sugar ring then the anomeric centre has the β-configuration. If the anomeric hydroxyl is below the plane of the sugar ring in a D-series sugar then the anomeric centre has the α-configuration. This definition is reversed for the L-series sugars, so for example, both fructoses in Figure 2 have the anomeric hydroxyl above the plane of the ring and therefore have the α-configuration.[9]

Monosaccharides may join together to form oligosaccharides. The monosaccharides units in an oligosaccharide are joined by bonds from the

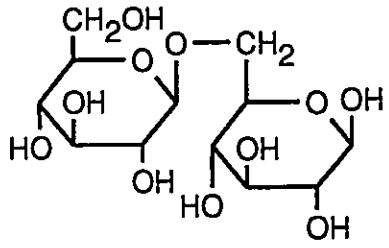

β - D -Glucopyranosyl-(1 → 6)-β - D -glucopyranose

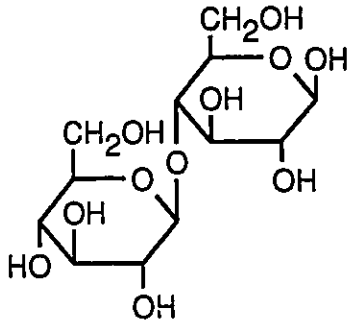

β - D -Glucopyranosyl-(1 → 4)-β - D -glucopyranose

Figure 3. (1→6)- and (1→4)-linkage isomers of glucose disaccharides.

anomeric centre of one molecule through an acetal linkage to a second molecule. The end of the oligosaccharide which contains an anomeric centre not linked to another monosaccharides is referred to as the reducing end of the oligomer. When an oligosaccharide becomes large it is referred to as a polysaccharide. Two examples of disaccharides are shown in Figure 3.

1.3 Mass Spectrometry

Mass spectrometry has proven to be valuable in the structure elucidation of organic compounds. This technique is based upon the generation of ions from neutral molecules in the gas phase. The ions may be fragment ions, molecular ions or molecular ion adducts (*e.g.* $[M+H]^+$). Mass spectrometry is used to determine the mass of these ions, thereby providing information which in turn may allow one to ascertain their structures and ultimately deduce the structure of the analyte.

The ions, produced in the source of a single focussing mass spectrometer, are accelerated through a potential difference and then are passed through a magnetic field which causes a deflection in their flight path. The magnitude of the deflection is a function of the mass and the charge (usually +1) of the ions traversing the magnetic field. The ions follow an arc of a given radius, such that:[10]

$$m/z = \frac{B^2 r^2 e}{2V} \qquad \text{eqn 1}$$

where: m is the mass of the ion
e is the charge on an electron
z is the number of electronic charges on the ion
B is the magnetic field strength
r is the radius of the ion path
V is the accelerating voltage

By placing a detector at an appropriate position and scanning either the accelerating voltage or the magnetic field, ions of different masses can be transmitted to the detector. A mass spectrum is then obtained by plotting *m/z* versus the relative abundance of the ions.

When generated in an ion source, ions have a range of kinetic energies and this range is not diminished when the ions are accelerated out of the source or deflected by the magnet. This property is reflected in the width of the ion beam and ultimately the mass resolution of a single focussing mass spectrometer. In order to improve the resolution of a mass spectrometer a kinetic energy "filter" is required; consequently, mass spectrometers were equipped with an electric sector. The electric sector, placed between the source and the magnet, transmits ions that follow a path such that:[10]

$$mv^2 = reE \qquad \text{eqn. 2}$$

where: m is the mass of the ion
v is the velocity of the ion
r is the radius of the ion path
e is the charge on an electron
E is the electric field strength.

Instruments equipped with an electric sector are referred to as double-focusing instruments and have markedly better resolution than the single-focusing instruments. Later variants of double-focusing mass spectrometers placed the electric sector after the magnetic sector and are referred to as reversed-geometry instruments.[10] The magnetic sector instruments used in this research are reversed-geometry double-focusing instruments and are schematically diagrammed in Figure 4.

1.3.1 Electron Ionization Mass Spectrometry

The first and still most commonly used mode of ionization is electron ionization (EI).[10] In EI-MS, vaporized sample molecules are ionized by a beam of electrons as described by equations 3a to 3d. Loss of an electron from the analyte results in the formation of a molecular ion $[ABCD]^{+\cdot}$ (eqn. 3a) which has an odd number of electrons. The molecular ion may then fragment to produce an even electron ion and a radical, species AB^+ and $CD^{\cdot}$, respectively, in equation 3b. Alternatively, the molecular ion may eliminate a neutral molecule to generate an odd electron fragment ion as in equation 3c. Finally, the molecular ion might undergo a re-arrangement during fragmentation as illustrated by equation 3d.

$$[ABCD] + e^- \rightarrow [ABCD]^{+\cdot} + 2e^- \qquad \text{eqn. 3a}$$

$$[ABCD]^{+\cdot} \rightarrow [AB]^+ + [CD]^{\cdot} \qquad \text{eqn. 3b}$$

$$[ABCD]^{+\cdot} \rightarrow [AB]^{+\cdot} + CD \qquad \text{eqn. 3c}$$

$$[ABCD]^{+\cdot} \rightarrow [AD]^{+\cdot} + BC \qquad \text{eqn. 3d}$$

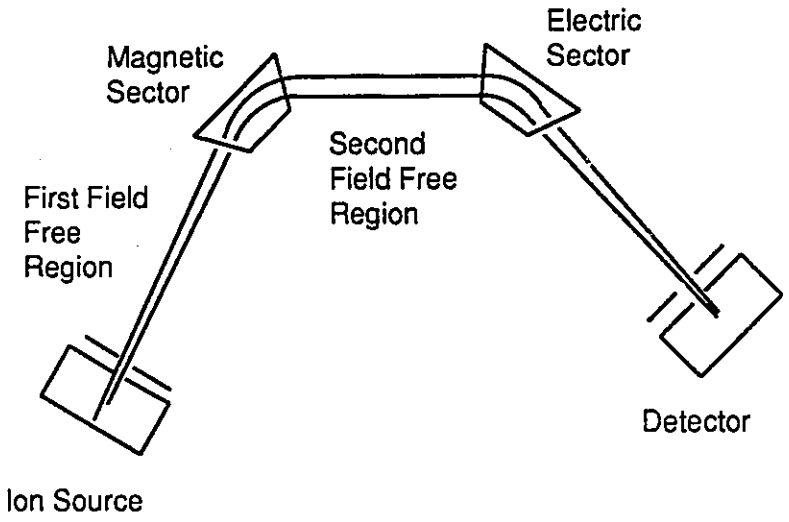

Figure 4. A schematic diagram of a double-focussing reversed-geometry mass spectrometer.

The ions are then accelerated from the source and mass analyzed. The electrons, used to generate the sample ions, typically have energies in the order of 70 eV. Such energies ensure that there is significant ionization and fragmentation of the analyte.

Unfortunately, EI-MS often fails to provide molecular weight information. Consequently, other ionization methods were developed which result in much less fragmentation of the organic molecules being studied. These other ionization modes are referred to as "soft" ionization techniques.[10,11]

1.3.2 Chemical Ionization Mass Spectrometry

Chemical ionization (CI) mass spectrometry (developed by Munson and Field[12]) is a commonly used "soft" ionization technique. This mode of ionization relies on the interaction of the analyte with a reagent plasma inside the ion source. The reagent plasma is generated by the interaction of a reagent gas with an electron beam. Subsequent ion-molecule reactions between the reagent ions and neutral reagent gas generate an equilibrium mixture of ions which interact with the analyte. The series of reactions which produces the reagent plasma is illustrated below for the case where ammonia is used as the reagent gas.[13] The relative abundance of the species present in the reagent plasma is dependent on both the source temperature and the reagent gas pressure.

$$NH_3 + e^- \rightarrow NH_3^{+\cdot} + 2e^- \qquad \text{eqn. 4}$$

$$NH_3 + e^- \rightarrow NH_2^+ + H^\cdot + 2e^- \qquad \text{eqn. 5}$$

$$NH_3^{+\cdot} + NH_3 \rightarrow NH_4^+ + NH_2^\cdot \qquad \text{eqn. 6}$$

$$NH_2^+ + NH_3 \rightarrow NH_3^{+\cdot} + NH_2^\cdot \qquad \text{eqn. 7}$$

$$NH_2^+ + NH_3 \rightarrow NH_4^+ + NH \qquad \text{eqn. 8}$$

$$NH_4^+ + NH_3 \rightarrow NH_4^+ \cdot NH_3 \qquad \text{eqn. 9}$$

$$NH_4^+ \cdot NH_3 + NH_3 \rightarrow NH_4^+ \cdot 2NH_3 \qquad \text{eqn. 10}$$

A wide variety of materials may be used to generate reagent plasmas, making CI-MS a very versatile technique. However, the focus of this thesis is on the use of ammonia as a reagent gas (See ref. 14 for a review of other reagent gas systems).

The analyte may react with the ammonia reagent plasma to generate adduct ions, $[M+H]^+$ or $[M+NH_4]^+$.[13] The formation of a protonated molecular adduct occurs when the proton affinity (PA) of the analyte is greater than that of ammonia, although both processes may occur. However, as the PA difference increases the ratio $[M+H]^+/[M+NH_4]^+$ will also increase and eventually only the $[M+H]^+$ ion will be formed in detectable amounts.[13] When the PA of the analyte molecule is the same or slightly less than that of ammonia the $[M+NH_4]^+$ ion is formed exclusively, and when the PA of the analyte is much less than that of ammonia no sample ions are observed.[13]

Unlike electron ionization, chemical ionization generally imparts little energy to the substrate. The energy transferred to the analyte during protonation

is equivalent to the difference in the proton affinity of the molecule being ionized and the ammonia reagent gas. Since ammonia has a fairly high proton affinity little energy is transferred and little fragmentation results.[10,13]

Baldwin and McLafferty[15] improved the standard CI technique by using an extended probe, which vaporizes the sample directly inside the ion source, unlike a conventional probe which vaporizes the sample outside of the source. This modification reduces pyrolysis of the sample and imparts less thermal energy to the molecule. The technique is referred to as desorption chemical ionization (DCI). It provides two major improvements over conventional chemical ionization, namely, spectra can be obtained with much less sample heating and the spectra exhibit more abundant high mass ions.

1.3.3 Fast Atom Bombardment Mass Spectrometry

The development of fast atom bombardment (FAB) mass spectrometry,[16] another soft ionization technique, greatly extended the utility of mass spectrometry in the analysis of large, labile biomolecules.[4,7] In FAB-MS the sample is first dissolved in a viscous, relatively involatile, liquid matrix such as glycerol. This mixture is then applied in a thin film to a probe that is inserted into the mass spectrometer. The sample is ionized by bombarding the film with a beam of energetic neutral atoms. A typical energy for such an atom beam is 8 keV and xenon is commonly used as the projectile atom.[10]

The dissolution of the sample in a liquid matrix has several advantages.

First, spectra can be generated from ionic species present in solution. Ionic compounds are generally too polar to be vaporized and ionized by EI or CI. Secondly, diffusion from lower layers of the film acts to replenish the sample as it is depleted from the film surface. Thus, FAB ionization enables spectra to be generated over an extended period of time.[10]

The generation of ions from neutral samples under FAB-MS conditions is not well understood.[17] The process is, at least in part, dependent on the choice of matrix. Barber *et al.*[18] have noted that FAB spectra, like CI spectra, exhibit even electron ions and Shröder *et al.*[19] have proposed that the FAB ionization process is similar to that of CI.

When glycerol, or related matrices such as 1-thioglycerol, is used analytes usually form $[M+H]^+$ ions. Other adduct ions may be observed also. For example, if the sample is contaminated with salts, adducts of the sample and a cation may be observed (*e.g.* $[M+Na]^+$). Additionally, adducts of the sample and the matrix, as well as combinations of the matrix and a cation, may be formed (*e.g.* $[M+glycerol+Na]^+$).

1.3.4 Metastable Ions

In the ionization process, ions of a given mass are formed with a wide range of internal energy.[10] When the internal energy is high the ions undergo fragmentation within the ion source. Sometimes the internal energy is insufficient to cause immediate fragmentation but fragmentation may occur while the ion is in

transit from the source to the detector. The ions which fragment outside the ion source are referred to as metastable ions.[10] If a metastable ion fragments between the source and the magnet of a single-focussing mass spectrometer, a "metastable peak" may be observed in the spectrum. Metastable peaks are easily recognized because they often appear at fractional masses and are more diffuse than regular peaks. The mass at which a metastable peak appears is governed by equation 11.

$$m^* = m_2^2/m_1 \qquad \text{eqn. 11}$$

where: m^* is the observed mass of the metastable peak
m_2 is the mass of the ion produced on decomposition of the metastable ion
m_1 is the mass of the metastable ion

The observation of metastable peaks can be very useful in sorting out fragmentation mechanisms; however, care must be taken in interpreting the origin of the peak appearing at m^*. Equation 11 has a large number of solutions so it is not always possible to attribute an observed metastable peak to a single parent ion.

1.3.5 Mass Analyzed Ion Kinetic Energy Scans

A number of techniques have been developed to probe the fate of selected ions[10] which do not suffer from the ambiguities inherent in metastable ion analysis. One such technique is known as mass analyzed ion kinetic energy scanning (MIKES).[20] The other techniques are hereafter collectively referred to as

daughter ion scans (see reference 10 and references therein).

In a MIKE scan the magnet is set to transmit a single ion, which decomposes in the second field free region between the magnet and the electric sector. The resulting ions (all derived from the single parent ion) then undergo a mass separation by scanning the electric sector to yield a spectrum with low resolution. The low resolution of MIKES spectra is a consequence of the poor mass resolution capability of the electric sector.

The analysis of MIKES spectra can be complicated by the presence of artefacts which result from decompositions in the first field free region of a double focusing mass spectrometer.[10] The products of these decompositions may possess the correct momentum and energy necessary to be transmitted to the detector. Ast and co-workers[21] have shown that artefacts of this type can dominate a MIKES spectrum. The effect is most pronounced when the relative abundance of the ion selected in the MIKES experiment is low. The relative abundance of these artefacts is very sensitive to the magnet setting in a MIKES experiment. Small changes in the magnet setting (*e.g.* a few tenths of a mass unit) can cause large changes in the abundance of the artefacts with respect to the abundance of the genuine MIKES ions, making it possible to identify the artefacts.

1.3.5.1 Collisional Activation

If the parent ion selected in a MIKES experiment lacks sufficient internal energy to undergo significant fragmentation, the abundance of the fragment ions

may be increased by collisional activation (CA).[22] In a collisional activation experiment the ion beam is passed through a collision cell placed just in front of the electric sector. The collision cell is filled with a small quantity of an inert gas with which the parent ions can collide. On collision with the gas some of the translational energy of the parent ions becomes converted to internal energy; this results in increased fragmentation.

1.4 Mass Spectrometry of Carbohydrates

Mass spectrometry has been widely applied[1-7] to the study of carbohydrates since the first demonstration of its utility in the analysis of this class of compounds. The use of volatile derivatives was found to facilitate the mass spectrometry of carbohydrates by increasing both the sensitivity and the reproducibility of the mass spectra.[2] Methyl ethers, acetate esters, and trimethylsilyl ethers have been most widely utilized in MS studies of carbohydrates.[3] However, of these three types of derivatives, carbohydrate peracetates have received the least amount of study.[3] The next few sections summarize what is known about the mass spectrometry of carbohydrate peracetates with respect to the ionization modes that have been employed in this study.

1.4.1 Electron Ionization Mass Spectrometry of Peracetylated Carbohydrates

Biemann and co-workers[23] appear to have undertaken the first

systematic investigation of peracetylated monosaccharides by EI-MS. Their work was followed by the work of Smale and Waight[24] with some tetraacetyl aryl glucosides and the work of Heyns and Müller[25] with some isotopically labelled peracetylated hexoses. The spectra exhibit no molecular ions (with the exception of some of the aryl glucosides) and are characterized by two main series of ions.

The first of these two principal series is initiated by the loss of the substituent at C-1 to afford a resonance stabilized oxonium ion (ion ***a***, Scheme 1). It was postulated that ion ***a*** fragments along several competing pathways as outlined in Scheme 1. It was proposed that the second principal ion series is initiated by the cleavage of the pyranose ring to yield an ion which immediately undergoes a rearrangement to afford the resonance stabilized ion ***b*** (Scheme 2). Ion ***b*** is considered to fragment along several competing pathways also.[25] Biemann *et al.*[23] proposed a one step route (Scheme 3) to ion ***c*** ; however, the route to ion ***c*** outlined in Scheme 2 is supported by the observation of a metastable ion resulting from the transition *m/z* 288-46 → *m/z* 242. The route to ***c***, as outlined in Scheme 2 is consistent also with the results obtained from the studies of isotopically labelled acetylated hexoses.[25] Ion ***c*** was postulated to undergo further rearrangements and fragmentations as outlined in Scheme 2.

A minor series of ions in the spectra of hexopyranoses results from the cleavage of the C-5, C-6 bond to afford the resonance stabilized ion ***d*** (Scheme

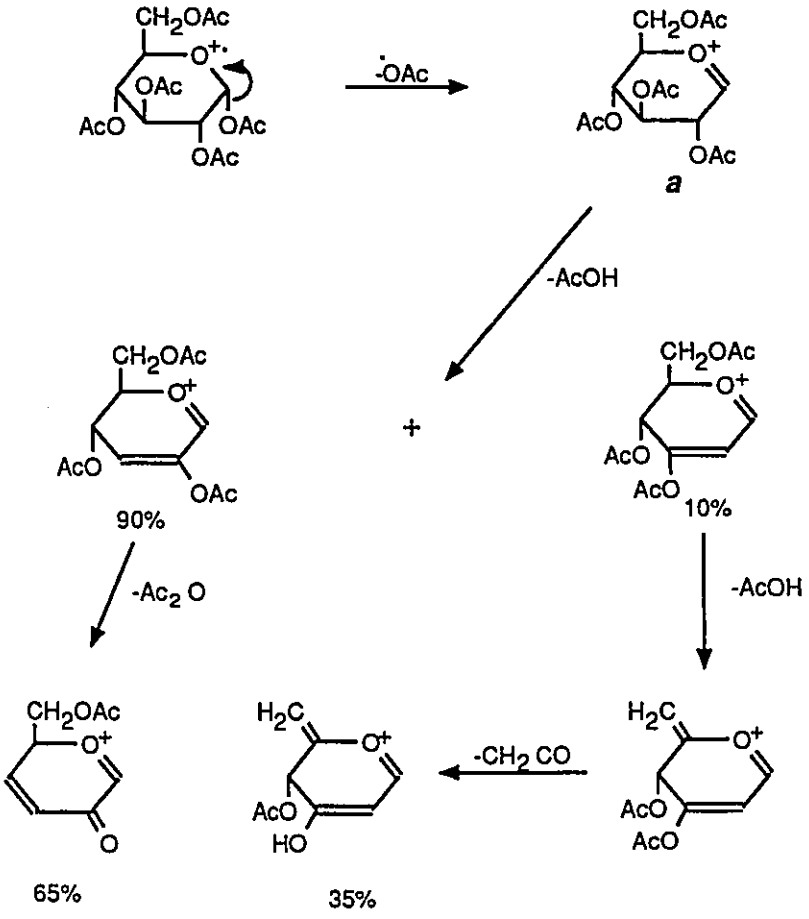
CH2OAc
O+·
OAc
AcO
OAc
OAc
-OAc
CH2OAc
O+
OAc
AcO
OAc
a
-AcOH
CH2OAc
O+
AcO
OAc
90%
+
CH2OAc
O+
AcO
AcO
10%
-Ac2 O
-AcOH
CH2OAc
O+
O
65%
H2C
O+
AcO
HO
35%
-CH2 CO
H2C
O+
AcO
AcO

Scheme 1

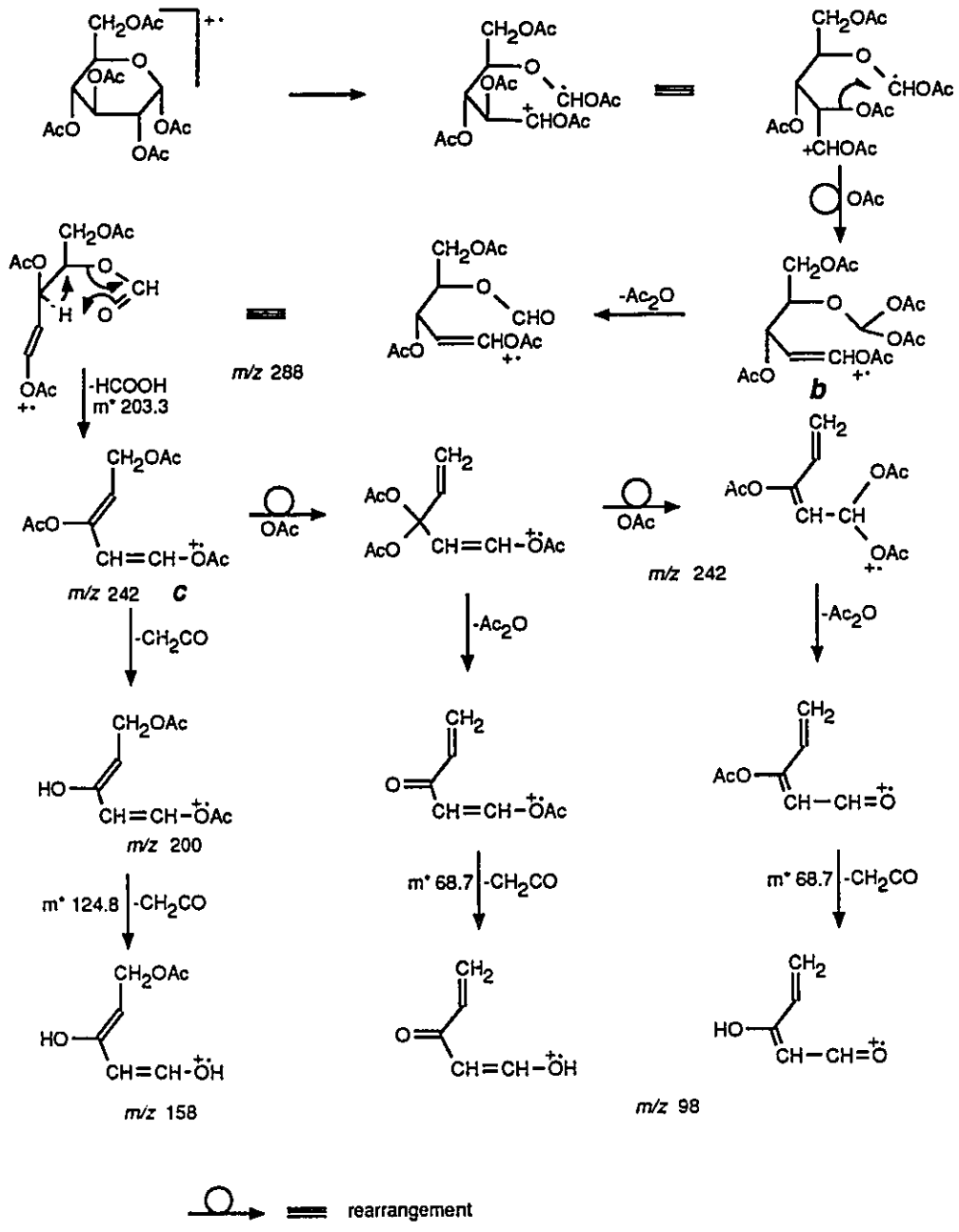
m/z 288
-HCOOH
m* 203.3
m/z 242 c
-CH2CO
m/z 200
m* 124.8
-CH2CO
m/z 158
-Ac2O
b
m/z 242
-Ac2O
m* 68.7
-CH2CO
m/z 98
m* 68.7
-CH2CO
rearrangement

Scheme 2

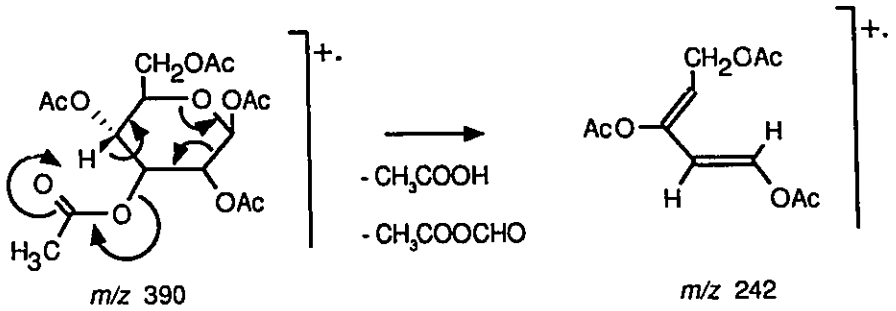

m/z 390 *m/z* 242

Scheme 3

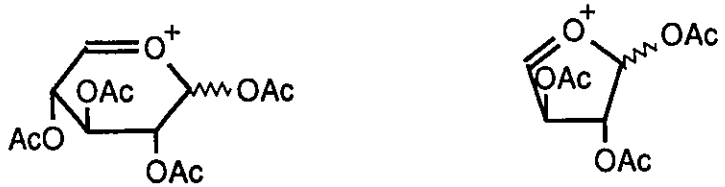

m/z 317 *m/z* 245

d ***e***

Scheme 4

4).[23] Ion ***d*** then undergoes losses of acetic acid and ketene. While this is a minor fragmentation process for hexopyranoses, the hexofuranoses exhibit a relatively intense ion at *m/z* 245 (ion ***e***, Scheme 4) corresponding to the analogous cleavage between C-4 and C-5.[23] This type of fragmentation provides a simple method for differentiating hexofuranoses from hexopyranoses.

Several groups have studied peracetylated oligosaccharides by EI-MS.[26-31] The spectra of the oligomers rarely exhibit abundant high mass ions. Those ions that are observed appear to result from the same modes of fragmentation that have been found in the monosaccharides.

Because of the high stability of the oxonium ions, or the manner in which the carbohydrate rings fragment, the majority of the ions observed in EI spectra of peracetylated oligosaccharides are derived from the non-reducing end of the sugar. A notable exception to this is an ion that appears at *m/z* 317 (see Scheme 5) in the spectra of peracetylated hexopyranose disaccharides (except for 1→1-linked disaccharides).

The ion in question has been studied by three groups.[27,28,30] Guerrera and Weill[30] determined that the *m/z* 317 ion in the spectra of peracetylated hexose disaccharides is not the same as that observed at the same mass in the spectra of peracetylated hexopyranoses (*i.e.* ion ***d***, Scheme 4). Later experiments by Das and Thayumanavan[27] showed that all the linkage isomers of peracetylated glucose disaccharides except (1→1)-linked isomers exhibited an *m/z* 317 ion. They proposed a mechanism for the formation of the *m/z* 317 ion which is similar to one

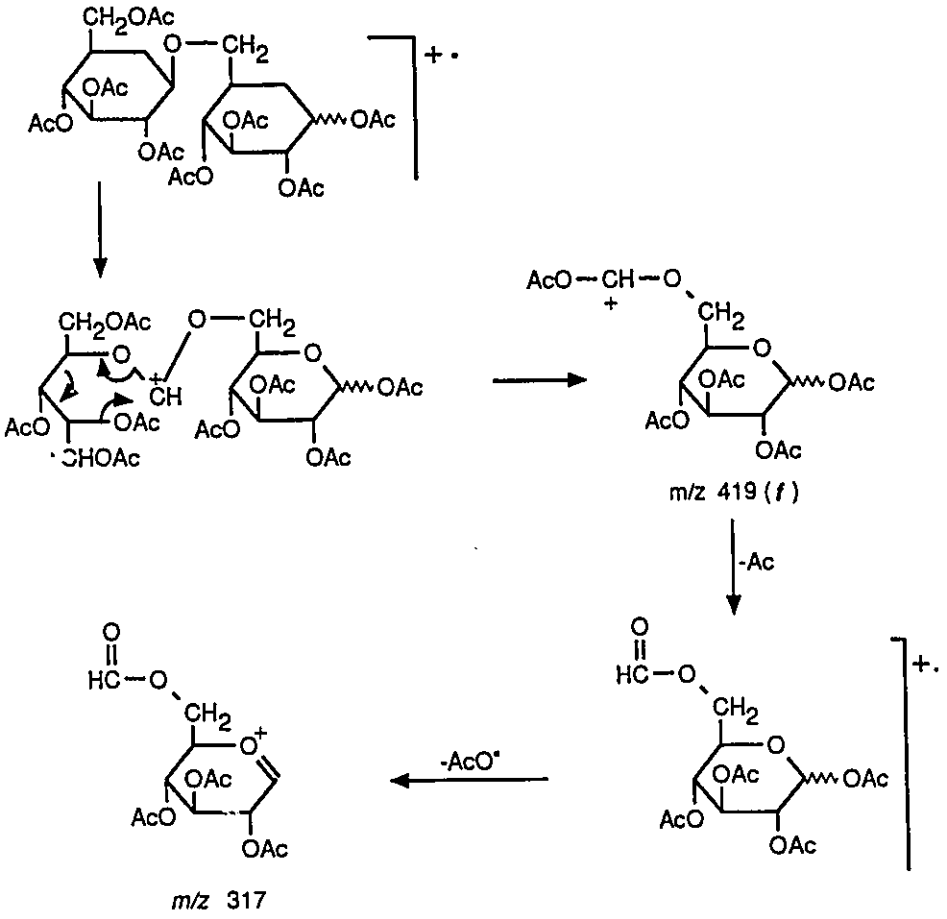

Scheme 5

proposed by Bosso *et al.* (Scheme 5) who examined a number of labelled compounds.[28] The nature of the intermediate between the ions at *m/z* 419 (*f*) and *m/z* 317 in Scheme 5 is unclear (it seems unlikely that *f* loses Ac·); however, Bosso *et al.*[28] were able to establish that the *m/z* 317 ion contains the carbon that was situated at C-1 of the non-reducing glycosyl unit. It has not been confirmed that the C-3 substituent of the non-reducing glycosyl unit undergoes the transfer (to C-1) outlined in Scheme 5. Chizhov *et al.*[31] have suggested that such a mechanism is reasonable based on the fact that studies of isotopically labelled *O*-methyl derivatives of glucose have shown that they undergo fragmentations which involve the transfer of the C-3 substituent to C-1.[1]

1.4.2 Chemical Ionization Mass Spectrometry of Peracetylated Carbohydrates

The methane and isobutane CI mass spectra of peracetylated mono- and oligosaccharides are similar to the corresponding EI mass spectra.[3] The spectra are dominated by oxonium ions and ions that result from the further fragmentation of the oxonium ions (by loss of acetic acid and ketene).[32,33]

Methane CI experiments with labelled glucopyranoses showed that there was a preferred sequence for the loss of the acetate groups around the ring.[32] The sequence is outlined in Scheme 6. Another interesting result of this experiment is that the acetates at C-2 and C-4 became scrambled. Hogg and Nagabushan[32] proposed that the rearrangement of the acetates proceeded as shown in Scheme 7.

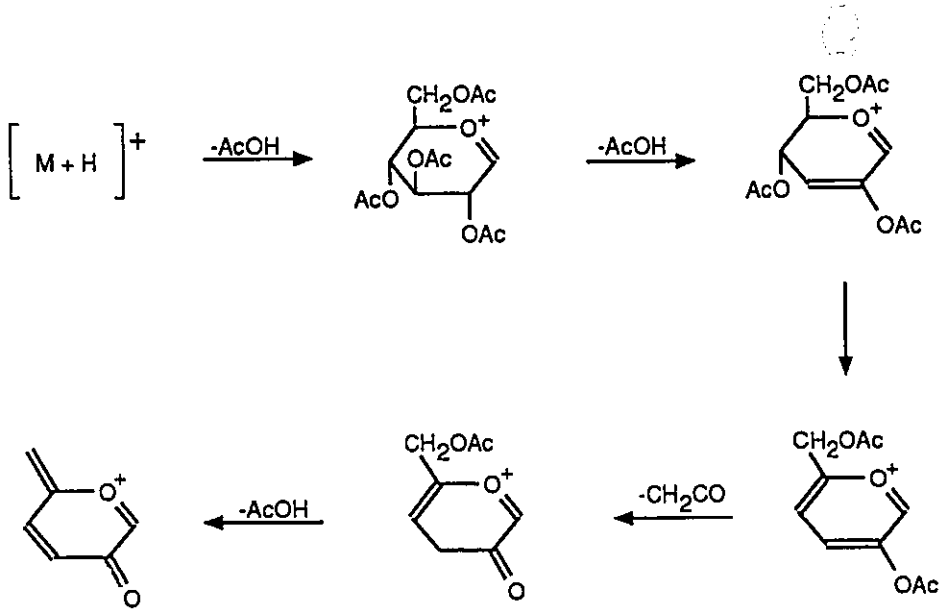

Scheme 6

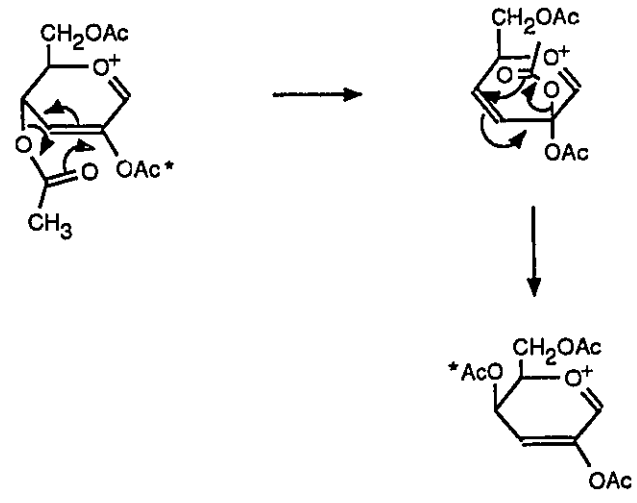

Scheme 7

Peracetylated oligosaccharides have been examined by CI-MS using ammonia[33,34] and mixtures of ammonia-isobutane[35] as the reagent gas. The spectra were dominated by even electron ions which contained ammonium. All the spectra exhibited an $[M+NH_4]^+$ ion and in many cases this ion was the most abundant ion in the spectrum. Many of the spectra exhibited $[M+NH_4-42]^+$, $[M+NH_4-60]^+$, and $[M+NH_4-77]^+$ ions, as well as ions resulting from further losses of 42 and 60 mass units from the aforementioned ions. The loss of 77 mass units from the $[M+NH_4]^+$ ion was attributed to the loss of ammonium and the C-1 acetate to form an oxonium ion. This conclusion was based on the observation that sucrose octaacetate, which could not undergo an analogous fragmentation, lacked an $[M+NH_4-77]^+$ ion in its spectrum.

Metastable ions, accounted for by decompositions of $[M+NH_4]^+$ to $[M+NH_4-60]^+$ and $[M+NH_4-77]^+$, were detected. However, no metastable ions were found for the loss of 42 mass units from the $[M+NH_4]^+$ ion. Dougherty *et al.*[35] proposed that this ion, for which no corresponding metastable ion was observed, was the result of 'thermolysis of the parent molecule followed by NH_4^+ attachment to the neutral fragments'.

Cleavage of the glycosidic bonds of oligosaccharides afforded a number of different types of ions, including oxonium ions and ions of the type shown in Figure 5. The ions in Figure 5 are derived formally by cleavage on either side of the glycosidic oxygen with attachment of H or CH_3CO to the glycosidic oxygen.

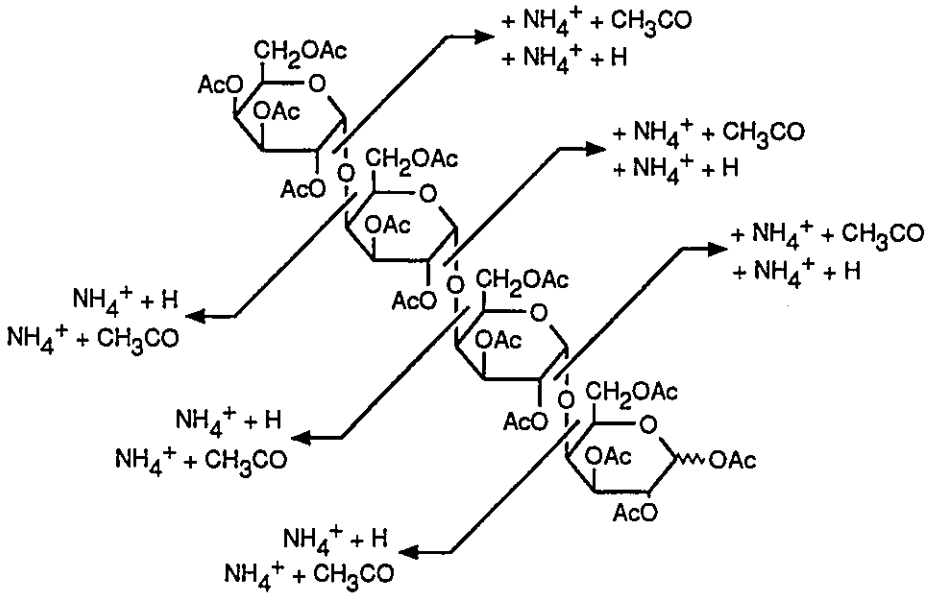

Figure 5. A partial fragmentation scheme for a peracetylated oligosaccharide.

These ions are hereafter referred to as hydrogen transfer ions and acyl transfer ions, respectively. Dougherty *et al.*[35] attributed the formation of these ions to thermolysis also.

1.4.3 Fast Atom Bombardment Mass Spectrometry of Peracetylated Carbohydrates

Fast atom bombardment mass spectrometry has been applied to the analysis of peracetylated oligosaccharides. Molecular weight related ions result from either the protonation of the carbohydrate or the formation of an adduct with a cation derived from a salt (*e.g.* Na^+).[7,36] Fragment ions are predominantly oxonium ions, although protonated hydrogen transfer ions and ions resulting from loss of acetic acid and ketene from the oxonium ions, are observed. MIKES studies on the oxonium ions indicate that they fragment in much the same manner as has been found under EI and methane CI conditions.[37-39] These studies indicated that the oxonium ions derived from peracetylated glucose, galactose and mannose could be distinguished by their MIKE spectra. This property has been used to assign the structure of a papulacandin antibiotic.[40]

A property of FAB-MS that distinguishes it from other ionization modes is the preferred cleavage of oligosaccharides at glycosidic linkages next to amino sugars. This type of preferred cleavage has been reported for a number of oligosaccharides containing glucosamine (2-amino-2-deoxyglucose).[36]

1.4.4 Linkage Analysis of Carbohydrates by Mass Spectrometry

The discrimination of linkage isomers of carbohydrates has been a recurring theme in mass spectrometric studies of carbohydrates. Early work in this area involved EI studies on permethylated disaccharides.[41] The linkage isomers were differentiated by comparing the relative abundance of a number of ions in the spectra. Later work, in which CI[42,43] and MIKES[44] were employed, refined the technique developed in the EI studies, but still involved the comparison of the abundance of a large number of ions.

More recently FAB-MS has been used to determine the linkage position in some underivatized oligosaccharides. Attempts to differentiate linkage isomers by positive ion FAB-MS proved only marginally successful. Dallinga and Heerma reported that the differences in the spectra are 'relatively small and do not always allow an unambiguous identification'.[45] The inability to differentiate linkage isomers by positive FAB-MS was attributed to the random protonation of the sugar hydroxyls; this resulted in non-selective fragmentation.[43]

Later work[46-49] using negative ion FAB-MS proved more successful. Daughter ion scans of the collisionally activated $[M-H]^-$ ions of disaccharides were found to be diagnostic of the type of linkage in the disaccharides. The selective fragmentation was attributed to the preferential deprotonation of the anomeric hydroxyl, which is more acidic than the other hydroxyls in a carbohydrate.[46] The ensuing fragmentation of the charge-bearing sugar residue is then directed by the position of linkage. The technique can be used also to determine every linkage

in an oligosaccahride by examining the daughter ion spectra of the ions produced by cleavage of the glycosidic linkages as shown in eqn. 12.[46,49]

$$R\text{-}O\text{-}R'\text{-}O^- \rightarrow R\text{-}O^- + R'O \qquad \text{eqn. 12}$$

where R=R'= a glycosyl unit

The ability to determine every linkage in an oligosaccharide and the need to compare only five ions to make the determination makes this method of linkage determination both simple and powerful; however, the analysis required a considerable amount of sample (up to 100 μg) for a mass spectrometric technique.

Dallinga and Heerma[49] demonstrated also that negative ion FAB-MS could be used to determine the configuration of the glycosidic linkage in a disaccharide. However, the spectra obtained were dependent on the configuration of the substituent at C-2 of the non-reducing glycosyl unit (glycosyl unit R in eqn. 12). This fact made it necessary to know the identity of the non-reducing residue before the linkage configuration could be assigned.

Positive ion FAB-MS was employed successfully to determine the interglycosidic linkages of peracetylated carbohydrates.[50,51,52] Domon *et al.*[50,51] found that 1,3- and 1,4-linkages could be identified by visual inspection of the daughter ion spectra of the collisionally activated oxonium ions of oligosaccharides. The daughter ion spectra of oxonium ions, substituted at C-3, exhibited an ion corresponding to a species from which the residue at C-3 was eliminated to afford a double bond, and the daughter ion spectra of oxonium ions, substituted at C-4, exhibited an abundant ion corresponding to the loss of acetic acid.

Identification of other linkage isomers required the aid of a computer pattern recognition routine and was reported only for a series of peracetylated disaccharides.[52] The computer performed a series of statistical analyses on the relative abundance of a set of ions in the daughter ion spectra of the collisionally activated disaccharide oxonium ions. The results of the calculations were plotted on a grid. Those carbohydrates with the same linkage had similar spectra and consequently ended up in the same region of the grid. An added benefit of this type of analysis is that it can also be used to determine the configuration of the linkage and the identity of the constituent monosaccharides. However, unambiguous assignment of structural features is not always possible because of the close proximity and, in some instances, overlap of the regions in the plot.

1.5 Lipopolysaccharides

1.5.1 Occurrence of Lipopolysaccharides

Lipopolysaccharides (LPS) are components of the cell envelope of Gram-negative bacteria.[53] The cell envelope consists of an inner cytoplasmic membrane surrounded by a peptidoglycan layer. The rigid peptidoglycan layer is surrounded by a more flexible bilayer. The inner monolayer of this bilayer is composed of phospholipids and proteins, while the outer monolayer contains the LPS and more proteins. The LPS, being at the cell surface, are important in the interaction of Gram-negative bacteria with other biological systems. The lipopolysaccharides of P. aeruginosa are, in fact, the major polysaccharide

polysaccharide antigens of that bacterium.[8]

1.5.2 Structure of Lipopolysaccharides

Lipopolysaccharides can themselves be divided into discrete regions which are common to all LPS isolated from Gram-negative bacteria. The innermost portion (with respect to the cell wall) of LPS is lipid A which is attached to the outer side chain polysaccharide through a core oligosaccharide.[54,55]

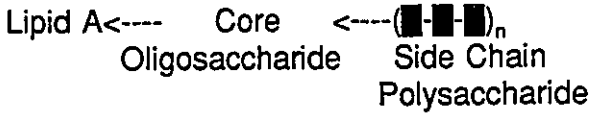

The structure of the core and lipid A regions of the LPS shows little variation within a species but the side chain polysaccharides can be highly variable. The individual regions of the LPS are described in greater detail below.

1.5.2.1 The Structure of Lipid A

The structure of P. aeruginosa lipid A has been determined by Kulshin *et al.*[56] (Fig. 6). It consists of a glucosamine disaccharide which is phosphorylated and contains both ester and amide linked fatty acids but was found to be heterogeneous with respect to the degree of acylation. This hydrophobic portion of the LPS anchors it to the cell wall through non-bonding interactions.[8] Thus, LPS is not chemically bound to the cell and can be isolated for analysis by extraction of whole cells with a suitable solvent.

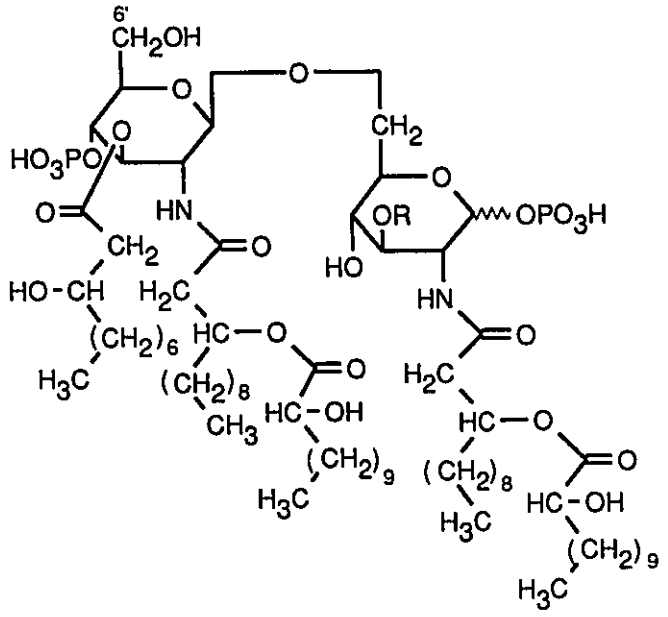

R=H or 3-hydroxy decanoyl

Figure 6. The structure of lipid A derived from P. aeruginosa[56]

The LPS, through lipid A, are attached to the cell through non-bonding interactions, but lipid A is chemically bound to the core portion of the LPS; the point of attachment is C-6′ of the glucosamine disaccharide.

1.5.2.2 The Structure of the Core Oligosaccharide

The core oligosaccharide (core) is a relatively low molecular weight oligomer which usually contains a number of different monosaccharides. The outer region of the core (in the case of P. aeruginosa) typically consists of neutral sugars while the inner core usually contains aminosugars, heptoses (some of which may be phosphorylated) and 2-keto-3-deoxy-octulosonic acid (KDO) (which may also be phosphorylated).[57-61] The core has so far always been found to be linked to lipid A through the acid labile ketal linkage of KDO. This linkage makes it possible to remove the lipid A from the LPS by very mild acid hydrolysis, yielding a water soluble carbohydrate that is much more easily analyzed.[8,53]

1.5.2.3 The Structure of the Side Chain Polysaccharide

P. aeruginosa elaborates two forms of LPS, each with a different side chain polysaccharide. The side chain polysaccharides are generally believed to be linked to the outer region of the core and are made up of a number of repeating oligosaccharide units.[8,54] One form of LPS has a side chain in which the repeating units are composed principally of rhamnose.[62,63] The other form of LPS is rich in acidic and amino sugars and is referred to as the O-antigen.[64] The number, type

and/or arrangement of the sugars in the O-antigen varies from one strain of bacterium to the next.[65] It is this variation that in fact differentiates the strains or, in immunological terms, determines their O-specificity.[8]

A number of schemes have been developed for differentiating or serotyping the numerous strains of P. aeruginosa, based on the differences in the O-antigen. These classification schemes have been reviewed and will not be discussed here.[66-68] However, in order to make comparisons of the results of this research with other work it is useful to know that the mutants studied here were derived from P. aeruginosa strain PAO1 serotype 05 (International Antigenic Typing System[68]).

The mutants that were actually studied (AK1012 and AK1401) are so-called non-typable mutants,[8] because the LPS of these two mutants lack a side chain polysaccharide.[69,70] The absence of the side chain makes it easier to isolate and analyze the cores of the LPS extracted from the mutants. Additionally, the AK1012 mutant lacks part of the core expressed by the parent strain.[69]

1.6 Carbohydrate Analysis

The complete analysis of an oligosaccharide involves the determination of all the aspects of its structure (section 1.2). A number of procedures have been developed to elucidate carbohydrate structure; the procedues combine chemical, chromatographic and spectroscopic techniques. Those procedures employed in this study are described below.

1.6.1 Compositional Analysis

The compositional analysis of an oligosaccharide may be accomplished by analysis of the alditol peracetates of its constituent monosaccharides by gas chromatography (GC) and gas chromatography-mass spectrometry (GC-MS).[71] For this analysis the oligosaccharide is hydrolysed, reduced with sodium borodeuteride and acetylated to yield a mixture of alditol peracetates. The mixture is then analyzed by GC-MS to identify the type of monosaccharides (ie. hexitol, deoxyhexitol, heptitol etc.) present in the mixture. The identification of the type of monosaccharides from their mass spectra is simplified by the fact that alditol peracetates fragment in a predictable manner. Scheme 8 illustrates the principal fragmentations of an alditol peracetate.

Once the types of alditols in the mixture have been determined, the identities of the individual components can be ascertained by comparison of their GC retention times with those of authentic standards. This procedure allows the identification of a large number of components in a single analysis without the necessity of isolating each component. In addition, integration of peak areas provides a measure of the relative amounts of the various monosaccharides in the carbohydrate being analyzed. In practice, care must be taken when comparing the peak areas because there may be non-stoichiometric formation of the various components. Thus, losses may be caused by degradation during hydrolysis or incomplete cleavage of hydrolysis-resistant glycosidic linkages (as in the case of aminosugars).[71]

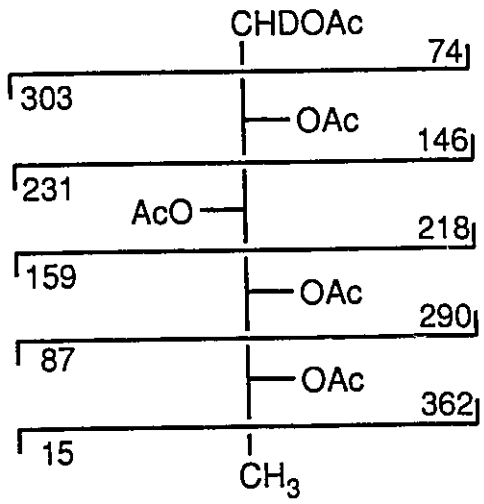

Scheme 8

1.6.2 Methylation Analysis

The determination of the position of linkage between glycosyl units in an oligosaccharide or a polysaccharide was greatly simplified by the application of GC-MS methods to methylation analysis.[72-74] This development made possible the determination of the linkages in a carbohydrate without the necessity of isolating the products of methylation analysis.

The two methods that are commonly used to permethylate oligosaccharides were developed by Hakomori[75] and Ciucanu and Kerek.[76] Following permethylation the sample is hydrolysed, reduced and acetylated to yield a mixture of partially methylated alditol acetate (PMAA). This mixture of PMAA's is then analyzed by GC-MS. Identification of the components relies on the fact that PMAA's fragment in a predictable manner. Fragmentation of the alditol backbone tends to occur next to methoxy rather than acetate groups. Thus, the dominant ions in the spectrum of the PMAA shown in Scheme 9 (1,5,6-tri-*O*-acetyl-2,3,4-tri-*O*-methyl hexitol) appear at *m/z* 117, *m/z* 161, *m/z* 189 and *m/z* 205. These ions indicate that there are acetate groups at C-1, C-5, and C-6, establishing that those positions were involved in bonding in the original carbohydrate. Thus, the PMAA in Scheme 9 corresponds to a 6-linked hexopyranose.

Ambiguities in this analysis can arise under certain circumstances. For instance, it is not possible to determine whether PMAA **a** (Scheme 10) was derived from a 3,6-linked hexopyranose or a 2,6 linked hexofuranose. This ambiguity can

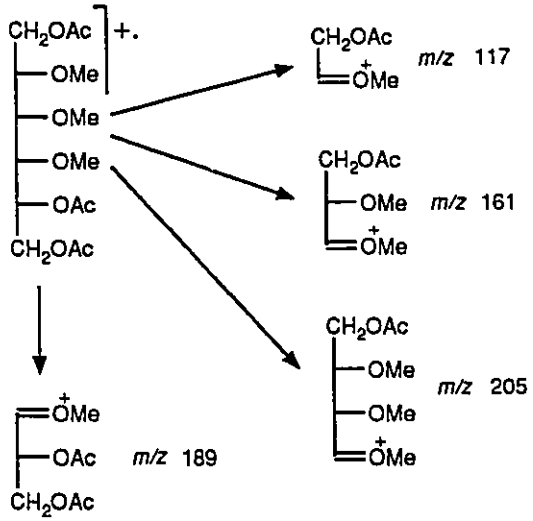

Scheme 9

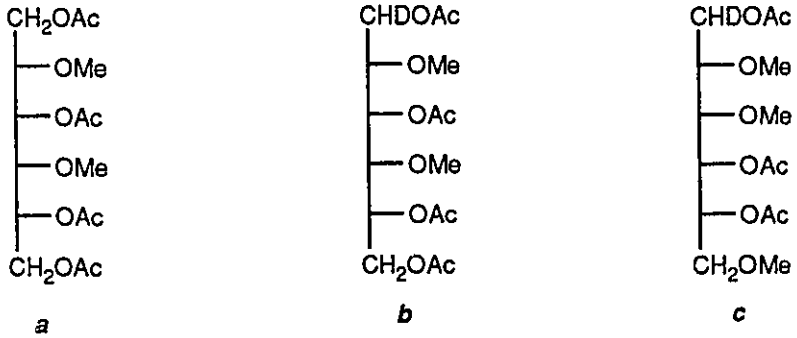

Scheme 10

be resolved by using $NaBD_4$ in the reduction step so that the anomeric carbon is labelled with a deuterium atom.[77] When so labelled it is clear that PMAA **b** (Scheme 10) is derived from a 3,6-linked hexopyranose. However, even with deuterium labelling it is impossible to determine whether PMAA **c** (Scheme 10) results from a 4-linked hexopyranose or a 5-linked hexofuranose. This type of ambiguity in the results of methylation analysis must be resolved by a different method of analysis.

1.6.3 Periodate Oxidation and Sodium Borodeuteride Reduction

Periodate oxidation and subsequent reduction (as outlined in Scheme 11) allows the selective degradation of an oligo- or polysaccharide. The selectivity of the periodate oxidation is based on its ability to cleave the carbon-carbon bonds between adjacent carbon atoms bearing hydroxyl groups. The products of this oxidation-reduction sequence can then be identified by compositional analysis. The carbohydrate components identified in the compositional analysis of the degraded carbohydrate will reflect the structure of the intact carbohydrate and may provide information on the identity of the monosaccharides in the intact carbohydrate that cannot be obtained from compositional analysis or methylation analysis alone.[78,79] For instance, a heptose for which no standards are available for comparison may be degraded to a hexose which can be identified by GC.

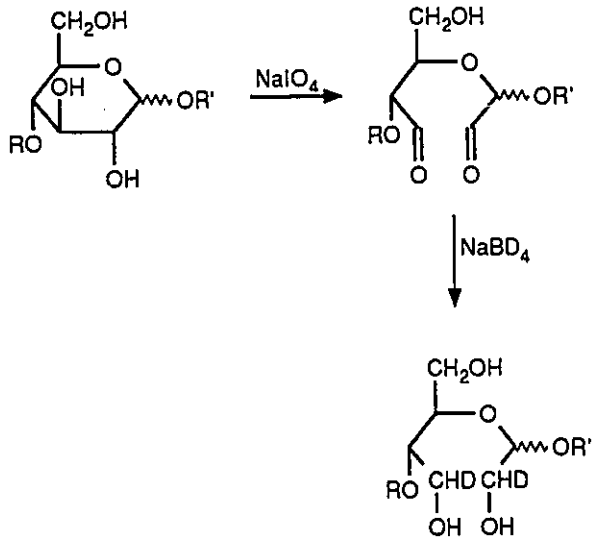
CH2OH
O
OH
OR'
RO
OH
NaIO4
CH2OH
O
OR'
RO
O
O
NaBD4
CH2OH
O
OR'
RO
CHD
CHD
OH
OH

Scheme 11

1.6.4 Absolute Configuration Determination

The determination of the absolute configuration of a monosaccharide requires the ability to distinguish between enantiomers. This may be done by isolating a pure sample of a monosaccharide of unknown absolute configuration (a task which may be difficult) and comparing its optical rotation with that of a standard. Leontein *et al.*[80] have developed a method for determining the absolute configuration of a monosaccharide that does not require prior isolation of the monosaccharide. The method is based on the principle that chromatographically inseparable D- and L-enantiomers may be made separable by converting them into a pair of diastereomers. Their method works as follows.

Once the identity of a monosaccharide has been established a standard sample of known absolute configuration is obtained (either enantiomer will do). The standard is reacted with an optically-pure chiral alcohol (either enantiomer) to obtain a glycoside which is then acetylated to facilitate analysis by GC or GC-MS. The same standard is then reacted with a racemic mixture of the chiral alcohol and subsequently acetylated. For the purpose of illustrating the technique assume the standard sugar has the D-configuration and the optically pure chiral alcohol is the (-)-isomer. In that case the first preparation decribed above would consist of glycosides formed from the D-sugar and the (-)-alcohol [D-(-) glycosides]. The second preparation described above would contain a mixture of glycosides formed from the D-sugar and the (-)-alcohol and the D-sugar and the (+)-alcohol [D-(+) glycosides]. The D-(-)-glycosides and the D-(+)-glycosides are diastereomers and

therefore chromatographically separable. However, the D-(+)-glycosides bear an enantiomeric relationship to the glycosides that would be formed from the corresponding L-sugar and the (-)-alcohol (L-(-)-glycosides). Since enantiomers co-elute the D-(+)-glycoside serves a a chromatographic standard for the for the L-(-)-glycoside. The absolute configuration of the unknown can then be detemined by preparing the volatile (-)-glycoside and comparing its retention time with those of the D-(-)-glycoside and the D-(+)-glycoside. If the unknown (-)-glycosides have the same retention time as the D-(-)-glycosides then the unknown sugar has the same configuration as the standard sugar. If the unknown (-)-glycosides have the same retention time as the D-(+)-glycosides then they must be enantiomers of the D-(+)-glycosides and therefore the unknown sugar has the opposite configuration of the standard sugar, namely the L-configuration.

1.6.5 Sequence Analysis

The analyses described above provide clues to the structure of an oligosaccharide but will generally be consistent with a number of structural isomers. In order to identify the correct isomer it is necessary to determine the sequence of the glycosyl residues in the oligosaccharide. Mass spectrometry is ideally suited to this task.

The mass spectra of oligosaccharides, or their volatile derivatives, exhibit ions resulting from the cleavage of the glycosidic linkages.[2-7] This fact, combined with a knowledge of the composition of the oligosaccharide and of the

linkage sites (as determined by the chemical analyses), allows one to assign possible structures to the ions in the mass spectrum of the oligosaccharide. These structures may then be used to deduce the sequence of glycosyl units in the oligosaccharide.

CHAPTER 2

EXPERIMENTAL

2.1 Materials

With the exception of the labelled gentiobioses (**5**,**6**), 2,3,4,6-tetra-*O*-acetyl-D-glucopyranose (**7**) and the core oligosaccharides, all the peracetylated carbohydrates used in this study were either purchased from, or prepared from sugars purchased from, Sigma Chemical Co., Inc., Aldrich, Inc. or Serva Biochemical, Inc. Compounds (**5-7**) and the AK1401 core oligosaccharide were provided by Professor W.A. Szarek, Queen's University, Kingston, Ontario Canada. Compound **5** was the pure β-anomer but compound **6** was a 6:4 mixture of α- and β-anomers as judged by its ^{1}H-NMR spectrum. The ammonia CI spectra of the two anomers were virtually identical as indicated by a GC-MS experiment The AK1012 core was provided by Professor A.M. Kropinski, Queen's University, Kingston, Ontario Canada. A complete description of the isolation and purification of the core oligosaccharides may be found elsewhere.[69] However, a brief outline of the procedure is included below for clarity.

Both the AK1012 and AK1401 P. aeruginosa cells were grown in a tryptic soy broth and were harvested by centrifugation. The cells were suspended in 0.1M potassium phosphate buffer and the cell walls were broken by mechanical action and then collected by centrifugation. The cell walls were dried by lyophilization and then extracted with a mixture of phenol (90% in H_2O):chloroform: petroleum ether=2:5:8 (v/v/v). The extracts were centrifuged and the supernatant

was collected. The volatile solvents were removed from the extract under vacuum and the LPS were precipitated by addition of water. The precipitated LPS were collected by filtration (AK1012) or centrifugation (AK1401) and then hydrolysed in acetic acid (1% in H_2O, v/v) at 100°C for 90 min. Hydrolysis of the LPS resulted in precipitation of the lipid A. The hydrolysate was cooled, then the lipid A was removed by filtration and the filtrate was lyophilized. The core samples were then purified by size exclusion chromatography using either Sephadex G-50 (AK1012) or Bio gel P-4 (AK1401) columns.

Unless stated otherwise, the core oligosaccharides were dephosphorylated[81,82] prior to subsequent analysis. The core sample (10-20 mg) was placed in a plastic screw cap vial and dissolved in 49% aqueous HF (2 mL). The solution was allowed to stand at approximately 2°C for 60 to 66 h, after which the aqueous HF was removed under vacuum. The residue was purified by size exclusion chromatography (1.5 cm x 22 cm column) using Sephadex G-10 gel and pyridinium acetate (0.2 M; 15 mL per hour flow rate) as the mobile phase. The void volume was collected and lyophilized to yield the dephosphorylated core (4-8 mg).

2.2 Instrumentation

2.2.1 Mass Spectrometry

CI and EI mass spectra were obtained on a VG Analytical ZAB-E mass spectrometer equipped with a VG-11-250J data system. The source temperature

was maintained at 200°C; the filament of the DCI probe was not heated unless otherwise indicated. An accelerating voltage of 7000 V was used in all experiments. In the EI mode the electron energy was 70 eV and in the CI mode the emission current was 1 mA. Spectra were acquired using a sample loading of 5 to 15 μg. The ammonia reagent gas (Matheson, anhydrous ammonia) was used at a pressure that resulted in a 20:1 ratio of $(NH_4)^+$ to $(N_2H_7)^+$; ammonia-d_3 was obtained from MSD Isotopes (99% isotopic purity).

FAB mass spectra were acquired on a VG Analytical ZAB-SE equipped with a VG-11-250 data system. An accelerating potential of 8 kV and an atom beam energy of 8 keV were employed. The sample loading was approximately 50 μg and the matrix was 1-thioglycerol.

MIKE spectra were acquired employing the EI or CI conditions described above. Under DEI conditions 20 μg of sample were used routinely and under DCI 40 to 60 μg of sample were required for each analysis. CA spectra were acquired employing helium as the collision gas at a pressure sufficient to attenuate the transmission of ions by 50%.

The GC-MS analysis of the anomers of labelled gentiobiose (**11**) was performed on a VG Micromass TRIO-2 mass spectrometer equipped with a VG-11-250J data system and a Hewlett-Packard 5890A Series II gas chromatograph. The anomers were separated on a 30 m, DB1701, wide-bore column (J & W Scientific) at 280°C isothermal, using helium as the carrier gas, at a head pressure of 1.5 psig. All other GC-MS experiments were carried out using a Hewlett-

Packard mass selective detector (MSD) equipped with a Hewlett-Packard 5890A Series II gas chromatograph and a Zenith Data Systems personal computer. The analyses on this instrument employed a 30 m, DB1701, narrow-bore column (J & W Scientific) with helium as the carrier gas at a head pressure of 4 psig. The temperature programs employed were (A) 50°C to 190°C at 60°C per min, hold for 20 min, then 4°C per min to 250°C and hold for 10 min, (B) 50°C to 160°C at 60°C per min and hold for 2 min, then 4°C per min to 260°C and hold for 10 min or (C) 50°C to 160°C at 60°C per min, then 6°C per min to 260 and hold for 35 min.

Mass spectral results are reported as *m/z* (% relative abundance of base peak). Ions in the mass spectra are plotted as percent relative abundance of the base peak versus *m/z*.

2.2.2 Nuclear Magnetic Resonance Spectroscopy

^{1}H-NMR experiments were recorded at 90 MHz on a Varian EM390 spectrometer. The spectra were recorded at ambient temperature and are reported in ppm relative to tetramethylsilane.

^{31}P-NMR spectra were recorded on a Bruker AM-500 spectrometer at 202.4 MHz at 70°C. The spectra are reported in ppm relative to H_3PO_4 as an external reference.

2.2.3 Gas Chromatography

Gas chromatography was performed on a Hewlett-Packard 5890

instrument equipped with a flame ionization detector maintained at 280°C. The separations were accomplished using a 30 m, DB-1701, wide-bore column (J & W Scientific) with helium as the carrier gas at a head pressure of 8 psig. Samples were injected on-column and the chromatograms were recorded on an HP3390A integrator. The temperature programs employed were as follows: (D) 190°C for 20 min, then 4°C per min to 250°C and hold for 20 min; (E) 280°C isothermal.

2.3 Analytical Methods

2.3.1 Compositional Analysis

The dephosphorylated core (~1 mg) was sealed in an evacuated tube with 2M trifluoroacetic acid (0.5 mL) and then heated at 120°C for 1.5 h at which time the hydrolysis tube was cooled to room temperature. The tube was then opened and the acid was evaporated under vacuum. The resultant monosaccharides were reduced with $NaBD_4$ (30 mg) in H_2O (5 mL) over a period of 12 h at which time the mixture was evaporated to dryness under vacuum. The residue was taken up in absolute methanol and the remaining $NaBD_4$ was decomposed by the addition of glacial acetic acid (2 drops). The boric acid was removed by co-distillation with the methanol and the remaining methanol was removed under vacuum. Acetic anhydride (2 mL) was added to the solid that remained after evaporation of the methanol. The mixture was heated at 100°C for 1 h and then the acetic anhydride was evaporated under vacuum. $CHCl_3$ was

added to the residue and the material that did not dissolve in the $CHCl_3$ was filtered off. The $CHCl_3$ solution was then analyzed by GC/MS and GC using temperature programs A and D, respectively. The relative quantities of the components were determined by integration of the area of each peak in the chromatogram.[71] External standards were used for glucose and rhamnose; the only components for which suitable standards were available.

2.3.2 Methylation Analysis

The dephosphorylated core (3-5 mg) was dissolved in dimethyl sulphoxide (DMSO, 1 mL), dried over CaH_2. Powdered KOH (~40 mg) was added, and the suspension was stirred under argon for 5 min. Methyl iodide (1 mL) was added and the mixture was stirred under argon for an additional hour. Water (2 mL) was added to the reaction vessel. The solution was extracted with $CHCl_3$ (2 x 2 mL) and the combined extract was washed with water 3 times and then dried over anhydrous Na_2SO_4. The solution was decanted and the $CHCl_3$ was evaporated under a stream of N_2 to yield the permethylated carbohydrate as a yellow oil.

The permethylated carbohydrate was sealed in an evacuated tube with 2M trifluoroacetic acid (0.5 mL) and heated at 120°C for 1.5 h. The hydrolysis tube was cooled, then opened and the hydrolysate was taken to dryness under a stream of N_2. The residue was reduced with $NaBH_4$ (40mg) in H_20 (2 mL) over a period of 6 h. The solution was again taken to dryness under a stream of N_2. The

residue was taken up in absolute methanol and the remaining $NaBH_4$ was decomposed by the addition of glacial acetic acid (2 drops). The boric acid was removed by co-distillation with methanol and the remaining methanol was evaporated under a stream of N_2.

Glacial acetic acid (1.0 mL) was added to trifluoracetic acid (2.0 mL) under argon and the mixture was allowed to stand for 5 min. The resultant mixed anhydride (0.5 mL/mg of carbohydrate) was added to the residue obtained after evaporation of the methanol and the solution was stirred under argon for 10 min. The solution was then taken to dryness under a stream of N_2. The product was analyzed by GC-MS (program B). The relative amonuts of the components were deterined by integration of the peaks areas in the total ion current chromatogram. The response factors were assumed to be approximately equal since no standards were available for comparison.[77]

2.3.3 Periodate Oxidation and Sodium Borodeuteride Reduction

The dephosphorylated core (2 mg) was dissolved in 0.1M sodium periodate solution (2 mL) and then stirred at room temperature in the dark for 24 h. An excess of $NaBD_4$ was added to the reaction mixture which was then stirred at room temperature for a further 12 h. The solution was then evaporated under vacuum and subsequently taken up in absolute methanol. Glacial acetic acid (2 drops) was added to the methanolic solution and the boric acid was removed by co-distillation with the methanol. The residual methanol was removed by

evaporation at reduced pressure. The periodate-oxidized/sodium borodeuteride reduced carbohydrate was then subjected to compositional analysis as described above.

2.3.4 Preparation of Samples for Absolute Configuration Determination[80]

The dephosphorylated core (2 mg) was hydrolysed with 2M trifluoroacetic acid (0.5 mL) at 120°C for 1.5 h. Volatile (-)-2-octyl glycosides were prepared from the core hydrolysate and analyzed as described below.

The carbohydrate (standard or hydrolysed core sample) to be analyzed (1-2 mg) was sealed in an evacuated ampoule with 2-octanol (0.5 mL; either (-)-2-octanol or (±)-2-octanol, as required) and trifluoroacetic acid (2 drops). The ampoule was heated at 140°C for 20 h, opened, and then the sample was taken to dryness under vacuum. The resulting oily brown residue was taken up in pyridine:acetic anhydride = 1:1 (v/v, 1 mL) and heated at 100°C for 1.5 h. The product was again taken to dryness under vacuum and then analyzed by NH_3-DCI MS and GC-MS (program C).

2.4 Preparation of Penta-*O*-acetyl-β-D-glucopyranose, **1**[83]

Acetic anhydride (50 mL) and powdered anhydrous sodium acetate (800 mg) were added to D-glucopyranose (1.0 g). The mixture was stirred at 100°C for 2.5 h and then poured into ice cold water (500 mL) in a flask, which was then shaken vigorously. A clear colourless oil coated the sides of the flask after 1-2

min. The water was decanted and another 500 mL of ice cold water was added to the vessel. The mixture was shaken for several more minutes and the water was again poured off. The oil slowly solidified on standing. The solid was taken up in methanol and was crystallized from a mixture of methanol and water. (1.52g, 70%, m.p.130-131°C, (corrected); lit. 130-132°C[83]

GC (program E): 1 component

MS (DCI, NH_3) *m/z* 408(100) $[M+NH_4]^+$

^1H NMR (90 MHz), $CDCl_3$, δ: 2.03 (3H, singlet, CH_3CO), 2.07 (6H, apparent singlet, $2CH_3CO$'s), 2.10 (3H, singlet, CH_3CO), 2.13 (3H, singlet, CH_3CO), 2.83 (1H, multiplet, H-5), 4.2 (2H apparent doublet of quartets, H-6), 5.13 (3H, overlapped signals at the indicated chemical shift, H-2, H-3, and H-4), 5.68 (1H, doublet, C-1).

2.5 Preparation of Monosaccharides **2** and **3** and Disaccharides **16** to **21**

Acetic anhydride (0.5 mL) and pyridine (0.5 mL) were added to the carbohydrate to be acetylated (0.5 mg). The mixture was heated at 100°C for 1.5 h. The resulting solution was evaporated under vacuum to yield a yellowish oil which was analyzed by GC (program E) and NH_3 DCI-MS.

Penta-*O*-acetyl-D-galactopyranose **2**

GC: 1 component

MS (DCI, NH_3): *m/z* 408(100) $[M+NH_4]^+$

Penta-*O*-acetyl-D-mannopyranose **3**

GC: 1 component

MS (DCI, NH_3): *m/z* 408(100) $[M+NH_4]^+$

Methyl hepta-*O*-acetyl-α-D-mannopyranosyl-(1→6)-α-D-mannopyranoside **16**

GC: 97% pure

MS (DCI, NH_3): *m/z* 668(100) $[M+NH_4]^+$

Methyl hepta-*O*-acetyl-α-D-mannopyranosyl-(1→4)-α-D-mannopyranoside **17**

GC: 99.5% pure

MS (DCI, NH_3): *m/z* 668(100) $[M+NH_4]^+$

Methyl hepta-*O*-acetyl-α-D-mannopyranosyl-(1→3)-α-D-mannopyranoside **18**

GC: 93% pure

MS (DCI, NH_3): *m/z* 668(100) $[M+NH_4]^+$

Methyl hepta-*O*-acetyl-α-D-mannopyranosyl-(1→2)-α-D-mannopyranoside **19**

GC: 88% pure

MS (DCI, NH_3): *m/z* 668(100) $[M+NH_4]^+$

Octa-*O*-acetyl-α-D-galactopyranosyl-(1→6)-D-galactopyranose **20**

GC: 91% pure

MS (DCI, NH_3): [illegible]100) $[M+NH_4]^+$

Octa-*O*-acetyl-α-D-galactopyranosyl-(1→4)-D-galactopyranose **21**

GC: 97% pure

MS (DCI, NH_3): *m/z* 696(100) $[M+NH_4]^+$

2.6 Preparation of 1,2,3,4-Tetra-*O*-acetyl-β-D-glucopyranose, **8**[84]

A solution of glucose (12 g) in pyridine (50 mL) was heated at 100°C in an oil bath. Trityl chloride (19.3 g) was added to the mixture while it was stirred. While continuing to stir the mixture, the temperature of the oil bath was raised slowly. When the temperature of the bath had reached 130°C the solid material in the reaction pot had dissolved to give a dark brown solution. Acetic anhydride (30 mL) was added to the mixture which was then allowed to cool to room temperature overnight.

In the morning the reaction product was poured into water (1.5 L). A precipitate formed immediately. The suspension was stirred with a mechanical stirrer until a fine suspension formed (4 h). The suspended solid was filtered off, but a large amount of the product adhered to the flask. Fresh water (1.0 L) was poured into the flask and then stirred for 4 h. On filtering, a fine powder was then obtained. The two batches of isolated product were separately crystallized, first from 95% ethanol and then from diethyl ether, to yield white needle-like crystals of 1,2,3,4-tetra-*O*-acetyl-6-*O*-trityl-β-D-glucopyranose. 1st batch 0.55g, m.p. 165.5-167°C (corrected) ; 2nd batch 1.48g, m.p. 163-166°C (corrected); lit. 166-167°C[84]

^{1}H NMR (90 MHz), $CDCl_3$, δ: 1.70 (3H's, singlet, CH_3CO), 2.00 (3H's, singlet,

CH_3CO), 2.02 (3H's, singlet, CH_3CO), 2.1 (3H's, singlet, CH_3CO), 3.20 (2H, apparent doublet of quartets, C-6 H's), 3.70 (1H, multiplet, C-5 H), 5.18 (3H, multiplet, H-2, H-3, and H-4), 5.72 (1H, doublet of doublets, C-1), 7.38 (15H, multiplet, trityl protons),

The entire first batch (0.55g) was dissolved in warm glacial acetic acid and then cooled to 10°C. HBr (0.26 mL, 30% by weight HBr in glacial acetic acid) was added to the solution. A precipitate formed immediately and was filtered off. The filtrate was poured into ice cold water and then extracted with $CHCl_3$. The extract was washed with water (5x10 mL) and dried over anhydrous Na_2SO_4. Evaporation of the $CHCl_3$ yielded a colourless oil. Crystallization of the oil from diethyl ether yielded a fine white solid, 116 mg, 35% (based on the intermediate tritylated compound). m.p. 126-127.5°C, (corrected); lit. 128-129°C.[84]

GC: 94% pure

MS (DCI, NH_3): *m/z* 366(100) $[M+NH_4]^+$

^1H NMR (90 MHz), $CDCl_3$, δ: 2.02 (6H's, apparent singlet, 2 CH_3CO's), 2.06 (3H's, singlet, CH_3CO), 2.12 (3H's, singlet, CH_3CO), 3.66 (3H's, overlapped signals centred at the indicated chemical shift, H-5 and two H-6's), 5.20 (3H's, overlapped signals centred at the indicated chemical shift, H-2, H-3, and H-4), 5.68 (1H, doublet, H-1)

2.7 The Preparation of the Isomeric Octa-*O*-acetyl-D-glucopyranosyl-D-glucopyranoses **10-15**

Glacial acetic acid and trifluoroacetic anhydride were combined in a 1 to 2 ratio (v/v) and allowed to sit for 5 min. The resulting mixed anhydride was added to the carbohydrate (0.5 mL/mg of carbohydrate) under argon. The reaction mixture was stirred for 10 min, after which the solution was evaporated under a stream of N_2. The product was analyzed by GC (program E) and NH_3-DCI MS.

Octa-*O*-acetyl-α-D-glucopyranosyl-(1→6)-D-glucopyranose **10**

GC: 89% pure

MS (DCI, NH_3): *m/z* 696(100) $[M+NH_4]^+$

Octa-*O*-acetyl-β-D-glucopyranosyl-(1→4)-D-glucopyranose **11**

GC: 94% pure

MS (DCI, NH_3): *m/z* 696(100) $[M+NH_4]^+$

Octa-*O*-acetyl-α-D-glucopyranosyl-(1→4)-D-glucopyranose **12**

GC: 93% pure

MS (DCI, NH_3): *m/z* 696(100) $[M+NH_4]^+$

Octa-*O*-acetyl-β-D-glucopyranosyl-(1→3)-D-glucopyranose **13**

GC: 92% pure

MS (DCI, NH_3): *m/z* 696(100) $[M+NH_4]^+$

Octa-*O*-acetyl-α-D-glucopyranosyl-(1→3)-D-glucopyranose **14**

GC: 88% pure

MS (DCI, NH_3): *m/z* 696(100) $[M+NH_4]^+$

Octa-*O*-acetyl-β-D-glucopyranosyl-(1→2)-D-glucopyranose **15**

GC: 96% pure

MS (DCI, NH_3): *m/z* 696 $[M+NH_4]^+$(100% rel. int.)

2.8 Preparation of Peracetylated Naringin **22** and Peracetylated Hesperidin **23**

Acetic anhydride (0.5 mL) and pyridine (0.5 mL) were added to the glycoside (2 to 3 mg) to be acetylated. The mixture was heated at 100°C for 1.5 h and then evaporated under vacuum to yield a yellow oil. The oil was analyzed by thin layer chromatography (TLC) (toluene:ethanol=9:1(v/v)) and NH_3-DCI MS.

Peracetylated Naringin, **22**

TLC: 1 component visible R_f 0.51

MS (DCI, NH_3): *m/z* 934(15) $[M+NH_4]^+$

Peracetylated Hesperidin, **23**

TLC: 1 component visible R_f 0.50

MS (DCI, NH_3): *m/z* 964(20) $[M+NH_4]^+$

CHAPTER 3

MASS SPECTROMETRY OF PERACETYLATED CARBOHYDRATES

RESULTS AND DISCUSSION

3.1 Introduction

In the first part of this chapter the NH_3-DCI mass spectra of a number of peracetylated mono- and disaccharides are examined. The structure of a number of ions in both classes of compounds have been clarified. In the case of the monosaccharides this was accomplished mainly by means of experiments in which ND_3 was used as the reagent gas. In the case of the disaccharides additional clarification was provided by comparison of the MIKES spectra of several ions with those derived from compounds of established structure and by the examination of the NH_3-DCI mass spectra of some labelled compounds. The spectra derived from the labelled compounds provided some insight into the fragmentation processes leading to the formation of hydrogen and acyl transfer ions and an ion that appears at *m/z* 317.

The second part of this chapter discusses experiments that enable one to determine the position of linkage in disaccharides comprised of either D-glucopyranose units or D-mannopyranose units. The determination is made by comparing the MIKES spectra of the *m/z* 317 ion, which appears in the DEI mass spectra of the (1→6)-, (1→4)-, (1→3)- and (1→2)-linked isomers. Examination of the MIKES spectra of the *m/z* 317 ion in the DEI spectra of the (1→6)- and (1→4)-linkage isomers of two galactose disaccharides suggests that this technique may

be applied also to disaccharides comprised of galactopyranose units. The technique was applied to the determination of the linkage in two flavonoid glycosides of known structure; the results of those experiments are discussed also.

3.2 Ammonia DCI MS of Some Peracetylated Monosaccharides

The ammonia DCI-MS spectra of peracetylated glucose, galactose, and mannose, structures **1-3**, respectively, were examined and found to be similar.

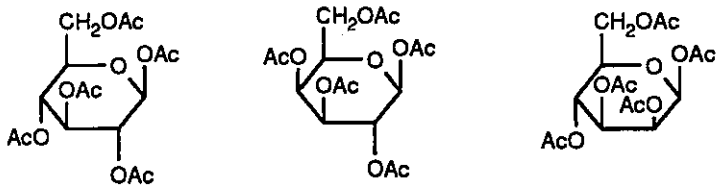

1 **2** **3**

The spectra were dominated by the $[M+NH_4]^+$ ion (Fig. 7). Several series of ions of low abundance were also evident. The ions at the high-mass end of the series corresponded to loss of ketene (*m/z* 366), acetic acid (*m/z* 348) or ammonium acetate (*m/z* 331) from the $[M+NH_4]^+$ ion. The other ions in the series corresponded in mass to subsequent losses of acetic acid and ketene from the ions of higher mass.

Peracetylated glucose (**1**) was examined under ND_3 DCI-MS conditions also. The high-mass ions in the spectrum shifted as indicated in Scheme 12. The $[M+NH_4]^+$ ion shows the expected shift of 4 mass units (ND_4 substituted for NH_4). The ion that corresponds to loss of ketene shifts by 5 mass units, indicating the presence of a free hydroxyl from which an H has exchanged for a D. The $[M-60+NH_4]^+$ ion splits into two ions at *m/z* 351 and *m/z* 352 (relative abundance

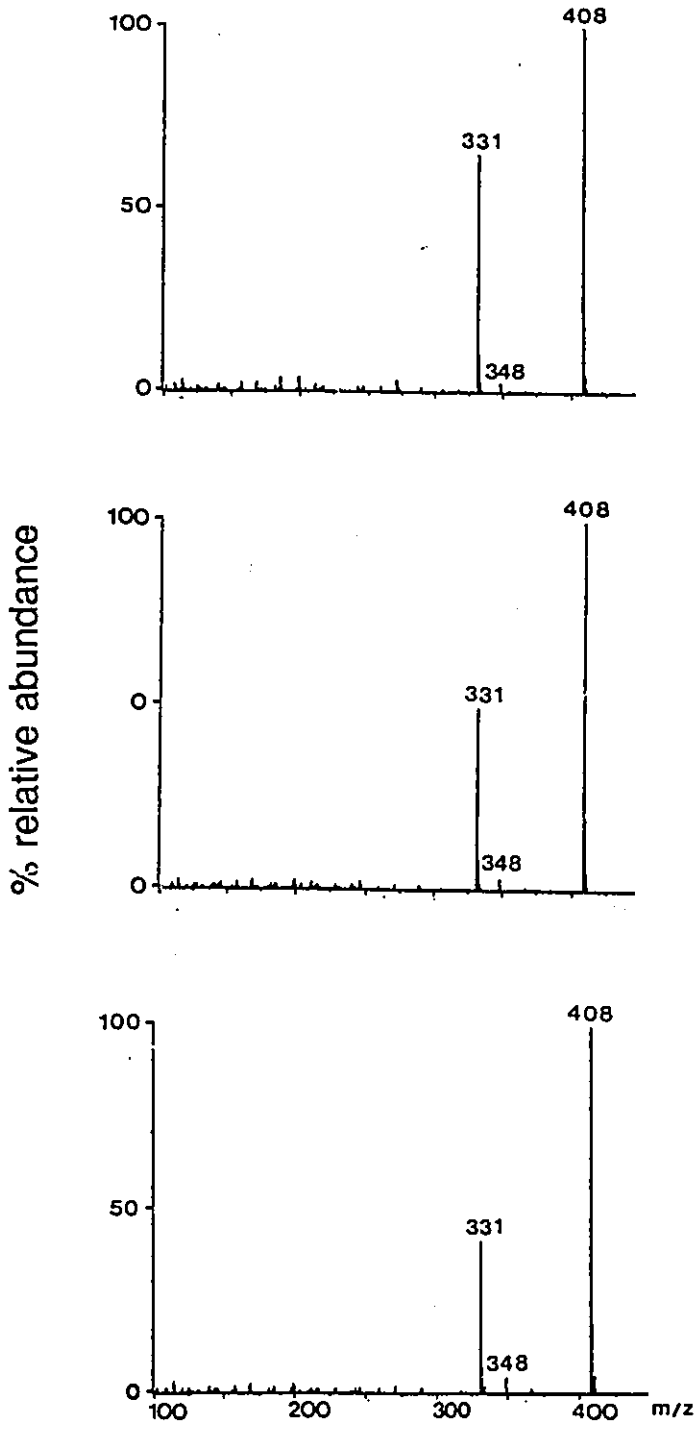

Figure 7. NH_3-DCI mass spectra of (a) peracetylated glucose; (b) peracetylated galactose; (c) peracetylated mannose.

NH_3 REAGENT GAS	ND_3 REAGENT GAS
$[M + NH_4]^+$ *m/z* 408	$[M + ND_4]^+$ *m/z* 412
$[M + NH_4 - 42]^+$ *m/z* 366	$[M + ND_4 - 42 - H + D]^+$ *m/z* 371
$[M + NH_4 - 60]^+$ *m/z* 348	$[M + ND_4 - 60]^+$ *m/z* 352
	$[M + ND_4 - 61]^+$ m/z 351

Scheme 12

~3:1). The ion at *m/z* 352 is derived from the corresponding ion at *m/z* 348 when ND_4^+ is substituted for NH_4^+. The ion at *m/z* 351 formally results from a loss of CH_3COOD from the $[M+ND_4]^+$ ion and may have the structure:

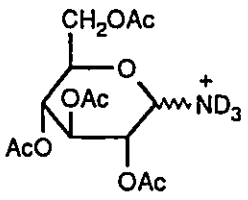

m/z 351

Ions of this type have been reported previously in the NH_3-CI spectra of permethylated oligosaccharides.[5,6]

MIKES experiments were performed on the $[M+NH_4]^+$ ions and the oxonium ions of compounds **1-3**. The only abundant ion observed in the MIKES spectra of the $[M+NH_4]^+$ ion of compounds **1-3** was the oxonium ion at *m/z* 331. An $[M-60+NH_4]^+$ ion (of low abundance, approximately 0.5% relative to *m/z* 331) was observed also in each spectrum.

The MIKES spectra of the oxonium ions at *m/z* 331, derived from **1-3**, are shown in Figure 8. The spectra obtained from peracetylated glucose (**1**) and peracetylated galactose (**2**) are similar to those reported by Guevremont and Wright for the respective compounds under FAB ionization conditions.[37] This suggests that fragmentation of the oxonium ions proceeds in a similar fashion under CI and FAB conditions. The MIKES spectrum of the oxonium ion of mannose resembles the MIKES spectrum obtained from the oxonium ion of

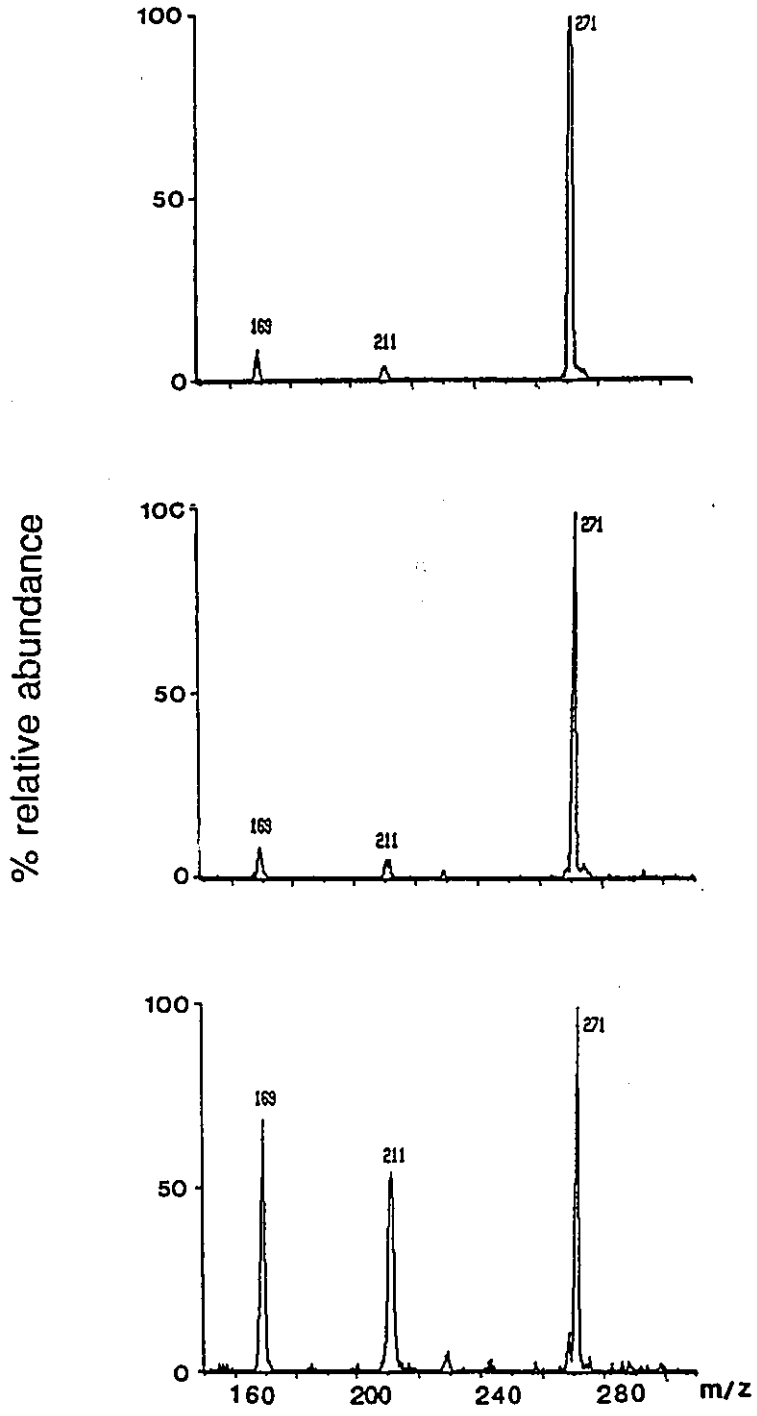

Figure 8. MIKES spectra of the *m/z* 331 ion in the NH_3-DCI spectra of (a) peracetylated glucose; (b) peracetylated mannose; (c) peracetylated galactose.

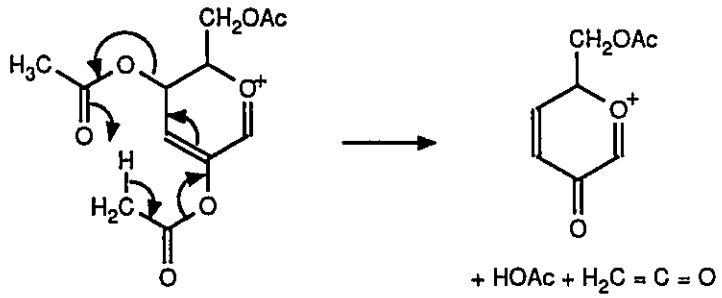

m/z 271 *m/z* 169

Scheme 13

glucose but not the MIKES spectrum obtained from the oxonium ion of galactose. Clearly the stereochemistry of the substituents around the sugar ring affects the fragmentation.

Guevremont and Wright[38] proposed a mechanism to explain the difference in the MIKES spectra of glucose and galactose which is based on the stereochemistry of the substituent at C-4 (Scheme 13). They suggested that the fragmentation outlined in Scheme 13 was more facile in the case of galactose because the C-4 acetate was axial and therefore could approach the C-2 acetate more closely. The proximity of the acetates was thought to enhance the rate of decomposition of the *m/z* 271 ion to the *m/z* 169 ion in the case of galactose.

3.3 Ammonia DCI MS of Some Peracetylated Oligosaccharides

The ammonia DCI spectra of the peracetylated oligosaccharides examined here are characterized by the same types of ions that were observed by Dougherty *et al.*[35], namely $[M+NH_4]^+$ ions, oxonium ions, hydrogen and acyl transfer ions (*i.e.* ions of the type illustrated in Fig. 5, p.26) and fragments resulting from losses of acetic acid and/or ketene from the aforementioned ions. The relative abundance of the hydrogen and acyl transfer ions is dependent on the structure and size of the oligomer. As the size of the oligomer increases there is a greater tendency for the formation of acyl transfer ions. However, the intensity of these ions is somewhat dependent on experimental conditions. Nevertheless, peracetylated carbohydrates are useful in the structure elucidation of

carbohydrates since the oxonium ions and the transfer ions present in the spectra of these carbohydrate derivatives provide sequence information.

In order to gain further insight into the fragmentation processes occurring under NH_3-DCI conditions we have examined the NH_3-DCI spectrum of octa-*O*-acetylgentiobiose (**4**) and the spectra of two isotopically-labelled octa-*O*-acetylgentiobioses (**5** and **6**). In compound **5** the system is labelled with trideuteroacetyl groups on the non-reducing moiety and in compound **6** with trideuteroacetyl groups on the reducing moiety (see Fig. 9). The presence of the deuterated acetates makes it possible to ascertain from which end of the disaccharide the ions observed in the spectra are derived. Some of the ions of interest, particularly the acyl transfer ions, are of low intensity in the spectra of the model compounds studied. In principle, either larger oligomers or other linkage isomers would have made better models; however, the compounds chosen (**5** and **6**) could be synthesized more easily than any of the compounds which exhibited more abundant ions.

3.3.1 Fragmentation of the Ammonium Adduct Ion of **4**, **5** and **6**

The spectra of **4**, **5**, and **6** are shown in Figure 10. The most abundant ion in each spectrum is the $[M+NH_4]^+$ ion which appears at *m/z* 696 (**4*a***) in the case of compound **4** and at *m/z* 708 in the spectra of **5** and **6**. MIKES experiments were performed on the $[M+NH_4]^+$ ion of **5** and **6** and the results are summarized in Scheme 14. Ion **5*a*** loses the elements of acetic acid and

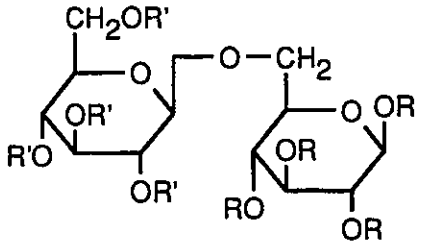

4. R = R' = CH_3CO
5. R = CH_3CO; R' = CD_3CO
6. R = CD_3CO; R' = CH_3CO

Figure 9. Peracetylated gentiobioses.

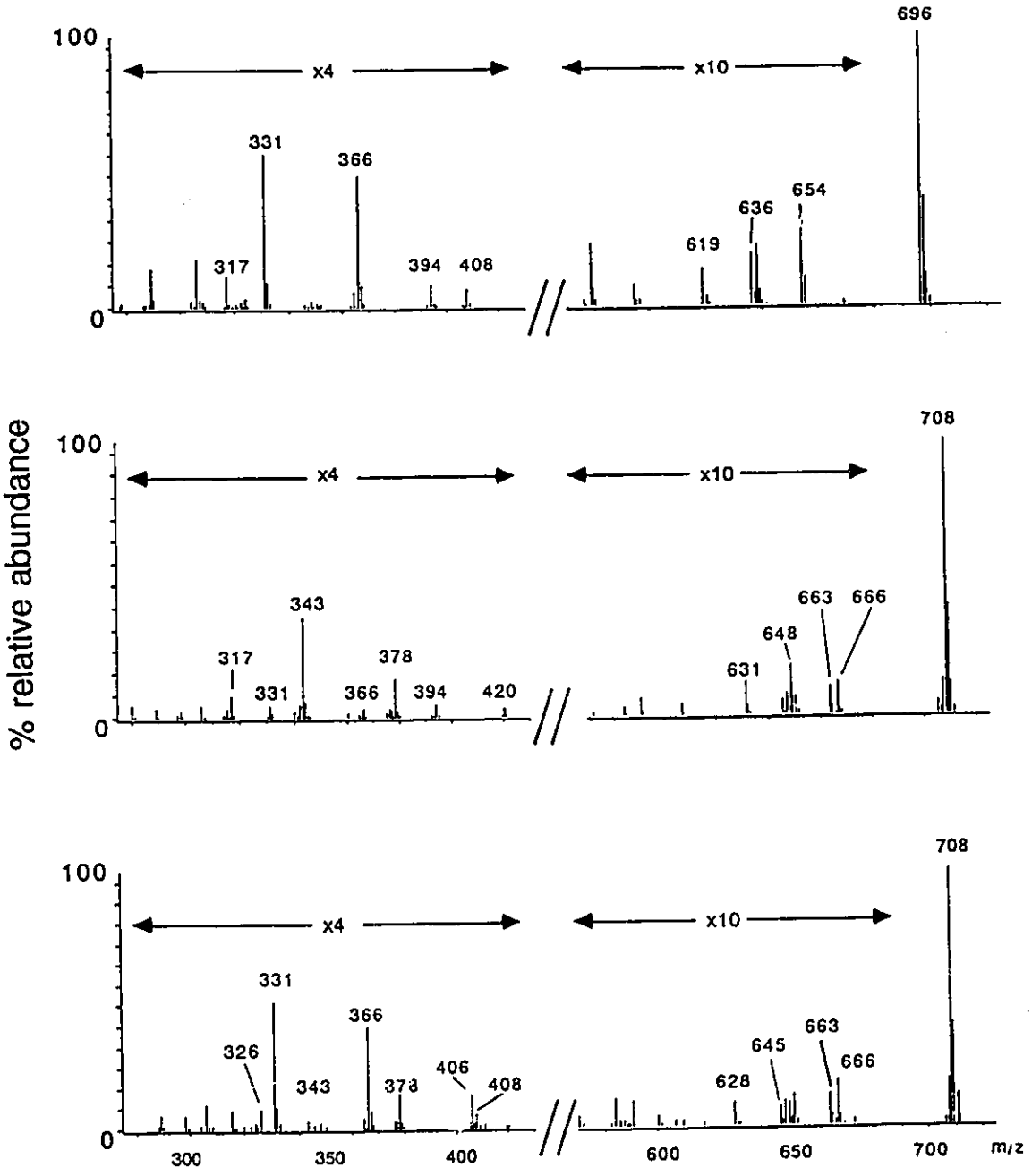

Figure 10. NH_3-DCI mass spectra of compounds **4**, **5**, and **6**.

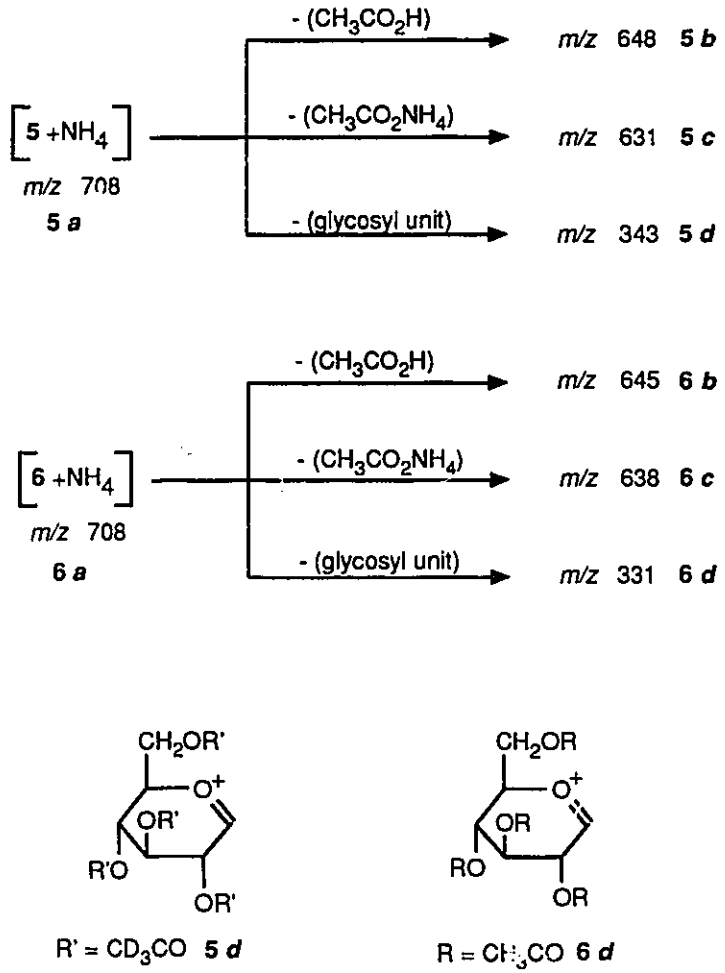
- (CH3CO2H)
m/z 648 5 b
[5 +NH4]
- (CH3CO2NH4)
m/z 631 5 c
m/z 708
5 a
- (glycosyl unit)
m/z 343 5 d
- (CH3CO2H)
m/z 645 6 b
[6 +NH4]
- (CH3CO2NH4)
m/z 638 6 c
m/z 708
6 a
- (glycosyl unit)
m/z 331 6 d
CH2OR'
O+
OR'
R'O
OR'
R' = CD3CO 5 d
CH2OR
O+
OR
RO
OR
R = CH3CO 6 d

Scheme 14

ammonium acetate to yield the ions at *m/z* 648 (**5*b***) and *m/z* 631 (**5*c***), respectively. There is no appreciable loss of acetic acid-d_3 or of the elements of ammonium acetate-d_3, suggesting that the ions in question are derived by losses almost exclusively from the reducing end of the molecule. The ion at *m/z* 343 (**5*d***) corresponds to the expected oxonium ion derived by fission at the glycosidic oxygen to yield the ion shown in Scheme 14. MIKES experiments indicate that the ions derived direct from the $[M+NH_4]^+$ ion of **6** include ions at *m/z* 645 (loss of CD_3CO_3H, **6*b***), *m/z* 628 (loss of the elements of $CD_3CO_2NH_4$, **6*c***) and *m/z* 331 (ion **6*d***). Once again the ions in question are derived by losses from the reducing end of the molecule indicating that there is little, if any, randomization of the acyl groups under the experimental conditions used in this study.

The spectrum of **5** exhibits also an ion at *m/z* 331, which is derived from the reducing end of the molecule. Its abundance relative to the ion at *m/z* 343 (**5*d***) is ~10%. MIKES experiments, both with and without collisional activation, provided no evidence that this ion (*m/z* 331) is derived from the $[M+NH_4]^+$ ion of **5**. This result suggest that the *m/z* 331 ion arises from a different precursor ion. An analogous ion is observed in the spectrum of **6** at *m/z* 343. Its intensity relative to that of *m/z* 331 (**6*d***) is also ~10%.

The spectrum of **4** exhibits ions at *m/z* 636 and *m/z* 619 which are derived from **4*a*** by the expected losses of acetic acid and the elements of ammonium acetate. The spectrum of **4** exhibits also an ion at *m/z* 331 which, in the light of the behaviour of **5** and **6**, is considered to be derived primarily, but not

exclusively, from the non-reducing end of **4**.

Ions corresponding to the loss of 42 mass units from the $[M+NH_4]^+$ ion of acetylated oligosaccharides have been attributed to the loss of ketene.[35] An ion is observed at *m/z* 654 (loss of 42 mass units from **4*a***) in the spectrum of **4** but, in the spectra of **5** and **6**, the ion at *m/z* 666 (loss of 42 mass units) is accompanied by an ion at *m/z* 663 (loss of 45 mass units); these ions therefore correspond to the respective replacement of CH_3CO and CD_3CO by H. Neither of these ions is observed in the MIKES spectra of the $[M+NH_4]^+$ ion of compounds **4**, **5** and **6**. The ions in question may arise from the addition of ammonium to a neutral species.

The losses of deuterated and undeuterated groups from **5** and **6** are approximately equal, indicating that the process is unlikely to involve a primary isotope effect, and that the loss is not specific to the reducing end of the molecule. The loss may be random and may be the result of ammonolysis of the acetates by the reagent gas and subsequent ionization of the neutral product. Ammonolysis of esters in NH_3-CIMS has been reported previously.[13,85]

3.3.2 Hydrogen Transfer Ions

The spectrum of **5** exhibits also ions at *m/z* 378 (**5*e***) and *m/z* 366 (**5*f***) (relative abundance ratio ~3:1). The difference in mass between these ions indicates that **5*e*** is derived from the non-reducing moiety and **5*f*** is derived from the reducing moiety. However, there is no evidence, either from MIKES or CA-

MIKES spectra, that these ions are derived from the $[M+NH_4]^+$ ion. The ions are assigned the structures shown in Scheme 15 and may formally be considered to arise from fission at either side of the glycosidic oxygen accompanied by attachment of a hydrogen and complexation with ammonium. Experiments in which ND_3 is used as the reagent gas confirm that these ions are ammonium ion complexes of a species with one labile proton; under these conditions there is a shift of 5 mass units to *m/z* 383 and *m/z* 371 for ions **5*e*** and **5*f***, respectively. Since the hydroxyl proton exchanges with the plasma it is not possible to determine whether ions **5*e*** and **5*f*** might arise from a mechanism involving inter- or intra-molecular H transfer.

In the spectrum of **6** the same ions are observed but the relative abundance of the ion at *m/z* 366 (**6*e***) is now greater than that at *m/z* 378 (**6*f***) ion. This result indicates that there is a greater tendency for cleavage of the glycosidic bond adjacent to the reducing sugar, namely, that fission at "x" predominates over fission at "y" (Scheme 15), although both process do occur. In the spectrum of **4** the peak at *m/z* 366 will consist of two ions corresponding in structure to ions **5*f*** and **6*e***.

MIKES experiments were performed on **5*e*** and **5*f*** and the results are summarized in Scheme 16. The ion at *m/z* 378 (**5*e***) suffers losses of 17 (*m/z* 361), 35 (*m/z* 343), 63 (*m/z* 315), and 80 mass units (*m/z* 298), attributed to the losses of NH_3, the elements of NH_4OH, CD_3CO_2H, and the elements of $CD_3CO_2NH_4$, respectively (Scheme 16).

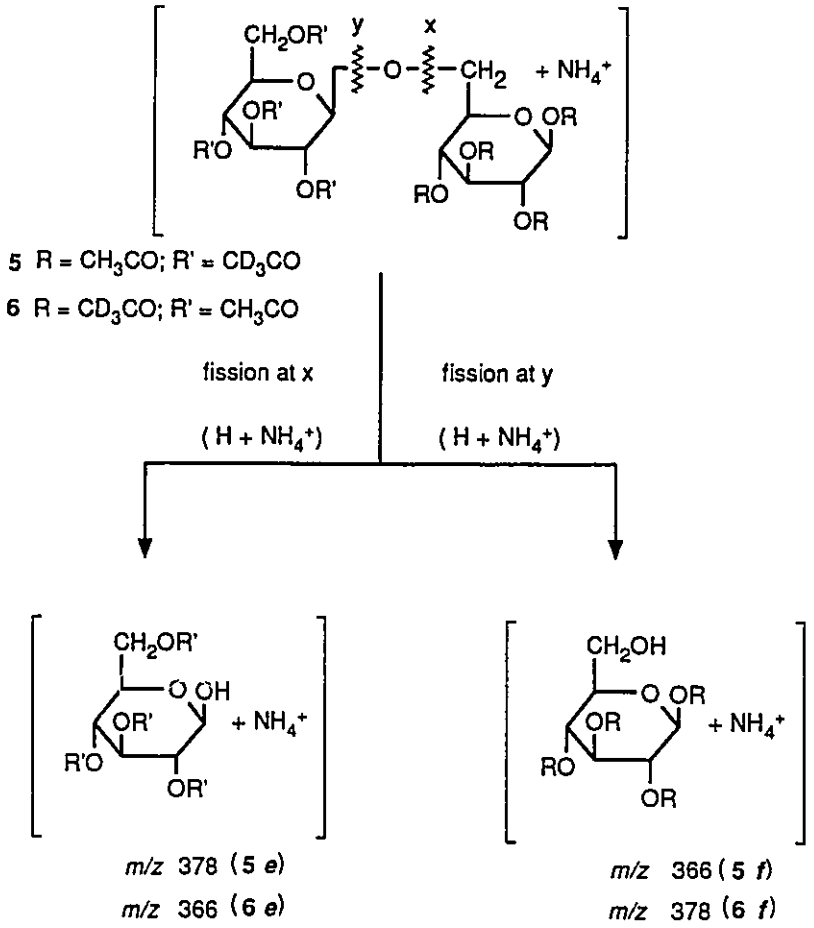
CH2OR'
y
x
O
OR'
R'O
OR'
O
CH2
+ NH4+
O OR
OR
RO
OR
5 R = CH3CO; R' = CD3CO
6 R = CD3CO; R' = CH3CO
fission at x
(H + NH4+)
fission at y
(H + NH4+)
CH2OR'
O OH
OR'
R'O
OR'
+ NH4+
CH2OH
O OR
OR
RO
OR
+ NH4+
m/z 378 (5 e)
m/z 366 (6 e)
m/z 366 (5 f)
m/z 378 (6 f)

Scheme 15

The ion corresponding to loss of the elements of NH_4OH was by far the most abundant, providing support for the contention that an OH group is situated at C-1 of **5*e***. MIKES experiments were performed on the ion at *m/z* 366 (**5*f***) also. An analogous series of losses were observed giving rise to ions at *m/z* 349 (NH_3), *m/z* 331 (NH_4OH), *m/z* 306 (CH_3CO_2H) and *m/z* 289 ($CH_3CO_2NH_4$). In the case of **5*f*** the loss of the elements of $CH_3CO_2NH_4$ was much greater than the loss of the elements of NH_4OH, indicating that the acetate that was lost in this process was probably situated at C-1 of **5*f***.

MIKES experiments performed on **6*e*** and **6*f*** are summarized in Scheme 17. The dominant ion (*m/z* 331) in the MIKES spectrum of **6*e*** arises by loss of the elements of NH_4OH, whereas the dominant ion (*m/z* 298) in the spectrum of **6*f*** arises by loss of the elements of $CD_3CO_2NH_4$. This result lends further support for the structures assigned to ions ***e*** and ***f***.

To confirm the assigned structures of ions ***e*** and ***f***, 2,3,4,6-tetra-*O*-acetyl-D-glucopyranose (**7**)[84] and 1,2,3,4-tetra-*O*-acetyl-D-glucopyranose (**8**)[84] were prepared and MIKES experiments were performed on their $[M+NH_4]^+$ ions. The MIKES spectra of ion **6*e*** and the $[M+NH_4]^+$ ion of **7** are shown in Figure 11 and those of ion **5*f*** and of the $[M+NH_4]^+$ ion of **8** in Figure 12. The spectra are virtually identical in each case, indicating that **6*e*** and **5*f*** likely have the same structure as the $[M+NH_4]^+$ ions of **7** and **8**, respectively. The origin of the peak at *m/z* 263 in the MIKES spectra of **6*e*** and **5*f*** has not been established. MIKES experiments, patterned after those of Ast *et al.*,[21] involving minor changes in the magnet setting

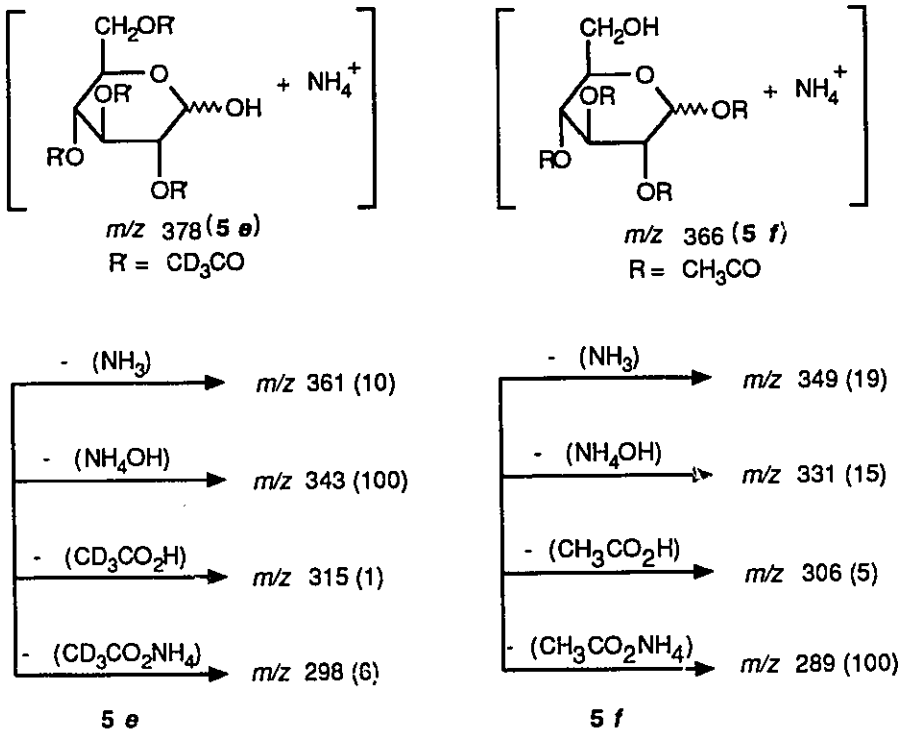
CH2OR
O
OR
OH
+ NH4+
RO
OR
m/z 378 (5 e)
R = CD3CO
CH2OH
O
OR
OR
+ NH4+
RO
OR
m/z 366 (5 f)
R = CH3CO
- (NH3)
m/z 361 (10)
- (NH4OH)
m/z 343 (100)
- (CD3CO2H)
m/z 315 (1)
- (CD3CO2NH4)
m/z 298 (6)
5 e
- (NH3)
m/z 349 (19)
- (NH4OH)
m/z 331 (15)
- (CH3CO2H)
m/z 306 (5)
- (CH3CO2NH4)
m/z 289 (100)
5 f

Scheme 16

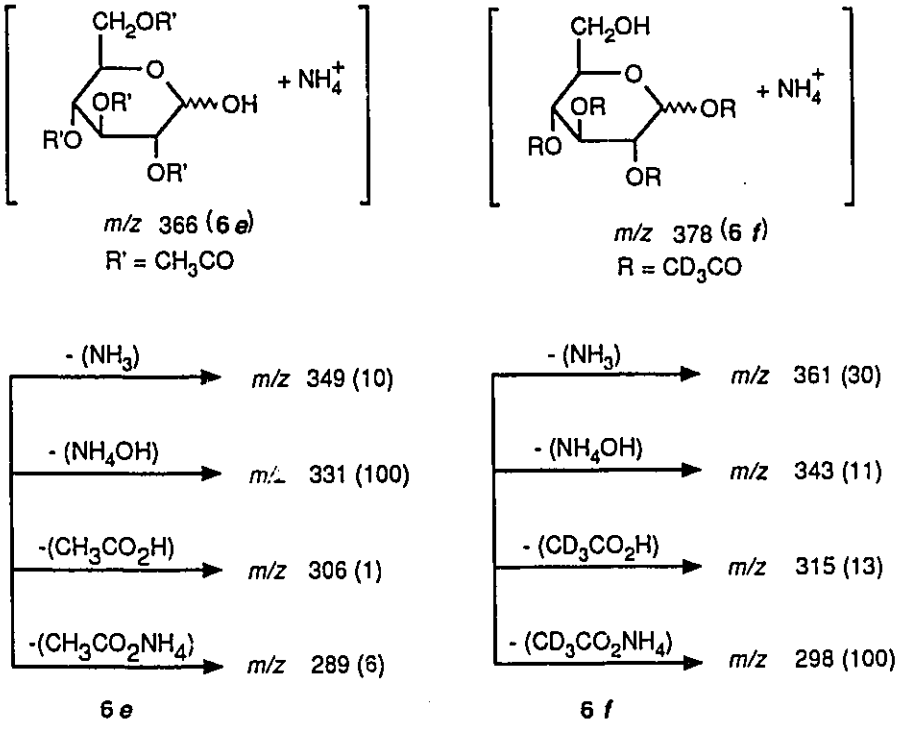
CH2OR'
O
OR'
OH
+ NH4+
R'O
OR'
m/z 366 (6 e)
R' = CH3CO
CH2OH
O
OR
OR
+ NH4+
RO
OR
m/z 378 (6 f)
R = CD3CO
- (NH3)
m/z 349 (10)
- (NH4OH)
m/z 331 (100)
-(CH3CO2H)
m/z 306 (1)
-(CH3CO2NH4)
m/z 289 (6)
6 e
- (NH3)
m/z 361 (30)
- (NH4OH)
m/z 343 (11)
- (CD3CO2H)
m/z 315 (13)
- (CD3CO2NH4)
m/z 298 (100)
6 f

Scheme 17

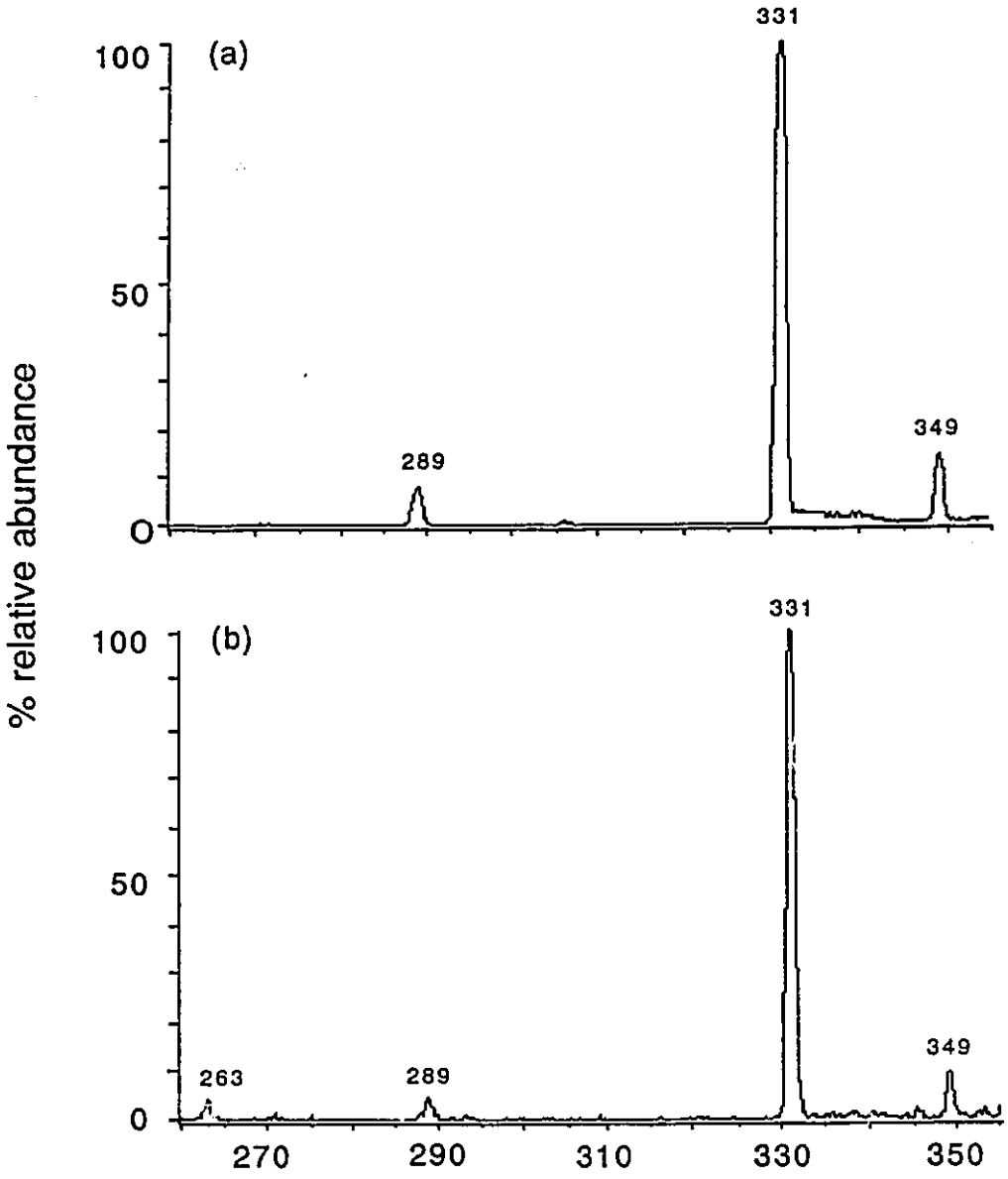

Figure 11. MIKES spectra of (a) the *m/z* 366 ion in the NH_3-DCI mass spectrum of 2,3,4,6-tetra-*O*-acetyl-D-glucopyranose and (b) ion **6*e***.

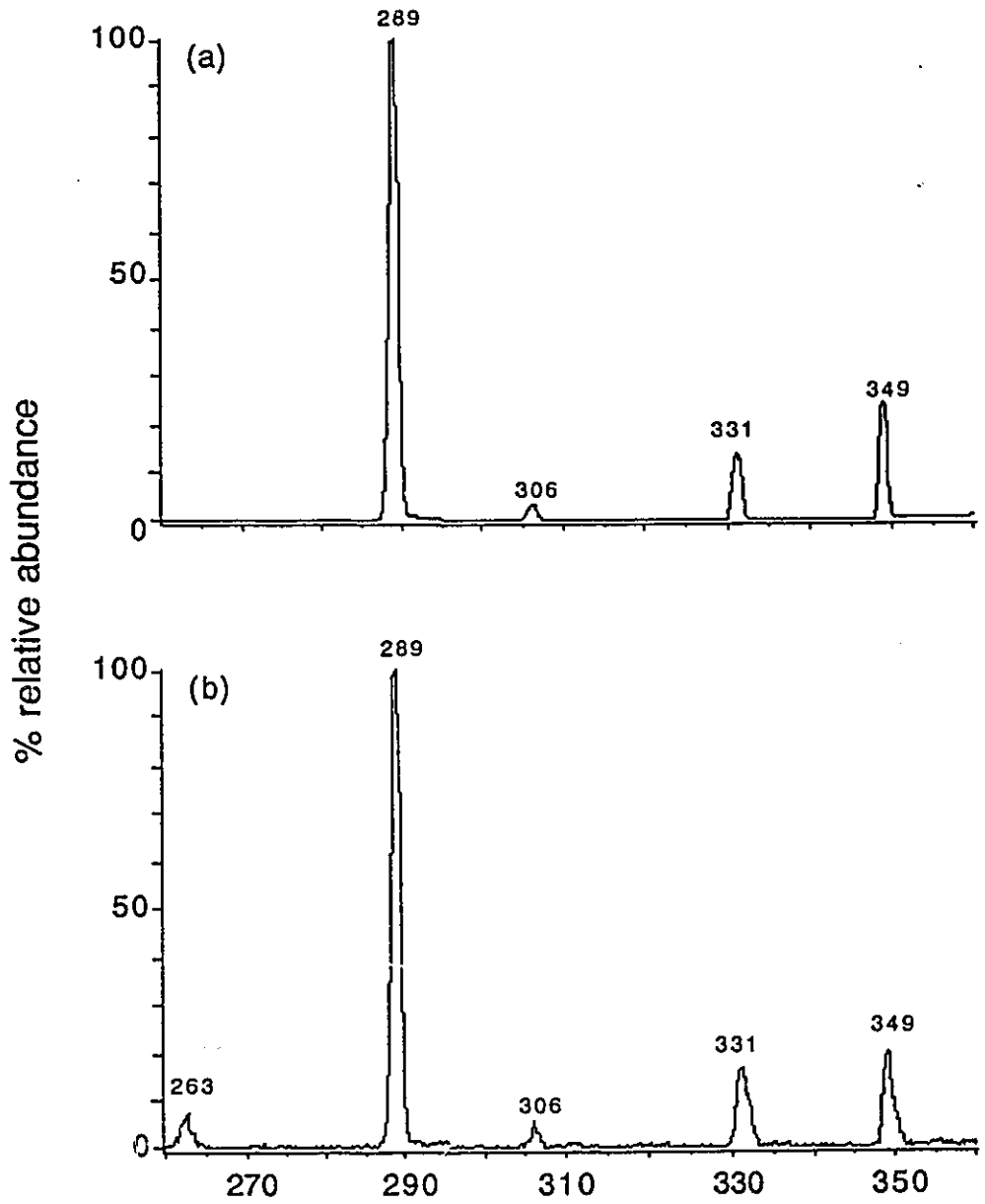

Figure 12. MIKES spectra of (a) the *m/z* 366 ion in the NH_3-DCI mass spectrum of 1,2,3,4-tetra-*O*-acetyl-D-glucopyranose and (b) ion **5*f***.

suggest that the *m/z* 263 ion is an artefact. The absence of a corresponding ion in the MIKES spectra of the deuterated analogues of **6*e*** and **5*f***, namely ions **5*e*** and **6*f*** suggests also that the *m/z* 263 ion is an artefact.

MIKES experiments have indicated that the $[M+NH_4]^+$ ion undergoes heterolytic cleavage at "y" (Scheme 18) to produce oxonium ion ***d***. Conservation of charge demands that a neutral species be produced in this process which might account for the formation of the hydrogen transfer ions ***f*** as shown in Scheme 18. However, there is no evidence in the MIKES spectra to suggest that heterolytic cleavage occurs at "x" to afford ions ***g***, a process which would indirectly afford hydrogen transfer ions ***e***. Nevertheless, ions corresponding in mass to ***d***, ***e***, ***f*** and ***g*** are all observed in the NH_3-DCI spectra. Heterolytic cleavage at "y" affords a more stable cation (***d***) than heterolytic cleavage at "x" (***g***) and should therefore predominate. However, hydrogen transfer ions ***e*** are more abundant than hydrogen transfer ions ***f***, a result which is contrary to what one might expect if the hydrogen transfer ions were formed exclusively by heterolytic cleavage of the glycosidic bonds. Therefore, there may be another more important process, in addition to heterolytic cleavage of a glycosidic bond, which results in the formation of the hydrogen transfer ions. The nature of this process has not been determined; however, it seems likely that it involves one or more neutral intermediate species since the formation of the hydrogen transfer ions could not be detected by MIKES.

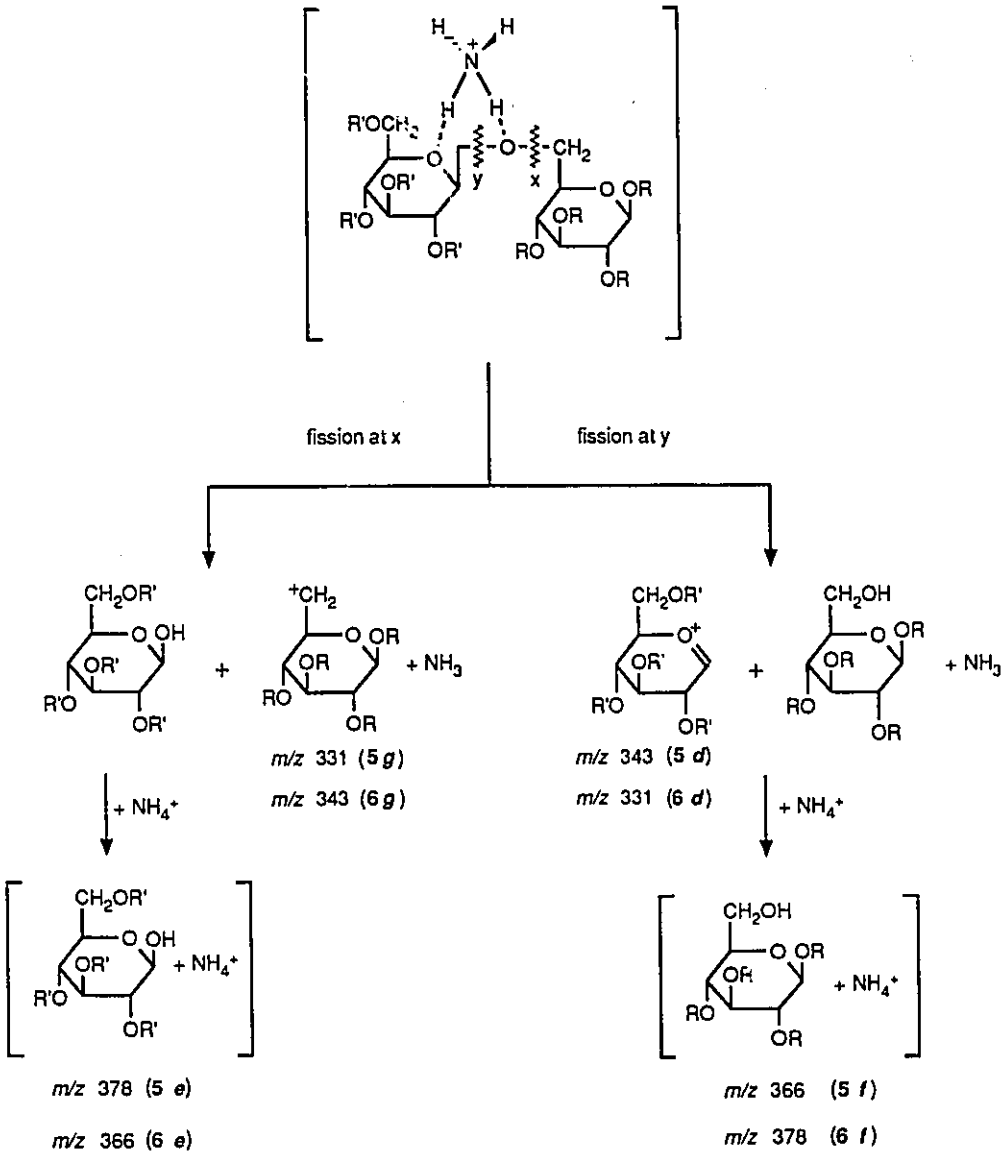
fission at x
fission at y
+ NH3
+ NH4+
m/z 331 (5 g)
m/z 343 (6 g)
m/z 343 (5 d)
m/z 331 (6 d)
m/z 378 (5 e)
m/z 366 (6 e)
m/z 366 (5 f)
m/z 378 (6 f)

Scheme 18

3.3.3 Acyl Transfer Ions

The ion at *m/z* 408 which is present in the NH_3-CI mass spectra of many peracetylated oligosaccharides[35] has been considered to be structurally similar to the $[M+NH_4]^+$ ion of 1,2,3,4,6-penta-*O*-acetyl-β-D-glucopyranose (**1**). The MIKES spectrum of the ion at *m/z* 408 in the spectrum (**4**) is virtually identical with that of the $[M+NH_4]^+$ ion of (**1**), indicating that they are likely of the same structure.

Acyl transfer ions, such as the one at *m/z* 408 in the spectrum of **4**, may formally be considered to arise by cleavage of the bond on either side of the glycosidic oxygen accompanied by attachment of an acyl group and complexation with ammonium. Experiments employing ND_3 as the reagent gas shift the *m/z* 408 ion to *m/z* 412, thereby confirming that it is an ammonium adduct ion.

In principle, **5** and **6** may each form four acyl transfer ions; ions ***h***, ***i***, ***j***, and ***k*** (Scheme 19). However, the spectrum of **5** exhibits only ion **5*h*** and the spectrum of **6** exhibits only ions **6*h***, **6*i***, and **6*j*** in a relative abundance of 5:2:1. The reason for the absence of the acyl transfer ions that could in principle be formed has not been established.

The spectrum of **5** exhibits an acyl transfer ion derived from the non-reducing end of the molecule only and in the case of **6** the acyl transfer ions derived from the non-reducing end (**6*h*** and **6*j***) are more abundant than the acyl transfer ion derived from the reducing end (**6*i***), thereby suggesting that acyl transfer ions are formed primarily, but not exclusively, by cleavage at "x" (Scheme 19) and transfer of an acyl group to the non-reducing end of the molecule.

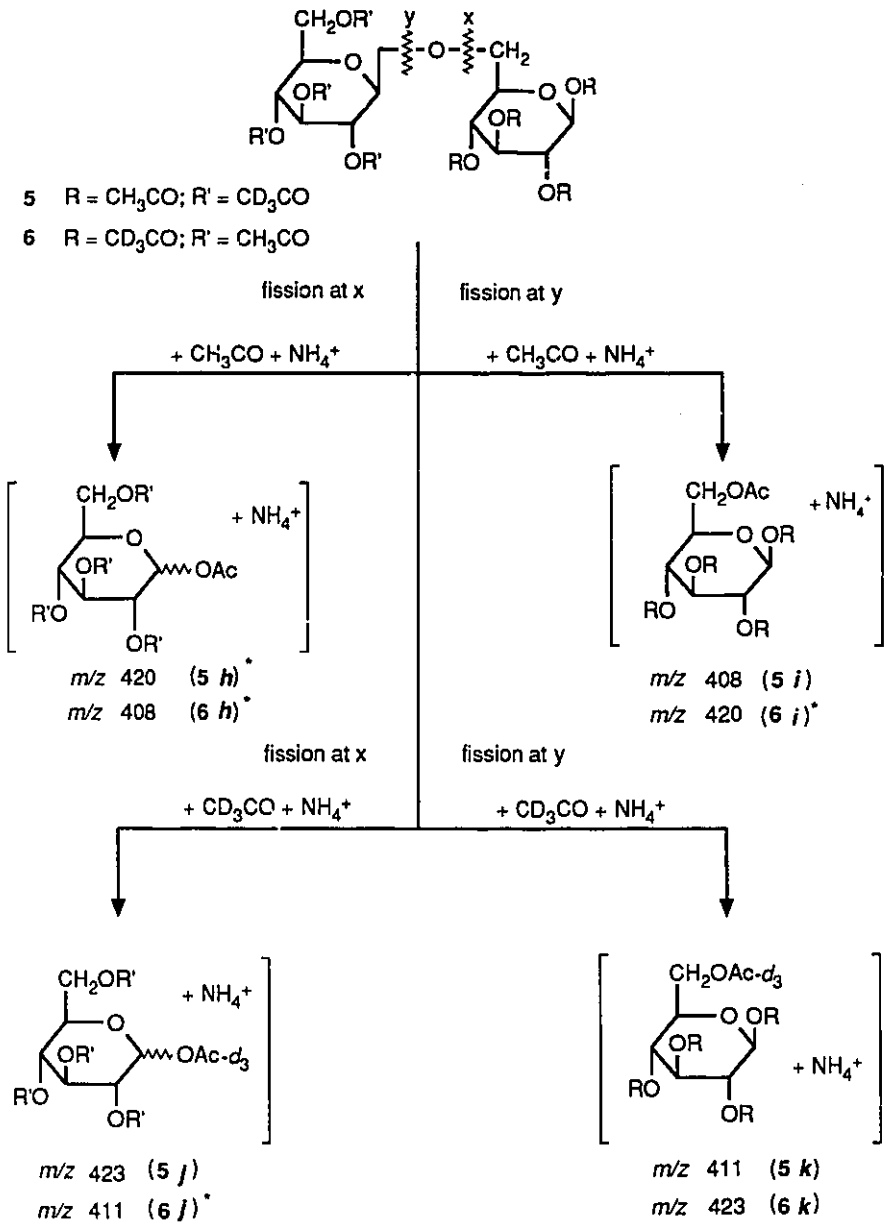

* ions observed in the spectra of **5** and **6**

Scheme 19

Only **5*h*** was sufficiently abundant to allow the acquisition of a clean MIKES spectrum. The dominant ion in the MIKES spectrum of **5*h*** was at *m/z* 343 corresponding to the loss of the elements of $CH_3CO_2NH_4$. This result suggests that the transferred acyl group was located at C-1 of **5*h***.

Ions **6*h*** and **6*j*** are separated by three mass units. This indicates that the acyl group that was transferred retains all of the hydrogen atoms (or deuterium atoms) that were attached to it before the transfer took place. Thus, the acyl transfer ions cannot be formed by the addition of ketene to a hydrogen transfer ion; addition of CD_2CO would afford an ion at *m/z* 410 instead of *m/z* 411 (**6*h***).

Two other processes that might account for the formation of the acyl transfer ions include the addition of an acetate ion to the ions at *m/z* 331 or *m/z* 343 and subsequent complexation by ammonium, or transesterification of a fragment containing a free hydroxyl (Scheme 20). These processes might be differentiated by examination of the NH_3-DCI mass spectrum of ^{18}O-labelled gentiobiose (**9**).

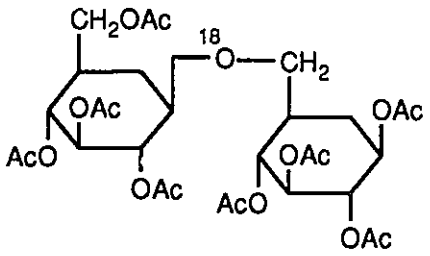

9

The ^{18}O-labelled glycosidic oxygen would not be incorporated into the acyl transfer ions if their formation involved the addition of an acetate to a cation. Alternatively,

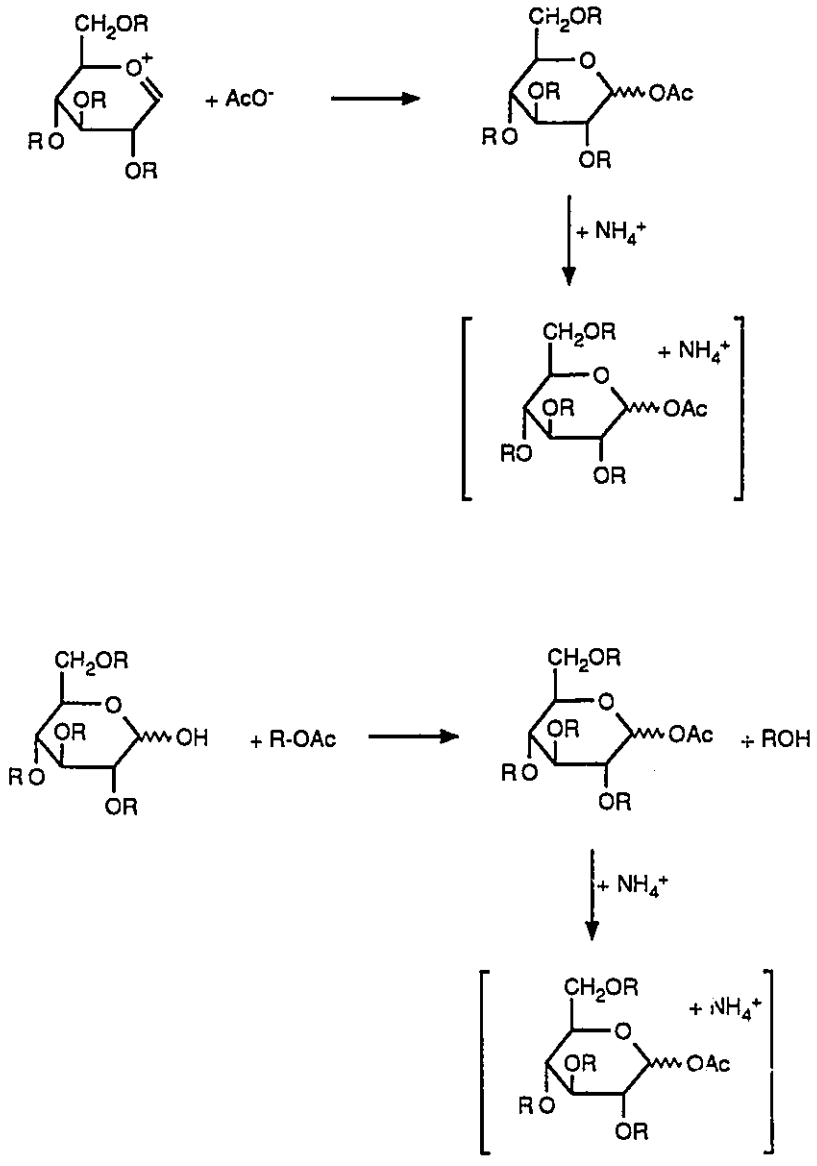

Scheme 20

a process involving the transesterification of a hydrogen transfer ion should not result in the loss of the labelled glycosidic oxygen, thereby resulting in a shift of the acyl transfer ions. The synthesis of **9** is being undertaken by Professor W.A. Szarek of Queen's University, Kingston, and it will be analyzed subsequently.

3.3.4 Ring Fragmentation of Peracetylated Oligosaccharides

A fragmentation of underivatized oligosaccharides that has been observed in FAB mass spectra,[4,52] in the NH_3-CI mass spectra of *O* -methylated oligosaccharides[5,6] and in the EI spectra of some peracetylated disaccharides[27,28,30] is also operative in the NH_3-DCI spectra of peracetylated oligosaccharides (Scheme 21). The $[M+NH_4]^+$ ions are postulated to undergo a ring fragmentation in the non-reducing moiety to afford ions ***l***, which in NH_3-DCI spectra appear as ammonium adducts. However, these ions are not observed in MIKES experiments on the $[M+NH_4]^+$ ions of **4**, **5**, or **6** and, like the acyl and hydrogen transfer ions, must be formed indirectly from $[M+NH_4]^+$ or from the neutral molecule. Ions ***l*** are converted through loss of ammonium acetate from **4** and **5** and through loss of ammonium trideuteroacetate from **6** into the oxonium ions ***m***. The masses of ions ***l*** and ***m*** derived from **4**, **5** and **6** (see Scheme 21) clearly indicate that the reducing moiety of the disaccharide is preserved in the fragment ions. Furthermore, the shift in mass from *m/z* 394 in the spectra of **4** and **5** to *m/z* 406 in the spectrum of **6** is consistent with the proposed structure of ion ***l***. Similarly the shift in mass of the *m/z* 317 ion to *m/z* 326 is consistent with the proposed structure of ion ***m***.

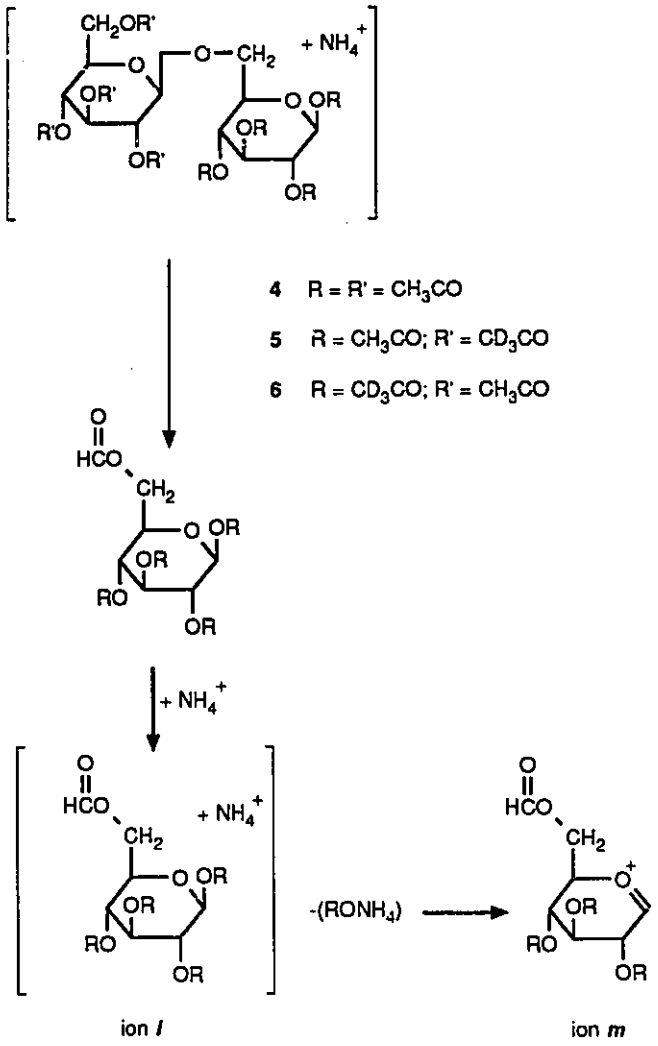

	m/z		
	4	**5**	**6**
$[M + NH_4]^+$	696	708	708
ion *l*	394	394	406
ion *m*	317	317	326

Scheme 21

Ions *l* may be formed in a reductive process (reductions of some functional groups are known to occur under NH_3-DCI conditions[86-90]). Addition of an electron to the $[M+NH_4]^+$ ion might result in the production of a number of neutral species as shown in Scheme 22. Addition of ammonium to the glycosyl unit that survives intact could then afford ion *l*. $[M+NH_4]^+$ ions of the other fragments produced on fragmentation of the ring are not observed in the spectra of **4**, **5** and **6**, possibly because they do not undergo efficient re-ionization. The mechanism differs from that proposed for formation of the same ion under EI-MS conditions (Scheme 5, p.22). Support for the mechanism in Scheme 22 might be provided by examination of the NH_3-DCI mass spectrum of a disaccharide in which the ring oxygen of the non-reducing moiety has been labelled with ^{18}O. In the mechanism proposed in Scheme 5 it was postulated that the non-reducing ring oxygen is lost on ring fragmentation, but the oxygen would be retained if the mechanism in Scheme 22 is correct.

3.4 Linkage Differentiation in Peracetylated Disaccharides

The determination of the position of linkage between the glycosyl units of oligosaccharides by mass spectrometry has been an area of widespread interest.[41-52] The presence of ions of type ***m-p*** at *m/z* 317 in the mass spectra of peracetylated disaccharides makes possible a new method for the determination of the position of linkage between the glycosyl units through the use of MIKES experiments on those ions. The ions at *m/z* 317 are labelled with a formyl group

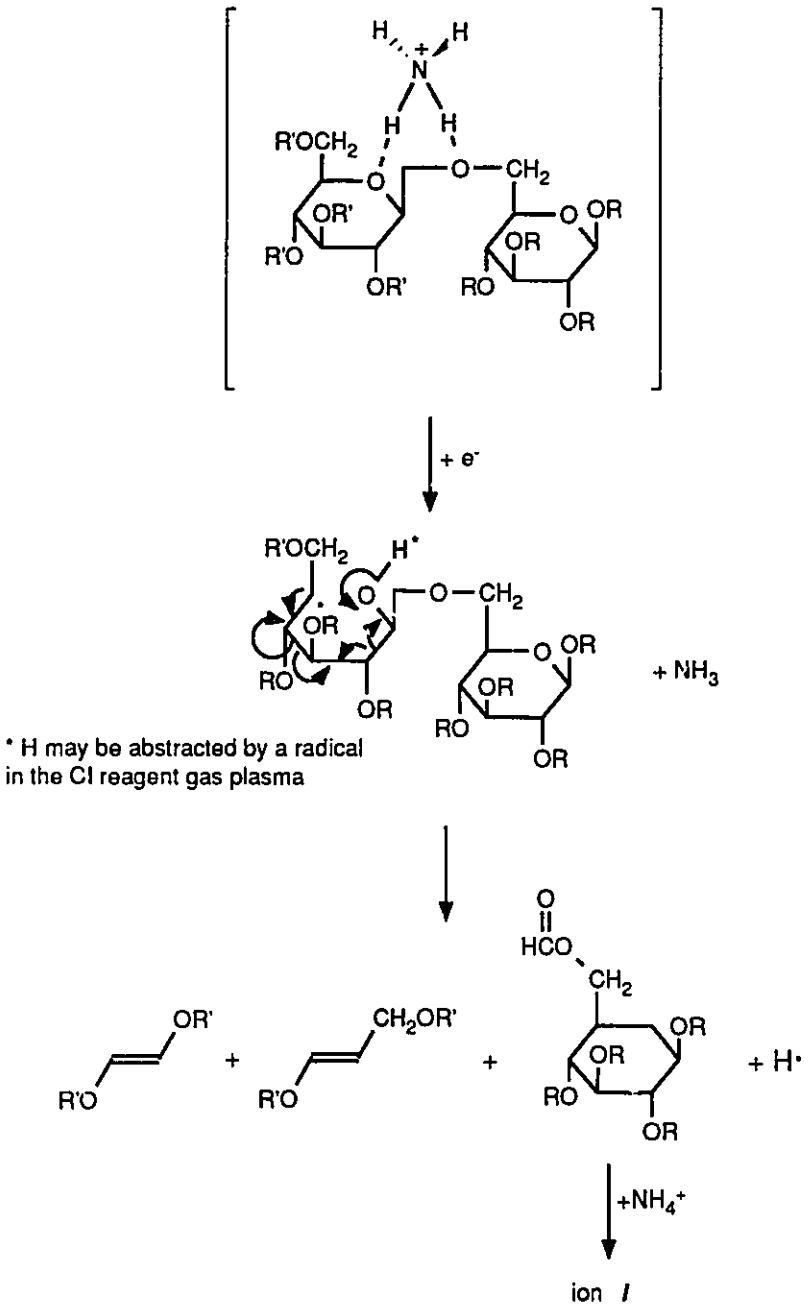
+ e⁻
+ NH3
* H may be abstracted by a radical
in the CI reagent gas plasma
+NH4+
ion I

Scheme 22

at the position of linkage between the two glycosyl units as shown in the structures ***m-p***, derived from (1→6), (1→4), (1→3), and (1→2)-linked disaccharides, respectively. The (1→1)-linked disaccharides cannot form an ion of this type and may therefore be differentiated from their linkage isomers by the absence of an *m/z* 317 ion in their mass spectra.

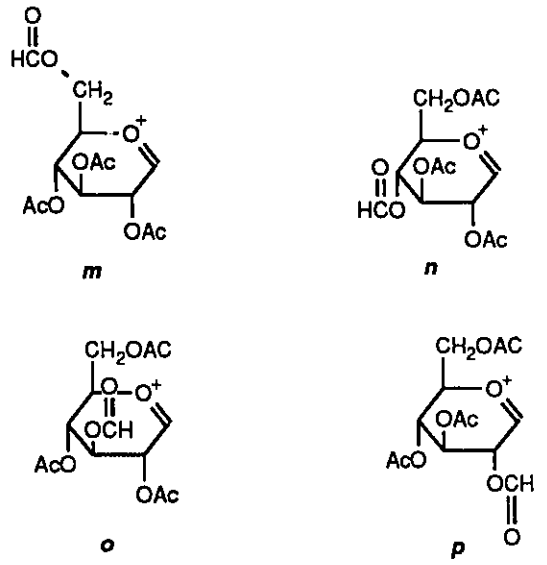

It has been demonstrated that there is a preferred sequence of losses of acetic acid and ketene from the oxonium ion (***d***) of peracetylated glucopyranoses.[23,25,39] It was therefore anticipated that the MIKES spectra of ions ***m-p*** would be distinct. Accordingly, compounds **4** and **10** to **15** were synthesized and the MIKES spectra of the *m/z* 317 ion in their NH_3-DCI mass spectra were acquired and examined. GC analysis of compounds **10** to **15** indicated that they contained some impurities. However, GC and MS analyses indicated that the impurities were all of low molecular weight and unlikely to interfere in the MIKES analyses on the *m/z* 317 ion. Since the work of Kondrat and Cooks[91] indicated

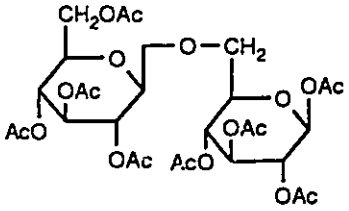

4

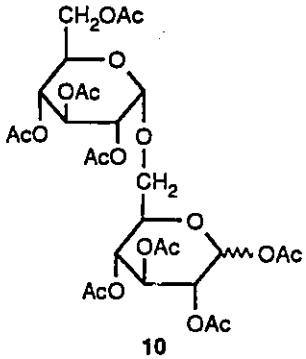

10

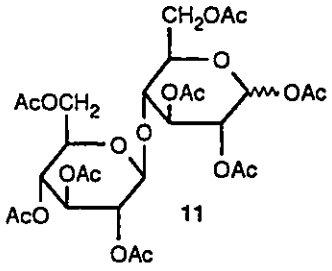

11

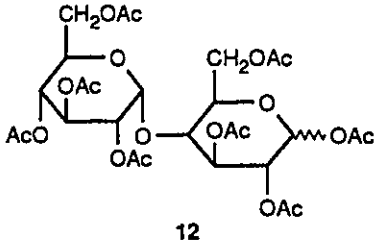

12

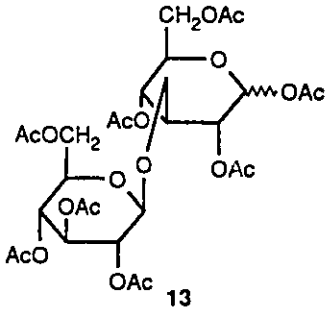

13

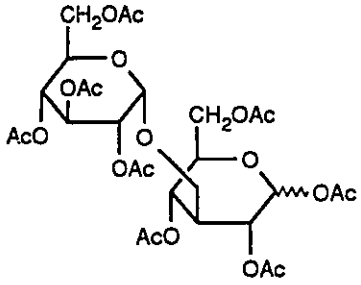

14

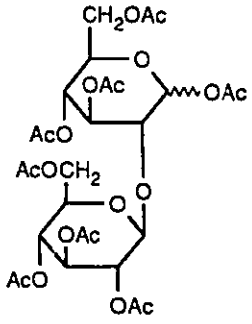

15

that it was possible to use MIKES to analyze a particular ion generated from a mixture of compounds the analysis was done without further purification of the acetylated disaccharides. The same arguments hold for the mannose and galactose disaccharides (compounds **16-21**).

Initially NH_3-DCI was used to generate the ions at *m/z* 317 for study by MIKES experiments. However, DEI yielded more abundant *m/z* 317 ions. The MIKES spectra could be acquired routinely in the DEI mode using only 20 μg of sample whereas 60 μg of sample were sometimes required when NH_3-DCI was employed. An example of the CA-MIKES spectra obtained on the ion at *m/z* 317 under NH_3-DCI and DEI conditions is given in Figure 13 for the case of peracetylated laminaribiose. Aside from the artefacts in the NH_3-DCI spectra the two spectra are similar, lending support to the contention that this ion has the same structure whether generated under DEI or NH_3-DCI conditions.

In Figure 14 the MIKES spectra of the ions at *m/z* 317 derived from the DEI spectra of **4** and **10-15** are shown. The spectra are sufficiently different to enable one to assign linkage positions by visual examination. The (1→3)-linked isomers, **13** and **14**, are unique because of the intense ion at *m/z* 271 in their spectra. The (1→4)-linked isomers, **11** and **12**, can be differentiated from the (1→6)-linked isomers, **4** and **10**, by virtue of the intense ion at *m/z* 169 in the former pair. Finally, the (1→2)-linked isomer, **15**, can be distinguished from the (1→6)-linked isomers because of the intense ion at *m/z* 169 in its spectrum and from the (1→4)-linked isomers because of the much more intense ion at *m/z* 197.

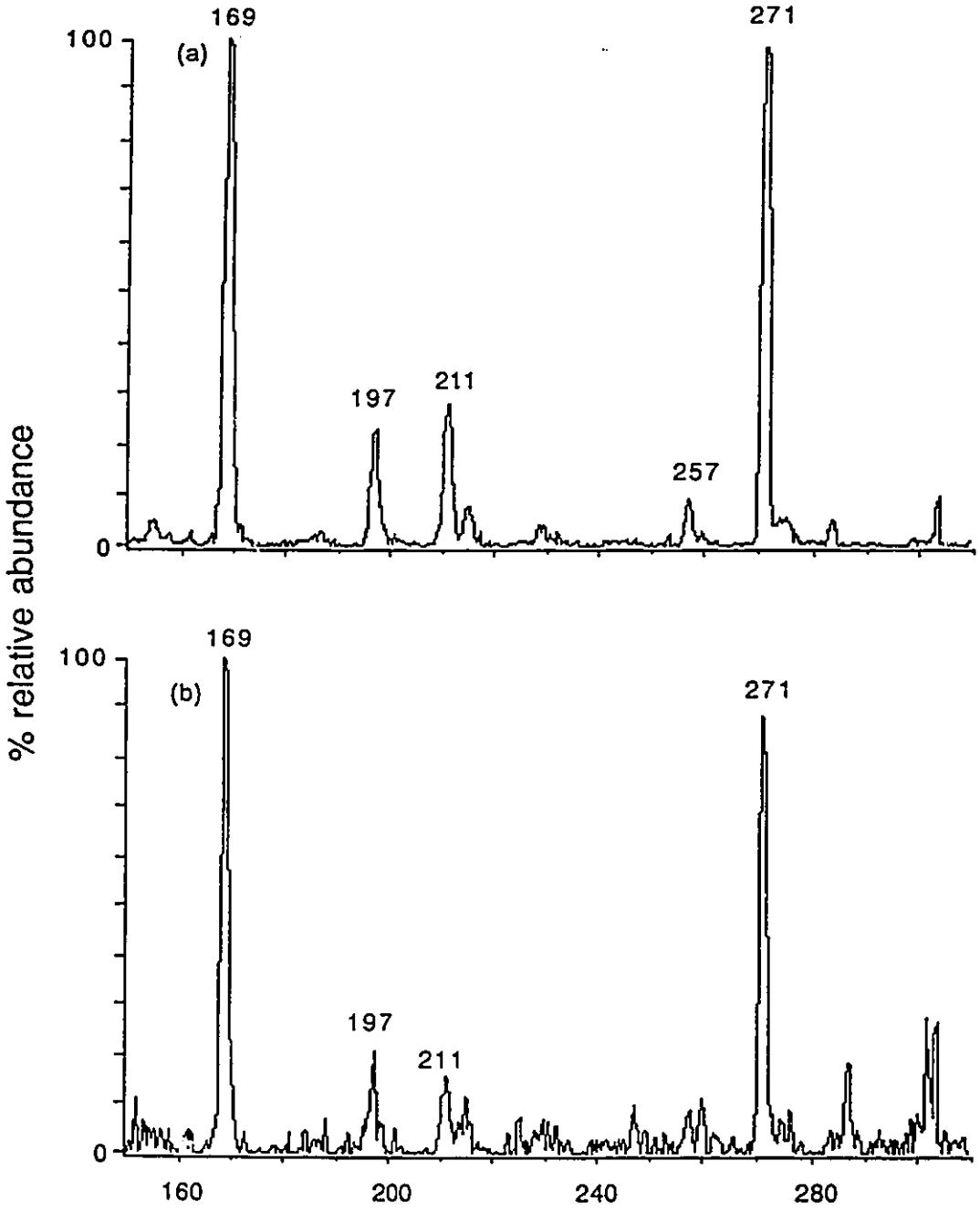

Figure 13. CA-MIKES spectra of the *m/z* 317 ion in the spectrum of **13** under (a) DEI conditions and (b) NH_3-DCI conditions.

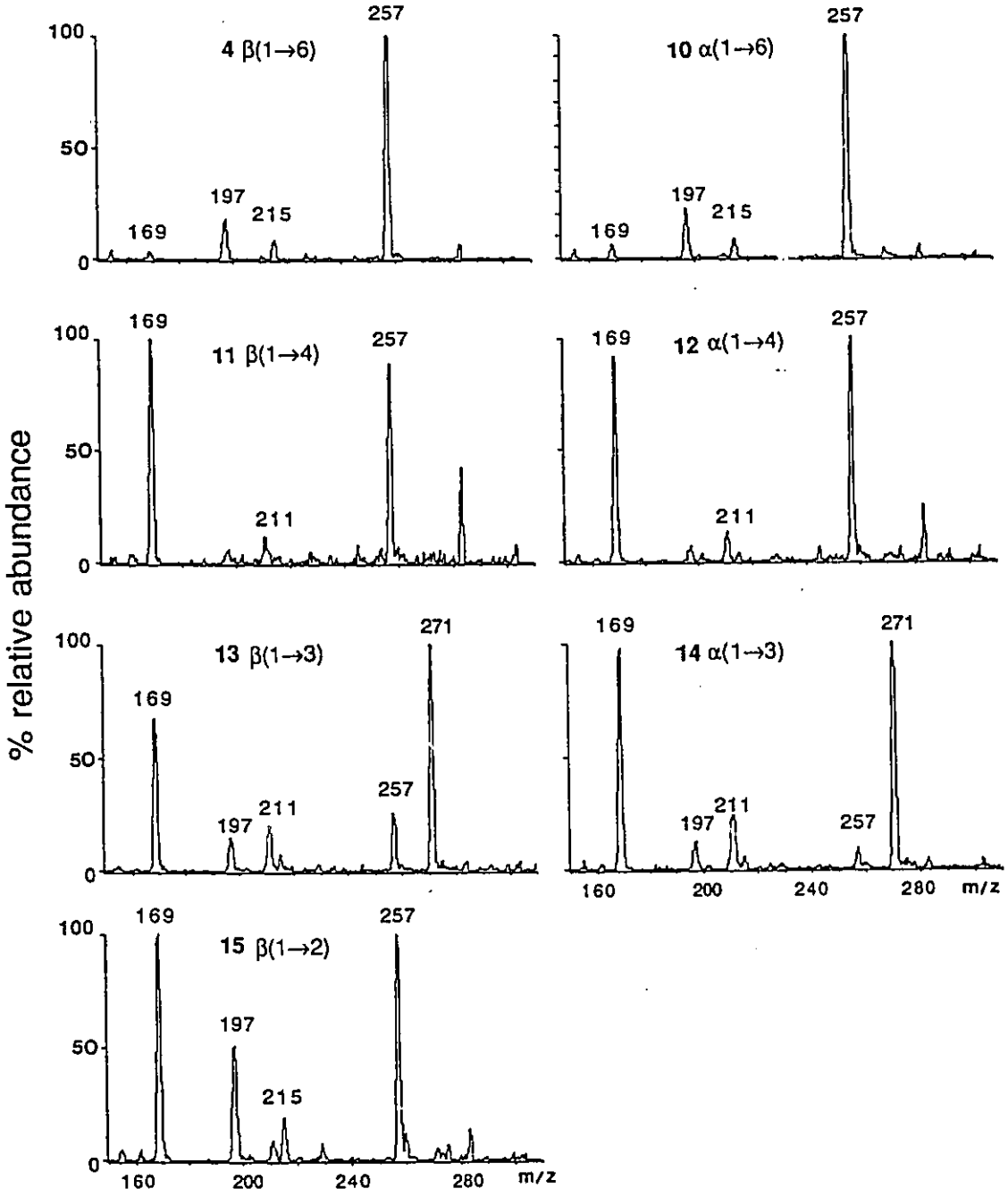

Figure 14. MIKES spectra of the *m/z* 317 ion in the DEI spectra of compounds **4** and **10-15**.

However, the spectra do not discriminate between isomers differing in configuration at the glycosidic centre, e.g. between **4** and **10**, or **11** and **12**, or **13** and **14**. The spectra of the (1→6)-linked isomers, **4** and **10**, are virtually the same; also the spectra of the isomeric pairs, **11** and **12**, and **13** and **14**, are very similar.

In order to explore the versatility of this technique the *m/z* 317 ions in the DEI mass spectra of compounds **16-23** were also examined by MIKES. The MIKES spectra of the *m/z* 317 ions of compounds **16-21** are shown in Figure 15. The fact that compounds **16-19** are methyl glycosides was not expected to affect the MIKES spectra of their *m/z* 317 ions since the substituent at C-1 of the reducing end of the disaccharide is lost in the formation of the ions at *m/z* 317. The anomeric configuration of the reducing moiety should have little effect on the MIKES spectra for the same reason.

The MIKES spectra of the four mannose disaccharides are again distinct (Fig. 15). The (1→6)-linked compound (**16**) has only one abundant ion which is at *m/z* 257. This distinguishes it from the (1→4)-linked compound (**17**) which has its only abundant ion at *m/z* 169. The (1→3)-linked isomer (**18**) is unique in that it is the only isomer to display an abundant *m/z* 271 ion in its MIKES spectrum. Finally, the MIKES spectrum derived from the *m/z* 317 ion in the DEI spectrum of the (1→2)-linked isomer (**19**) exhibits three relatively abundant ions at *m/z* 257, 197, and 169 which differentiates this isomer from the other three.

The MIKES spectra (Fig. 15) derived from the *m/z* 317 ions in the NH_3-DCI mass spectra of the two galactose disaccharides (**20**, (1→6)-linked and **21**,

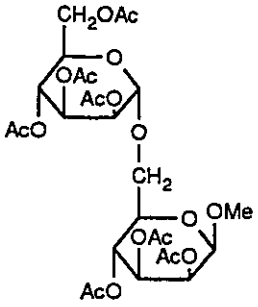

16

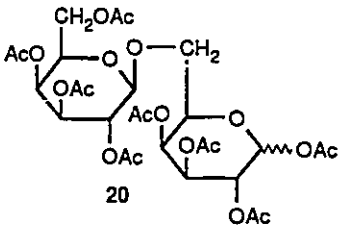

20

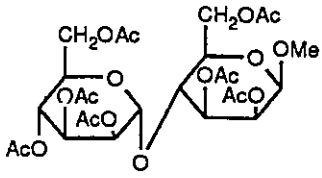

17

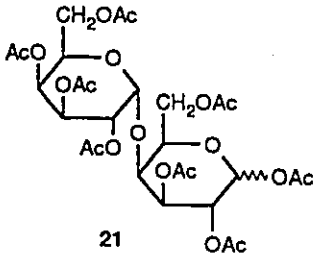

21

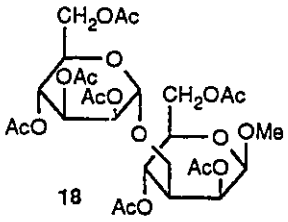

18

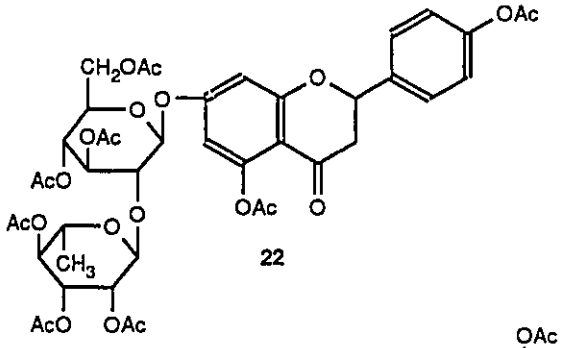

22

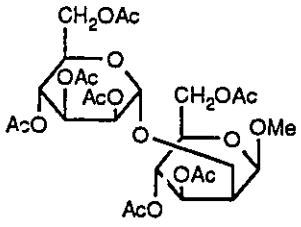

19

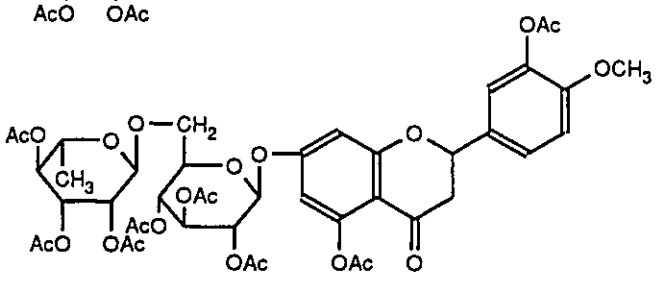

23

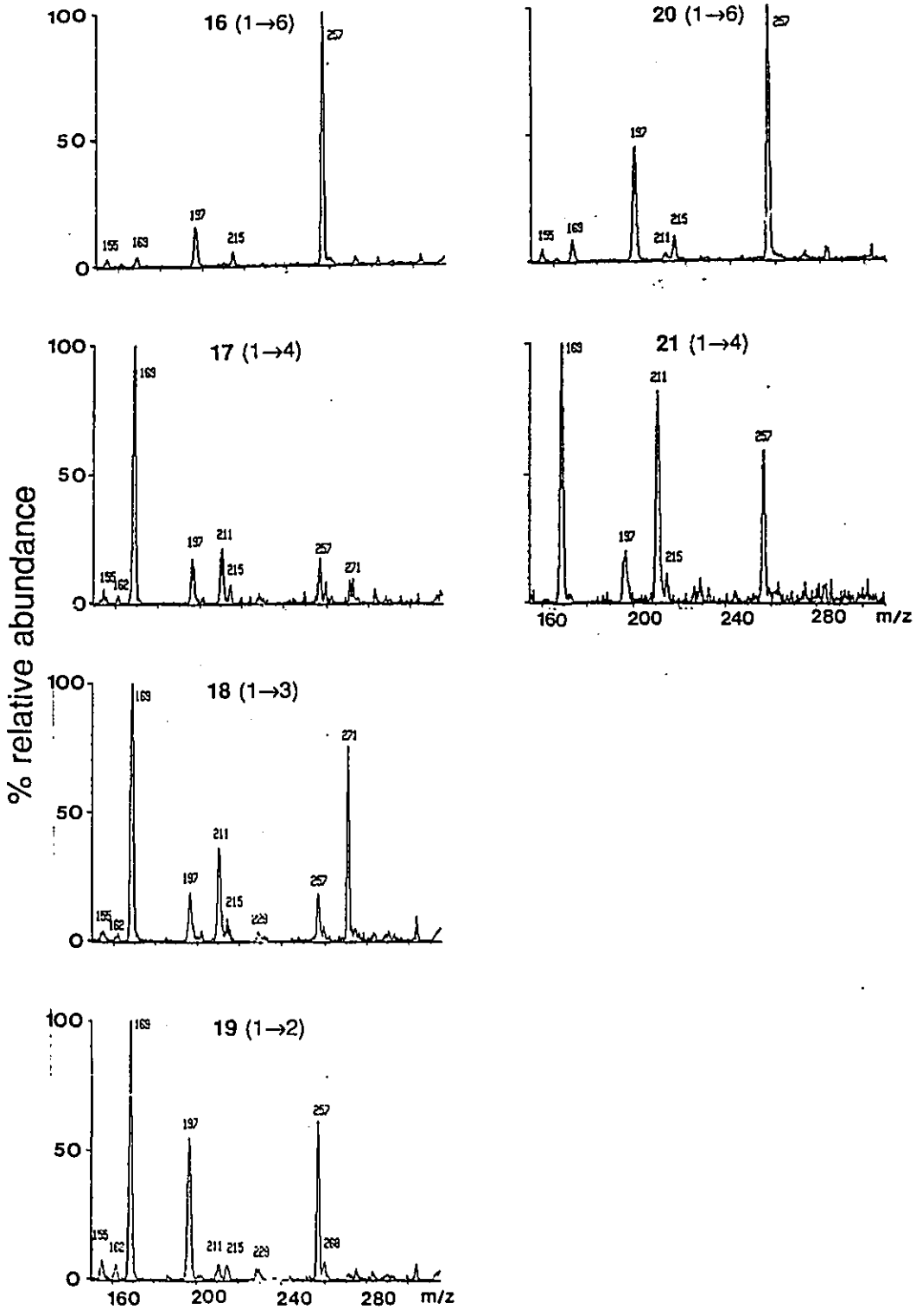

Figure 15. MIKES spectra of the *m/z* 317 ion in the DEI mass spectra of mannose disaccharides **16-19** and galactose disaccharides **20** and **21**.

(1→4)-linked) may be distinguished from each other also. It therefore seems likely that it will be possible to distinguish the four linkage isomers of this disaccharide series.

The MIKES spectra of the *m/z* 317 ions in the DEI mass spectra of compounds **22** and **23** are shown in Figure 16. The spectra are complicated by the presence of artefacts (as determined by making small changes in the magnet setting[21]). However, comparison of the relative abundance of the "real" MIKES ions with those in the MIKES spectra obtained from the glucose disaccharides shows that the MIKES spectrum derived from **22** closely matches that of the (1→6)-linked isomer and the MIKES spectrum derived from **23** closely matches that of the (1→2)-linked isomer. The MIKES spectra of the *m/z* 317 ions in the DEI spectra of **22** and **23** can therefore be used to assign the position of linkage between the glycosyl units in these glycosides.

The peaks appearing in the MIKES spectra of the *m/z* 317 ions may be accounted for in terms of losses of acetic acid, formic acid, ketene, and carbon monoxide. The various losses appear to follow the pattern postulated by Guevremont and co-workers[37-39] for the elimination of acetic acid and ketene from oxonium ion (***d***). Thus, the first loss appears to involve the elimination of the substituent at C-3 to afford a double bond between C-2 and C-3. This loss always gives rise to an abundant ion (for **4** and **10-15**) and in the case of the (1→3)-linked compounds (**13** and **14**) involves the loss of formic acid to afford the abundant *m/z* 271 ion that is unique to that isomer. In the case of the (1→3)-linked isomers (**13**

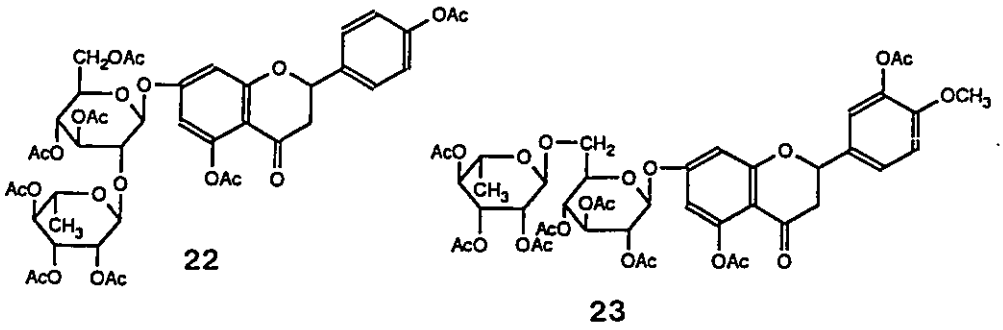

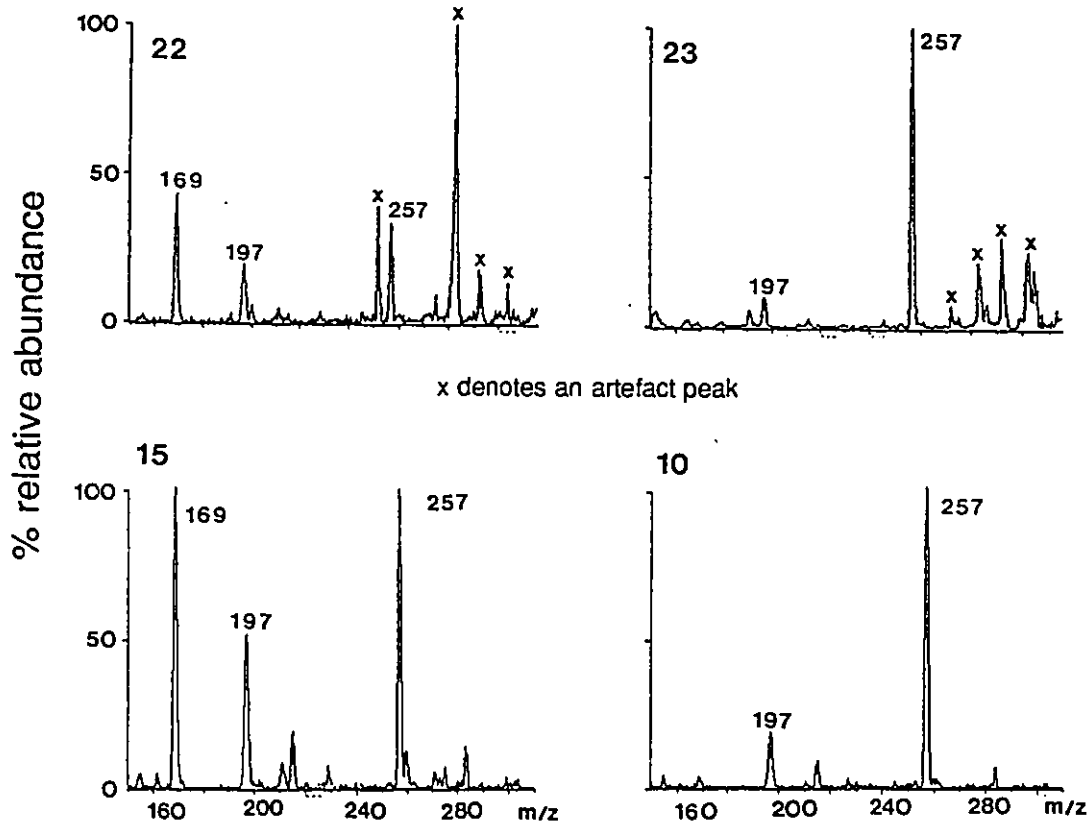

Figure 16. MIKES spectra of the *m/z* 317 ion in the DEI mass spectra of compounds **22**, **23**, (1→2)-linked glucose disaccharide (**15**) and (1→6)-linked glucose disaccharide (**10**).

and **14**) there is also a significant *m/z* 257 ion (corresponding to elimination of acetic acid), so in this isomer there is a loss from a position other than C-3 of the *m/z* 317 ion. Only the MIKES spectra of the (1→3)-linked isomers exhibit any evidence that there is competition with the elimination of the C-3 substituent of the *m/z* 317 ion, suggesting that the elimination of formic acid is less facile than that of acetic acid.

Subsequent fragmentation appears to proceed along three principal pathways (although other pathways may be operative also), in analogy with the processes described by Guevremont *et al.*,[39] as shown in Schemes 23-26 for the (1→6)-, (1→4)-, (1→3)-, and (1→2)-linked isomers, respectively. Pathway A involves the elimination of the substituent at C-2 to afford a carbonyl at that position. Pathway B entails the simultaneous elimination of the substituents at C-2 and C-4 in a manner analogous to that proposed by Guevremont and Wright[38] (Scheme 13, p.64). Pathway C involves elimination of the C-4 substituent to afford a double bond between C-4 and C-5.

In the case of the fragmentation of the *m/z* 257 ion derived from the (1→6)-linked isomers (**4** and **10**) all three pathways (Scheme 23) are operative. Pathway C, involving the loss of acetic acid to afford the ion at *m/z* 197, is most important and pathway B, involving the simultaneous loss of acetic acid and ketene, is least important but none of the pathways dominates the others as is the case for the other linkage isomers. The fragmentation of the *m/z* 257 ion derived from the (1→4)-linked isomers (**11** and **12**) is dominated by the simultaneous loss

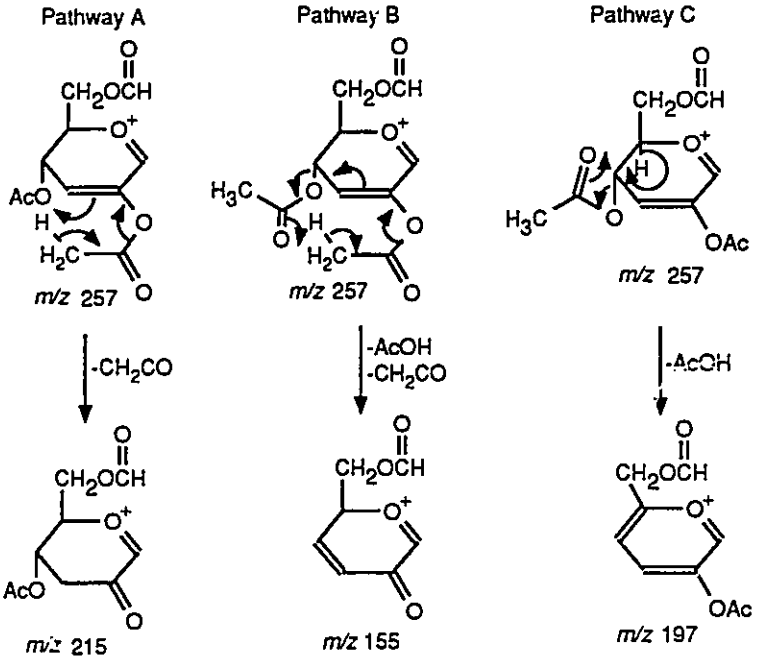

Scheme 23

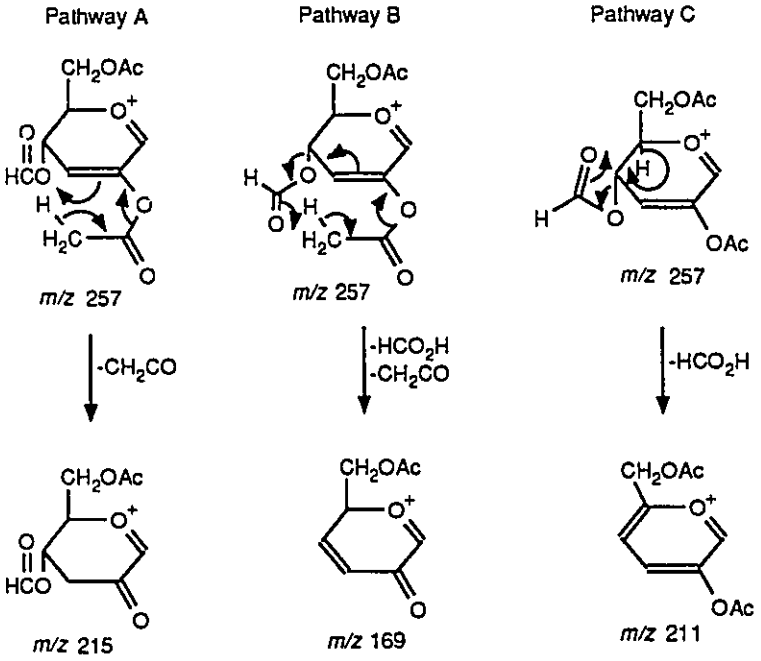

Scheme 24

of formic acid and ketene (pathway B, Scheme 24). Pathway C, involving loss of formic acid, is operative also. The loss of ketene from the *m/z* 257 ion (pathway A Scheme 24) does not appear to be significant.

Similarly, pathway B (*i.e.* simultaneous loss of acetic acid and ketene) yields the most abundant ions in the spectra of the (1→3)-linked isomers (**13** and **14**)(Scheme 25). Loss of acetic acid from the *m/z* 271 ion (pathway C) is operative also, while loss of ketene to afford an ion at *m/z* 229 (pathway A) appears to be insignificant. Additional ions are evident in the spectra of the (1→3)-linked isomers at *m/z* 197 and *m/z* 215 which appear to be derived from the *m/z* 257 ion by losses of acetic acid and ketene, respectively.

The (1→2)-linked isomer (**15**) yields the most complicated spectrum in terms of the number of low abundance ions that are observed. Nevertheless, the two most abundant ions below *m/z* 257 may be accounted for by two of the pathways outlined in Scheme 26. The ion at *m/z* 169, resulting from fragmentation along pathway B is most abundant but pathway C (*i.e.* loss of acetic acid) is a major fragmentation route also. Loss of carbon monoxide (pathway A) from the ion at *m/z* 257 to afford an ion at *m/z* 229 does not appear to be an important process. It may be that pathway A is less facile when a formate, rather than an acetate is situated at C-2, thereby allowing the ion at *m/z* 257 to fragment along a different pathway to yield the ions at *m/z* 215 and *m/z* 211. The *m/z* 257 ion shown in Scheme 26 cannot readily lose formic acid to yield the ion at *m/z* 211. Thus it seems likely that the ion at *m/z* 211 results from a process involving the

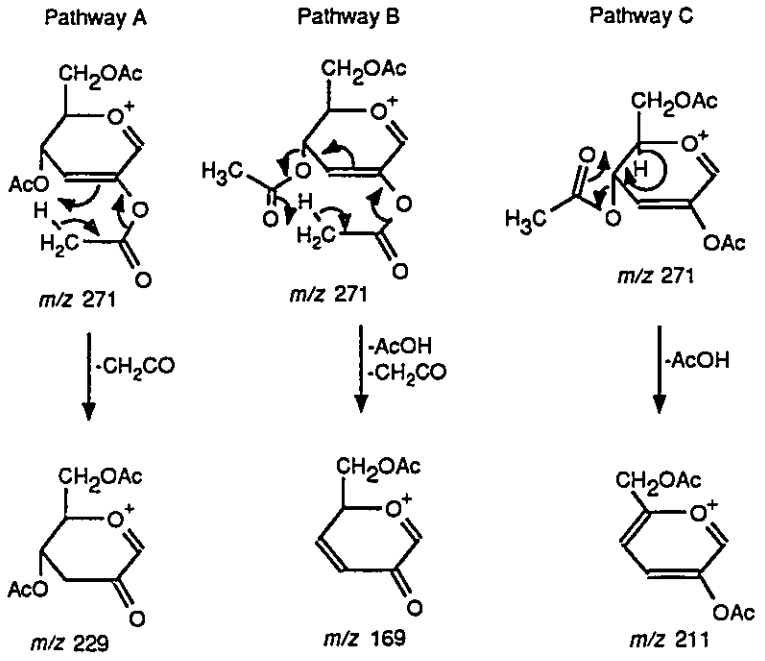

Scheme 25

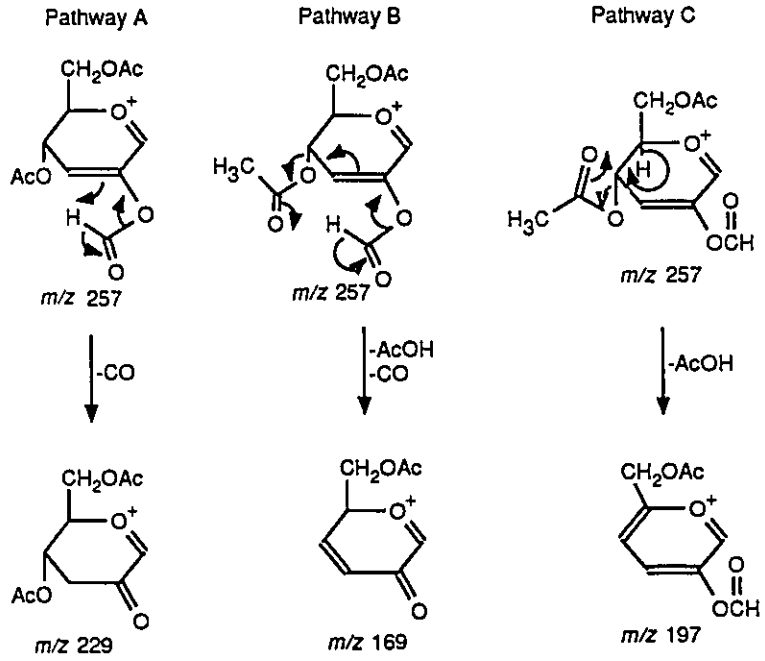

Scheme 26

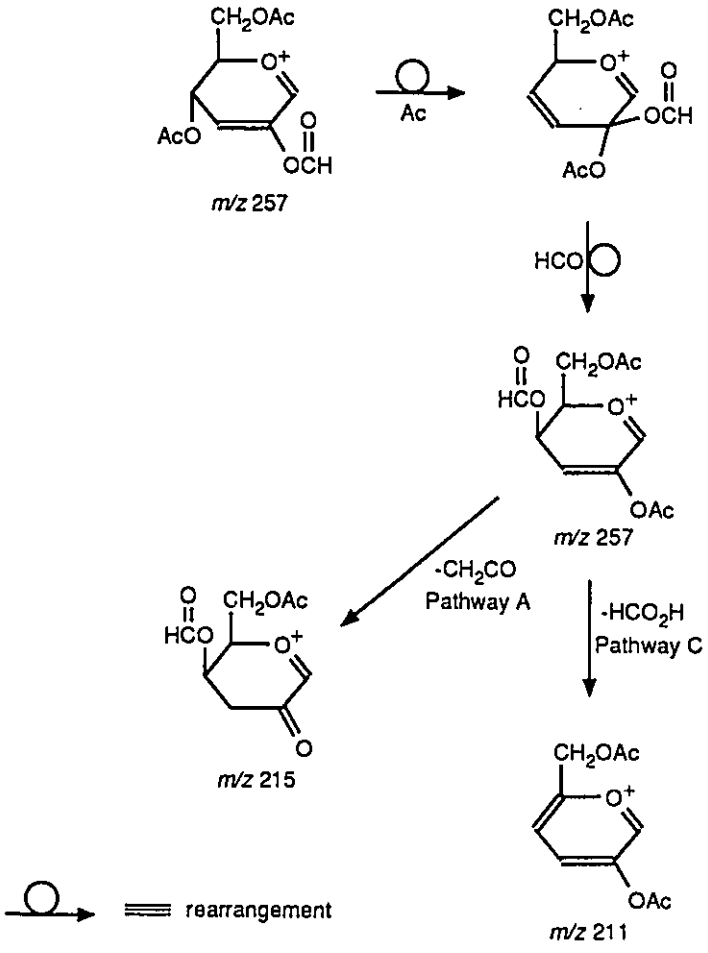
CH2OAc
O+
AcO
O
OCH
m/z 257
Ac
CH2OAc
O+
O
OCH
AcO
HCO
O
HCO
CH2OAc
O+
OAc
m/z 257
-CH2CO
Pathway A
-HCO2H
Pathway C
O
HCO
CH2OAc
O+
O
m/z 215
CH2OAc
O+
OAc
m/z 211
rearrangement

Scheme 27

rearrangement of the ion at *m/z* 257. Scheme 27 illustrates a mechanism, which if operative, accounts for the formation of the ions at *m/z* 215 and *m/z* 211. The scrambling of the substituents at C-2 and C-4 is analogous to the process that was proposed by Hogg and Nagabhushan (Scheme 7, p.24).[32]

The MIKES spectra derived from the *m/z* 317 ion in the DEI mass spectra of the (1→6)-, (1→3)- and (1→2)-linked mannose disaccharides are similar to the MIKES spectra of the corresponding glucose disaccharides. Glucose and mannose differ only in the configuration of the substituent at C-2. Once the substituent at C-3 has been eliminated, the chirality at C-2 is destroyed, thereby yielding the same *m/z* 257 ion (Scheme 28). Consequently the spectra of the glucose and mannose disaccharides are similar. However, the (1→4)-linked mannose disaccharide (**17**) is anomalous in that its MIKES spectrum does not exhibit an intense ion at *m/z* 257, corresponding to loss of the C-3 substituent from the ion at *m/z* 317. The reason for the anomalous behaviour of the *m/z* 317 ion derived from **17** cannot be explained unless the purported structure is wrong. NMR experiments will need to be undertaken to confirm the structure of **17**.

In the case of the galactose disaccharides, the same general fragmentation schemes seem to apply. However, fragmentation pathway C, involving elimination of the C-4 substituent from the *m/z* 257 ion, is much more important in the case of the galactose disaccharides than it is for the corresponding linkage isomers of the glucose and mannose disaccharides. Since the galactose disaccharides have a different configuration at C-4 it is likely that the

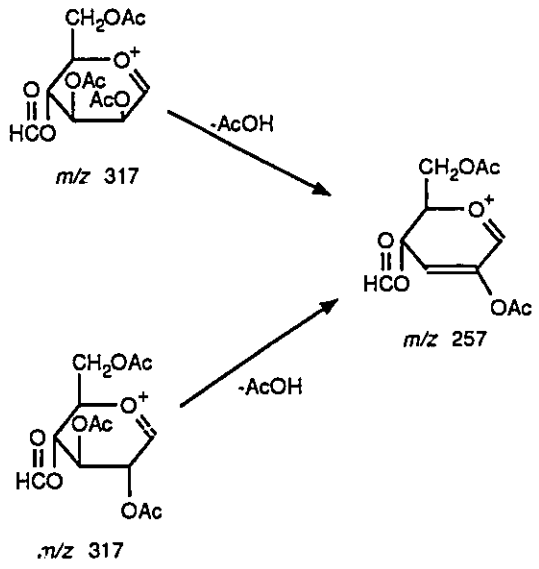
CH2OAc
O+
OAc
AcO
O
HCO
m/z 317
-AcOH
CH2OAc
O+
O
HCO
OAc
m/z 257
CH2OAc
O+
OAc
O
HCO
OAc
m/z 317
-AcOH

Scheme 28

relative stereochemistry at C-4 influences the fragmentation; however, the reason for this effect is still unclear.

3.5 Summary

A number of peracetylated monosaccharides were examined by NH_3-DCI mass spectrometry. Their spectra are characterized principally by ammonium adduct ions although oxonium ions are evident in the spectra also. The $[M+NH_4]^+$ ions fragment to yield oxonium ions at *m/z* 331 which undergo further fragmentation by subsequent losses of acetic acid and ketene. The losses of acetic acid and ketene appear to follow the pattern of losses observed in the FAB mass spectra of the same acetylated monosaccharides. An additional mode of fragmentation that may be operative is the displacement of the acetate at C-1 by NH_3.

Several peracetylated disaccharides were examined, two of which were isotopically labelled; the most abundant ion in their spectra was the $[M+NH_4]^+$ ion. Many of the fragment ions in the spectra were adduct ions; however, oxonium ions were again present. The $[M+NH_4]^+$ ion fragments by loss of acetic acid, by loss of the elements of ammonium acetate and by cleavage of the glycosidic bond to afford an oxonium ion. Other ions observed in the spectra indicated that the disaccharides undergo heterolytic cleavage on both sides of the glycosidic oxygen but this could not be confirmed by MIKES experiments on the $[M+NH_4]^+$ ion. Hydrogen and acyl transfer ions were observed in the spectra. The relative abundances of the hydrogen and acyl transfer ions derived from the non-reducing

end of the disaccharides was greater than the relative abundance of the same type of ions derived from the reducing end. This result is contrary to what one would expect if the formation of these ions involves heterolytic cleavage of the glycosidic bonds. Thus, another process, in addition to heterolytic cleavage of the glycosidic bonds, may be involved in the formation of the observed acyl and hydrogen transfer ions; however, the origin of these ions could not be determined. In addition to the fragmentations described above, the disaccharide underwent a fragmentation involving the decomposition of the non-reducing ring to yield a formate group at the point of linkage in the reducing ring of the disaccharide.

The ions that result from the cleavage of the non-reducing ring to yield a formylated monosaccharide are also observed in the DEI mass spectra of acetylated disaccharides. These ions are more abundant in the DEI than in the DCI mode and can be studied by MIKES experiments. Since the position of the formate group is dependent on the position of linkage in the disaccharide, linkage isomers afford isomeric ions containing a formate group. These isomeric ions yield distinct MIKES spectra, which enable one to assign the position of linkage in the disaccharide. This technique could differentiate the linkage isomers of glucose and mannose disaccharides. Experiments with the (1→6)- and (1→4)-linkage isomers of galactose disaccharides showed that they were also distinguishable. This technique for differentiating linkage isomers of disaccharides involves the comparison of fewer ions than the technique of de Jong *et al.*[41-44] Less sample is needed for the analysis (20 μg *vs* 100 μg) than is required by the technique used

by Dallinga *et al.*,[48,49] although their technique could be used to study the linkage positions in larger oligomers. Unlike the technique of Domon *et al.*[52] a computer analysis is not required to interpret the spectra.

CHAPTER 4

ANALYSIS OF THE CORE OLIGOSACCHARIDES

RESULTS AND DISCUSSION

4.1 Analysis of the Core Oligosaccharides from AK1012 and AK1401

Samples of the AK1012 and AK1401 cores were received from Professor W.A. Szarek and Professor A.M. Kropinski, respectively. Unless otherwise stated the cores were dephosphorylated prior to analysis. Once dephosphorylated the cores were subjected to a number of chemical analyses, namely compositional analysis, methylation analysis, and selective degradation followed by compositional analysis. The absolute configurations of the glucose and rhamnose in the AK1401 core were determined. Additionally, peracetylated core samples were analyzed by mass spectrometry and the native cores were analyzed by ^{31}P-NMR spectrometry. The results of these analyses are discussed in the following sections of this chapter.

4.2 Compositional Analysis

Alditol peracetates were prepared from the dephosphorylated cores by hydrolysis, reduction with $NaBD_4$, and acetylation. The resulting mixture was analyzed by GC and GC-MS. The molecular weights of the various carbohydrates in the mixture were determined from the spectra obtained in the GC-MS analysis (spectra are included in Appendix 2). The alditol peracetates were then identified by co-elution with authentic standards (except for the heptose for which no

standards were available). The relative abundance of each component (as determined by GC of the alditol peracetates) was determined from the average of three analyses. The results of the compositional analysis are summarized in Table 1.

All of the carbohydrates detected in this analysis were labelled with deuterium at C-1 as a result of reduction with $NaBD_4$, indicating that all the alditol peracetates were derived from aldoses. Thus, the AK1012 core contains heptose and 2-amino-2-deoxy-galactose (galactosamine) and the AK1401 core contains glucose and rhamnose in addition to heptose and galactosamine.

Previous work on the structure of the core oligosaccharides derived from mutants of P. aeruginosa strain PAO1 indicated that the core contained KDO and alanine also.[61] The alanine was detected using an automated amino acid analyzer and the KDO was detected using a spectrophotometric assay. The inability to detect KDO and alanine in this study is attributed to the basic conditions used for acetylation. After acetylation, the acidic KDO and alanine would be present in the mixture of alditol peracetates as carboxylates which are too polar to be eluted from a GC column. Analyses that will be discussed below indicate that alanine and KDO are present in the both the AK1012 and the AK1401 core.

The relative abundance of the alditol peracetates detected in the compositional analysis is indicated in Table 1. The values are non-integral making the stoichiometric proportions of the monosaccharides in the cores uncertain.

Table 1. Composition of the mixture of peracetylated alditols derived from the core oligosaccharides, from AK1012 and AK1401.

Retention time (min)	Components[a]	AK1012 Relative abundance[b]	AK1401 Relative abundance[b]
10.8	rhamnitol	----	4.1
25.8	glucitol	----	16.2
33.5	heptitol	3.7	4.8
35.0	galactosaminitol	1.0	1.0

[a] Components were analyzed as their alditol peracetates and their identities were confirmed by co-elution with authentic standards.

[b] The reported relative abundances are the average of three analyses.

4.3 Methylation Analysis

The methylation analysis of the dephosphorylated core involved the permethylation of the intact cores followed by hydrolysis, reduction with $NaBH_4$ and, finally, acetylation. This sequence of reactions yielded a mixture of partially methylated alditol acetates (PMAA's) which were analyzed by GC-MS. The results of this analysis are summarized in Tables 2 and 3 for the AK1012 and AK1401 cores, respectively. The bulk samples were analyzed by NH_3-DCI MS also. Spectra of the identified components are included in Appendix 2.

Analysis of the AK1012 core PMAA's by GC-MS indicated that the core contains a terminal heptose, a 3-linked heptose, a 3,7-linked heptose, and an 8-linked KDO. The PMAA corresponding to the 3-linked heptose was the major component, the others being present in minor amounts. The NH_3-DCI mass spectrum of the mixture of PMAA's exhibited ions which corresponded in mass to the $[M+NH_4]^+$ ions of the PMAA's identified by GC-MS. The PMAA's are present in non-integral amounts so no conclusions can be drawn regarding the relative abundance of the heptoses and KDO.

The presence of an acetate at C-1 and at C-5 in the PMAA's derived from the heptoses indicates that these monosaccharides exist in the pyranose form in the core. Acetates at C-2 and C-6 in the PMAA derived from KDO indicate that this monosaccharide exists in the pyranose form also.

The permethylation analysis of the AK1401 core indicated that this core contains a 3-linked heptose and a 3,7-linked heptose; again the 3,7-linked heptose

contains a 3-linked heptose and a 3,7-linked heptose; again the 3,7-linked heptose was the minor component. The other PMAA's detected indicate that the AK1401 core contains both terminal and 6-linked glucoses and a 2-linked rhamnose in a relative abundance of approximately 2:2:1. The proportion of total glucose to rhamnose is similar to that obtained from the compositional analysis, which suggests that the observed relative abundances are representative of the actual relative abundance of these components in the core. The other PMAA's are present in non-stoichiometric amounts making their actual relative abundance uncertain. The NH_3-DCI mass spectrum of the PMAA mixture derived from the AK1401 core is again consistent with the results of the GC-MS analysis.

Acetates at C-1 and C-5 of the glucoses, the rhamnose and the heptoses indicate that the monosaccharides from which they are derived exist in the pyranose form.

Neither the AK1012 core nor the AK1401 core yielded PMAA mixtures containing a component corresponding to the galactosamine that was detected in the compositional analysis. Furthermore, the AK1401 core was expected to contain a terminal heptose and an 8-linked KDO based on the results obtained from the AK1012 core. Attempts to optimize the PMAA preparation conditions for these components proved unsuccessful. The amino sugars seem to be particularly susceptible to degradation under the reaction conditions necessary to ensure complete methylation and complete hydrolysis of the methylated oligosaccharide. This fact may account for the absence of this component in the PMAA mixture.

The reasons for the absence of the PMAA's corresponding to the terminal heptose and the KDO are still not known, especially since the results discussed below give indirect evidence that these components are present in the AK1401 core. However, it is possible that a terminal heptose, if present in the AK1401 core, may have a residual phosphate. This phosphate would not be removed during the the preparation of the PMAA's; thus, a PMAA corresponding to a terminal heptose would not have been observed in the methylation analysis.

Table 2. Components detected in the methylation analysis of the AK1012 core oligosaccharide.

Component	Retention time (min)	Deduced origin of the component
1,5-di-*O*-acetyl-2,3,4,6,7-penta-*O*-methyl heptitol	19.6	terminal heptose
1,3,5-tri-*O*-acetyl-2,4,6,7-tetra-*O*-methyl heptitol	22.4	3-linked heptose
1,3,5,7-tetra-*O*-acetyl-2,4,6-tri-*O*-methyl heptitol	26.2	3,7-linked heptose
methyl 2,6,8-tri-*O*-acetyl-(3-deoxy)-4,5,7-tri-*O*-methyl octanoate	31.9	8-linked KDO

Table 3. Components detected in the methylation analysis of the AK1401 core oligosaccharide.

Component	Retention time (min)	Deduced origin of the component
1,2,5-tri-*O*-acetyl-6-deoxy-3,4-di-*O*-methyl hexitol	14.7	2-linked rhamnose
1,5-di-*O*-acetyl-2,3,4,6-tetra-*O*-methyl hexitol	15.6	terminal glucose
1,5,6-tri-*O*-acetyl-2,3,4-tri-*O*-methyl hexitol	19.1	6-linked glucose
1,3,5-tri-*O*-acetyl-2,4,6,7-tetra-*O*-methyl heptitol	22.4	3-linked heptose
1,3,5,7-tetra-*O*-acetyl-2,4,6-tri-*O*-methyl heptitol	26.2	3,7-linked heptose

4.4 Periodate Oxidation and Sodium Borodeuteride Reduction of the AK1012 and AK1401 Cores

The dephosphorylated cores were selectively degraded by oxidation with $NaIO_4$. The oxidation product was then reduced with $NaBD_4$ to mark the sites that had been oxidized by the $NaIO_4$. The resulting product was subjected to compositional analysis as described above, with the exception that $NaBH_4$, instead of $NaBD_4$, was used for the reduction. A summary of the results of this compositional analysis can be found in Table 4.

Glycerol-d_1 triacetate was the largest single component in this analysis. The terminal and 6-linked glucoses, the 2-linked rhamnose, and the terminal heptose would all yield glycerol-d_1 triacetate when the cores are treated as described above. Since most of the monosaccharides present in the core produce glycerol triacetate in this analysis the presence of this component provides no structural information.

Erythritol-d_1 tetraacetate was produced from both cores. It could in principle be derived from a 4-linked glucopyranose; however, the AK1012 core does not contain glucose and the methylation analysis indicated that none of the glucose residues in the AK1401 core was a 4-linked glucopyranose. Erythritol tetraacetate could also be derived from a 7 or 8-linked KDO if the KDO was in the pyranose form.

The methylation analysis of the AK1012 core indicated the presence of an 8-linked KDO in the pyranose form, which suggests that it was the source of the erythritol

tetraacetate. The erythritol tetraacetate derived from the AK1401 core likely originates from the same source as in the AK1012 core.

Mannitol hexaacetate-d_1 was present in the product mixture of both cores. This monosaccharide was not detected in the compositional analysis and therefore must result from oxidation and subsequent reduction of the cores. The methylation analysis indicated that both cores contain a 3-linked heptopyranose. This heptose would be degraded to a hexose when subjected to periodate oxidation and subsequent reduction. Thus, the heptose from which the mannitol hexaacetate was derived must have had the mannose configuration. Only one heptose was detected in the compositional analysis of the cores (Table 1). When the mixture of alditol acetates was re-analyzed on the same column using a different temperature program (210°C isothermal) the same result was obtained, suggesting that the three heptoses have the same structure. A heptose in both cores survives the periodate oxidation as indicated by the presence of a heptitol heptaacetate in the product mixture. The methylation analysis indicated that both cores contain a 3,7-linked heptopyranose, a unit that would survive the periodate oxidation intact.

Galactosamine was found to survive the periodate oxidation of the AK1401 core only. Both the 4,6-linked pyranose form or the 5,6-linked furanose form of an N-acylated galactosamine would survive periodate oxidation. Consequently, it is not possible to distinguish which of these isomers of galactosamine exists in the core, based on the results of the periodate oxidation.

Table 4. Components detected in the GC-MS analysis of the alditol acetates derived from the product of the periodate oxidation and $NaBD_4$ reduction of the AK1012 and AK1401 core oligosaccharides.

Core	Alditol[a,b]	Possible source of the alditol
AK1012	glycerol-d_1	
	erythritol-d_1	- 7 or 8-linked KDO
	mannitol-d_1	- 3-linked mannoheptopyranose
	heptitol	- 3,7-linked heptopyranose
AK1401	glycerol-d_1	
	erythritol-d_1	- 7 or 8-linked KDO
	mannitol-d_1	- 3-linked mannoheptopyranose
	heptitol	- 3,7-linked heptopyranose
	galactosaminitol	- 3 or 4-linked galactosamine (in the pyranose ring form) - 5- or 6-linked galactosamine (in the furanose ring form)

[a] Alditols were analyzed as their peracetates.

[b] Where possible, alditols were identified by comparison of their GC retention times with those of authentic standards.

4.5 Absolute Configuration Analysis of Glucose and Rhamnose

The absolute configuration of the glucose and rhamnose found in the AK1401 core was determined by the chiral glycoside method of Leontein *et al.*[80] The absolute configuration of the remaining monosaccharides could not be determined by this method because either the glycosides could not be formed or suitable standards were not available.

The chiral (-)-2-octyl and (±)-2-octyl glycosides were prepared from L-rhamnose and D-glucose by heating them with 2-octanol under acidic conditions. The glycosides were then acetylated for analysis by GC-MS. The reactions described above produced a number of isomeric glycosides; however, only some of the components are necessary to determine the absolute configuration of the carbohydrates. Figures 17 and 18 display the regions of the chromatograms in which the components of interest elute.

The total ion chromatogram (TIC) in Figure 17a exhibits two peaks (peaks 1 and 2). These peaks are assigned to the two glycosides produced from L-rhamnose and (-)-2-octanol. The chromatogram in Figure 17b exhibits two additional peaks (peaks 3 and 4). These additional peaks are only present when the L-rhamnose is glycosylated with the racemic octanol. GC-MS analysis indicates that these components are octyl glycosides also. Therefore, the additional components observed in Figure 17b correspond to the glycosides formed from the L-rhamnose and the (+)-2-octanol. The mass chromatogram of the octyl rhamnosides derived from the dephosphorylated hydrolysed AK1401 core (Fig.17c)

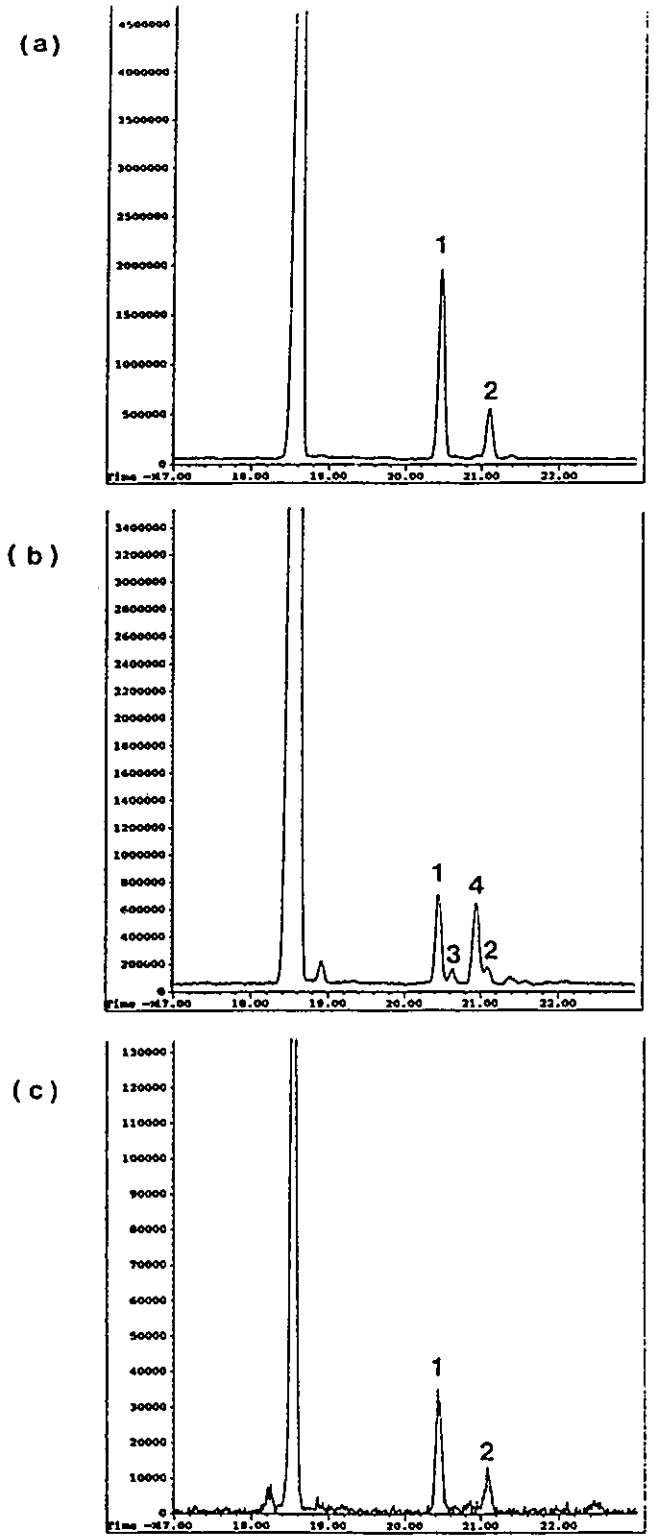

Figure 17. GC-MS chromatograms of (a) acetylated (-)-2-octyl-L-rhamnosides, (b) acetylated (±)-2-octyl-L-rhamnosides, (c) acetylated (-)-2-octyl-rhamnosides, from hydrolysed AK1012 core

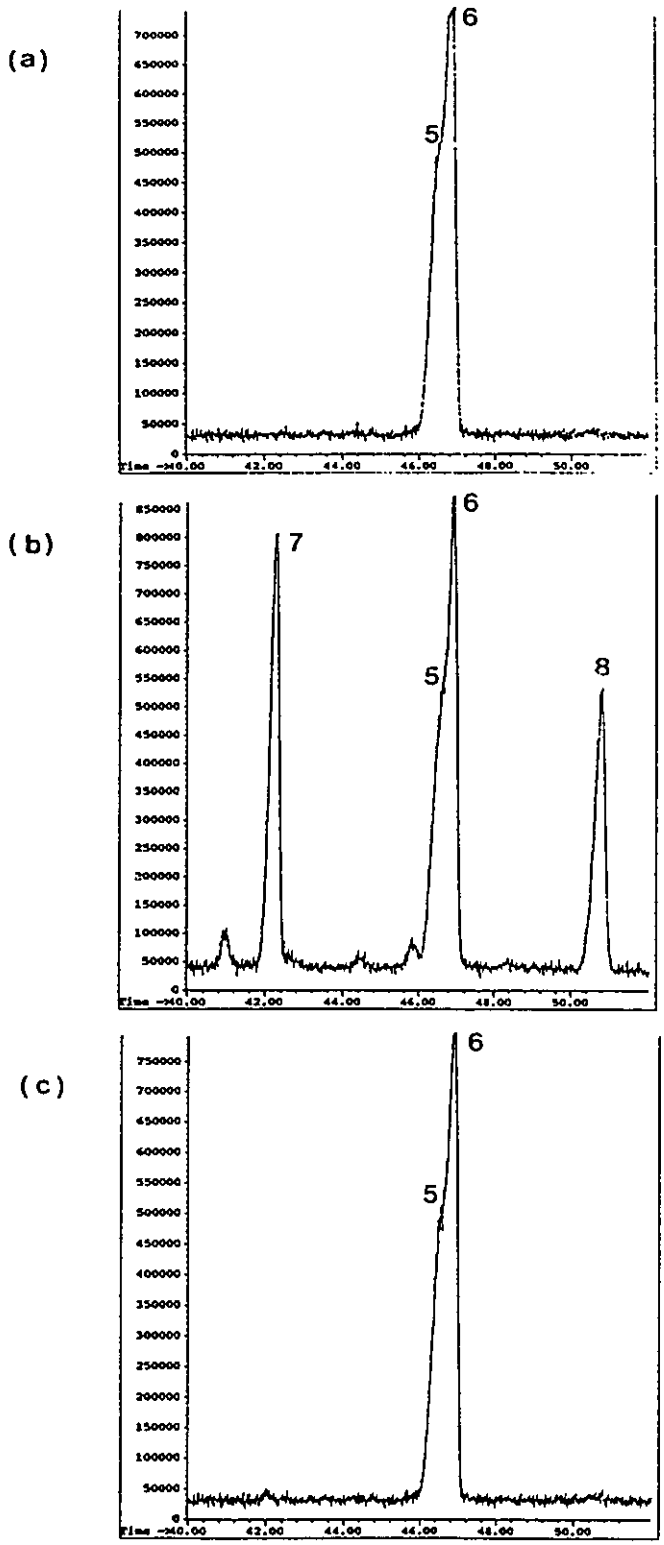

Figure 18. GC-MS chromatograms of (a) acetylated (-)-2-octyl-D-glucosides, (b) acetylated (±)-2-octyl-D-glucosides, (c) acetylated (-)-2-octyl-glucosides, from hydrolysed AK1401 core

exhibits peaks 1 and 2 only. A mass chromatogram of the *m/z* 115 ion was used in Figure 17c because there was an interfering component present which obscured the components of interest in the total ion chromatogram. Thus, the rhamnose found in the AK1401 core has the L-configuration.

Figure 18a exhibits the portion of the TIC in which the (-)-2-octyl-D-glucosides of interest elute (peaks 5 and 6). Peaks 5 and 6 are not resolved under the conditions used but resolution of these components is not required for this analysis. Once again additional peaks (peaks 7 and 8 Fig. 15b) are observed when the racemic octanol is used to make the glycosides. The partial chromatogram of the octyl glucosides derived from the dephosphorylated hydrolysed AK1401 core exhibits peaks 5 and 6 only (Fig. 18c). Thus, the glucose found in the AK1401 core has the D-configuration.

4.6 Summary of the Results from the Chemical Analyses of the AK1012 and AK1401 cores

The chemical analyses discussed above indicated that the AK1012 core contains a terminal, a 3-linked, and a 3,7-linked heptose. The branched heptose indicates that the core must have two non-reducing termini. The terminal heptose would account for one of these non-reducing termini. Since the nature of the core is such that the KDO forms the reducing end of the oligosaccharide, the galactosamine detected in the compositional analysis must be the other non-reducing terminus, which suggests three possible structures for the AK1012 core (Fig.19).

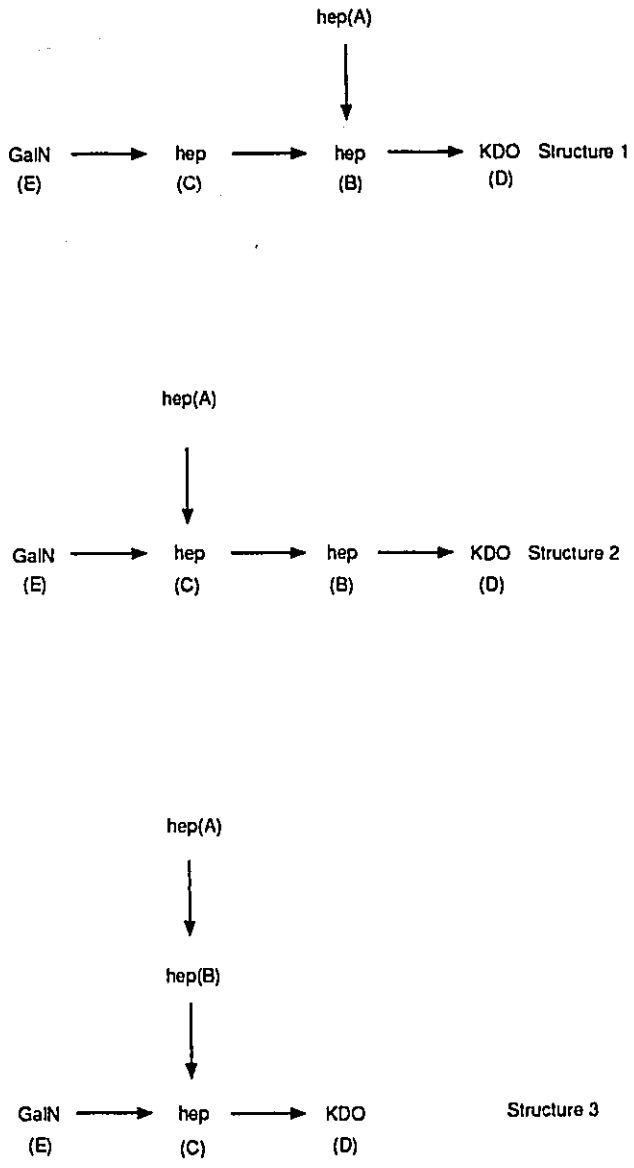

Figure 19. Possible isomeric structures of the AK1012 core.

An examination of the NH_3-DCI and FAB spectra of the acetylated core was undertaken in an attempt to differentiate among the three structures (Fig. 19). The results of the mass spectrometric analysis of the peracetylated dephosphorylated AK1012 core will be discussed in section 4.6.

The AK1401 core is expected to share a common inner core structure with the AK1012 core. The results of the chemical analyses are consistent with this hypothesis. The lack of a PMAA corresponding to a terminal heptose suggests that a heptose may be a point of attachment of the outer core to the inner portion of the AK1401 core. Alternatively, the PMAA corresponding to the terminal heptose may simply not have been detected. Additionally, the fact that the galactosamine survives the periodate oxidation and reduction of the AK1401 intact, suggests that this is a point of attachment of the outer core also. The methylation analysis indicated that there are two terminal glucose residues. The outer core region must therefore, have two non-reducing termini. The core fragments containing these termini may both be attached to the galactosamine or one may be attached to the galactosamine and one may be attached to the heptose. Both fragments cannot be attached to the heptose because the galactosamine must be substituted in order to survive the periodate oxidation and subsequent reduction intact. The results of the chemical analyses are therefore consistent with the isomeric structures in Figure 20. Mass spectrometry was used in an attempt to differentiate among these isomers. The results of the mass spectrometric analysis of the peracetylated AK1401 core are discussed below.

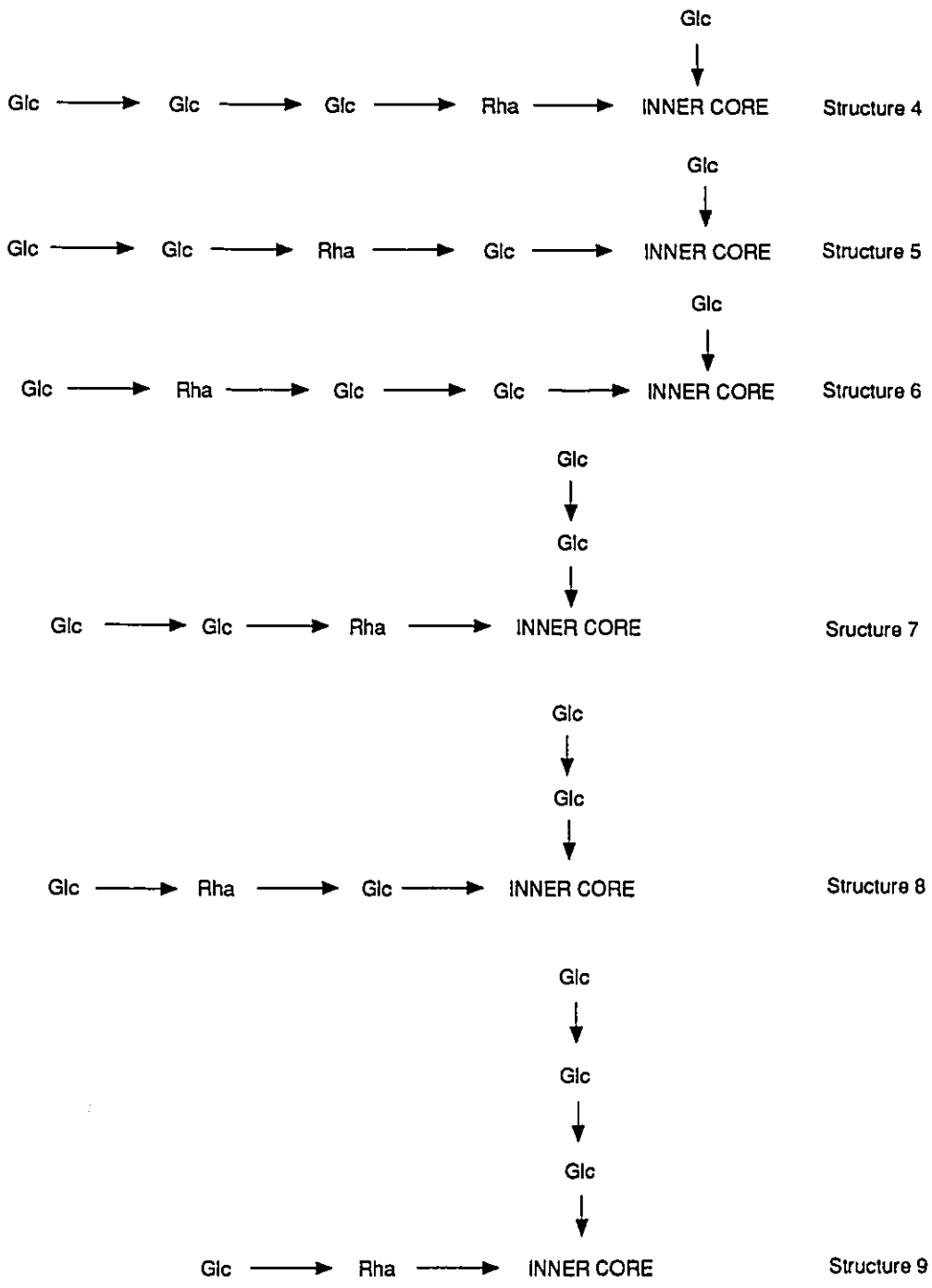

Figure 20. Possible isomeric structures of the AK1401 core.

4.7 Mass Spectrometry

Dephosphorylated AK1012 core was acetylated with a mixture of acetic acid and trifluoroacetic anhydride. The dephosphorylated AK1401 core would not dissolve in the reagents used to acetylate the AK1012 core and was therefore acetylated using acetic anhydride and pyridine. The acetylated cores were then analyzed by NH_3 DCI-MS and FAB-MS. The spectra obtained in these analyses are shown in Figures 21-25. Each of the spectra exhibits a number of diagnostic ions (proposed structures may be found in Table 5). In the CI spectra some of the diagnostic ions are oxonium ions but many of the ions are ammonium adducts. The FAB spectrum of the AK1012 core exhibits a number of unusual ions which are discussed below. The FAB spectrum of the AK1401 core is dominated by ions derived from the outer core region. Many of the ions are attributed to fragments which result from the transfer of an acyl group or a hydrogen to the observed ion. Such processes are common in both FAB[7,92] and CI mass spectrometry of peracetylated carbohydrates. The structures attributed to the ions in the mass spectra are described below. Many of the ions visible in the spectra (Fig. 21-25) are not discussed but are considered to be derived from the ions described in Table 5 by one or more losses of acetic acid, ketene, or water.

4.7.1 Mass Spectrometry of the AK1012 Core

The NH_3-DCI spectrum of peracetylated AK1012 core is shown in Figure 21. The ion at *m/z* 378 corresponds in mass to ion ***a*** (Table 5). This ion

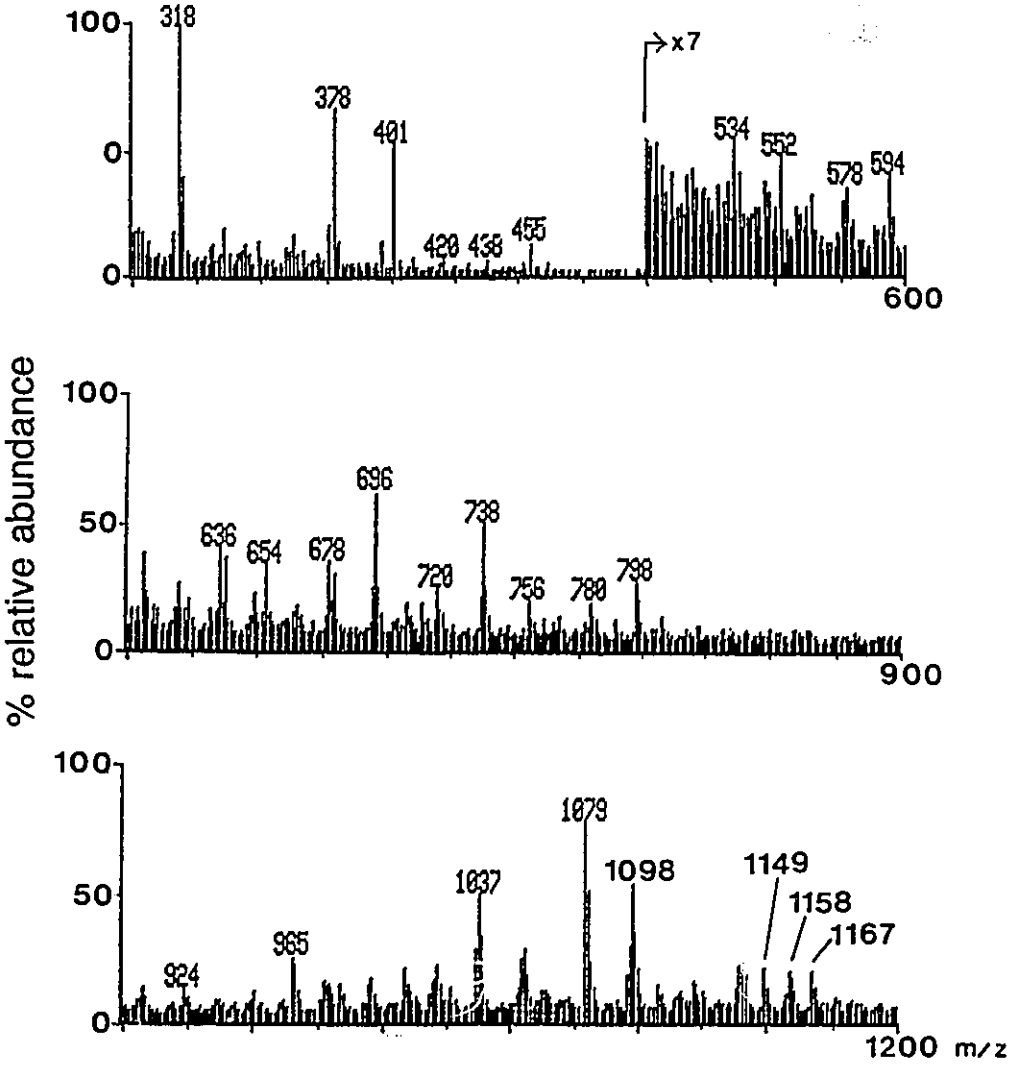

Figure 21. NH_3-DCI mass spectrum of acetylated AK1012 core.

may be derived from ion ***c*** by loss of a molecule of acetic acid. The ion at *m/z* 401 corresponds to oxonium ion ***b*** in Table 5. The alanyl moiety is assigned to the 2-position because the *m/z* 401 ion is still present in the spectrum when the core has been subjected to mild base hydrolysis prior to acetylation and MS. The base hydrolysis would have removed an *O*-linked alanyl group. The *m/z* 401 ion is consistent with the presence of a terminal galactosamine in the AK1012 core; this residue is hereafter referred to by the designation GalNAla. The GalNAla moiety is consistent with all three structures in Figure 19. A second diagnostic ion appears at *m/z* 438 and is assigned structure ***c***. This ion is consistent with the presence of a terminal heptose in the core (although it may be derived from an internal heptose) and may be derived from heptose A in each of the structures in Figure 19. Another ion appears at *m/z* 798 and corresponds in mass to ion ***d***. This ion can most easily be derived from units A and B of structure 3 (Fig. 19).

A number of trisaccharide fragment ions are observed also. An ion appears at *m/z* 1079 which corresponds in mass to the oxonium ion ***e***. The ion at *m/z* 1158 corresponds in mass to the heptose trisaccharide ***f***. This ion suggests that the heptoses are linked together but does not indicate which of the structures in Figure 19 is correct. Finally, there is an ion at *m/z* 1167 that corresponds to a proton adduct of a peracetylated trisaccharide assigned structure ***g***. The presence of the amides in the GalNAla moiety renders this fragment basic enough to form a proton adduct rather than the ammonium adduct usually observed in the NH_3 CI spectra of acetylated oligosaccharides. Ion ***g*** indicates (barring re-arrangements)

Table 5. Possible structures of the ions observed in the NH_3 DCI and FAB mass spectra of the peracetylated dephosphorylated AK1012 and AK1401 cores.

m/z	Designation	Possible Structure[a]
378	***a***	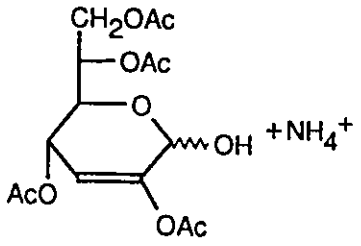
401	***b***	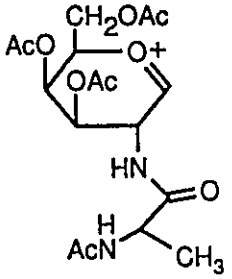
438	***c***	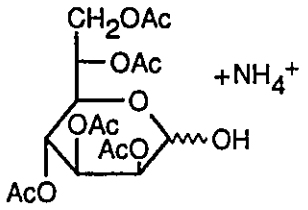
798	***d***	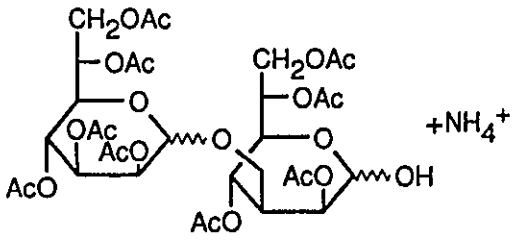

Table 5. continued

m/z	Designation	Possible Structure[a]
1079	*e* *	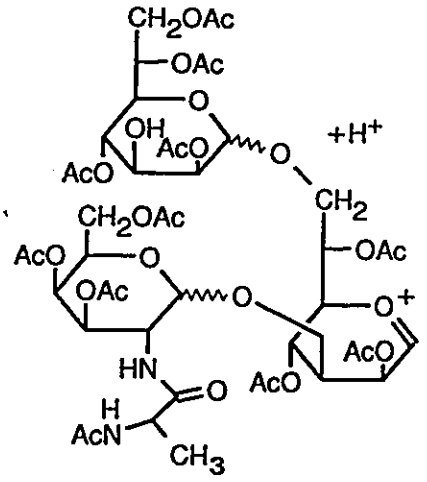
1158	*f*	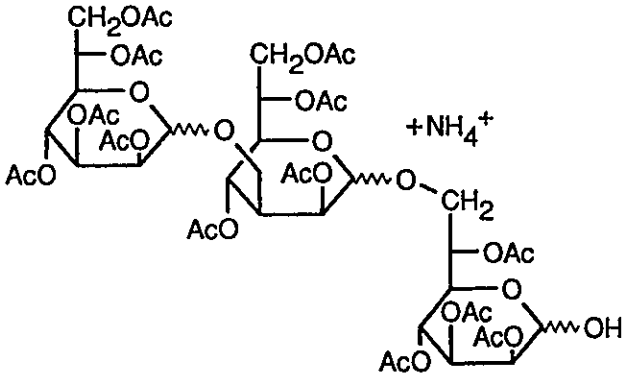
1167	*g*	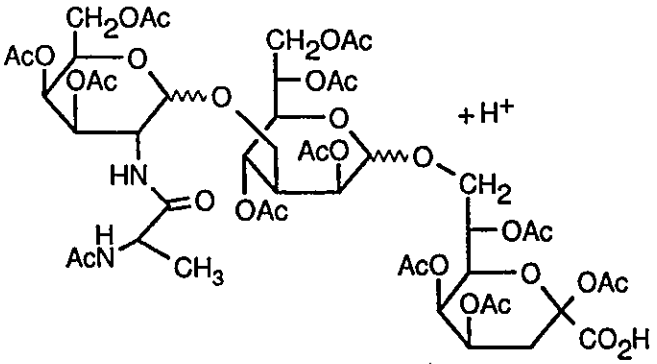

* alternatively, *e* may be derived from *g* by loss of formic acid and ketene

Table 5. continued

m/z	Designation	Possible Structure[a]
331	***h***	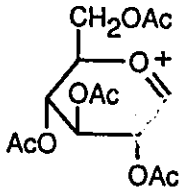
366	***i***	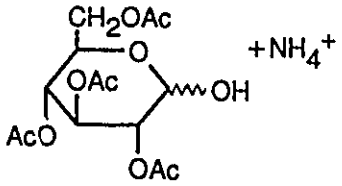
408	***j***	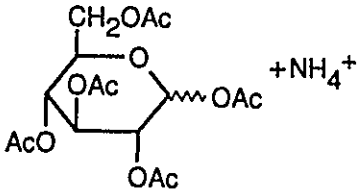
561	***k***	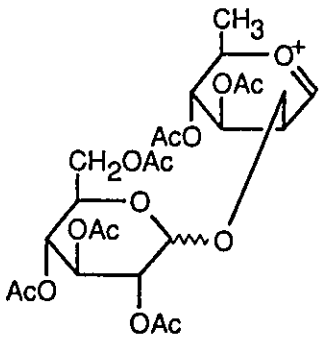
596	***l***	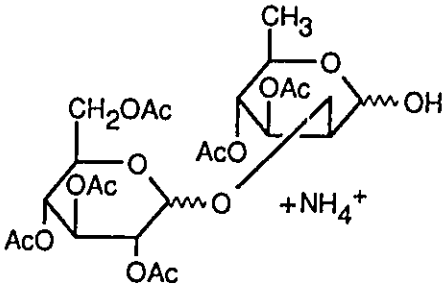

Table 5. continued

m/z	Designation	Possible Structure[a]
654	***m***	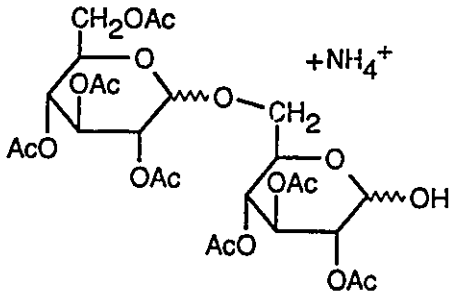
696	***n***	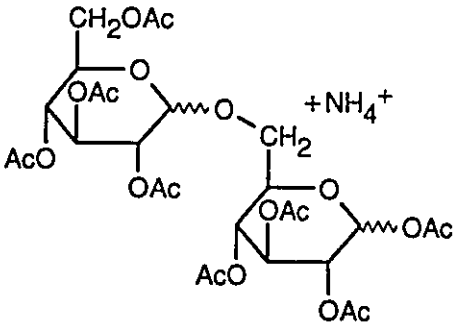
884	***o***	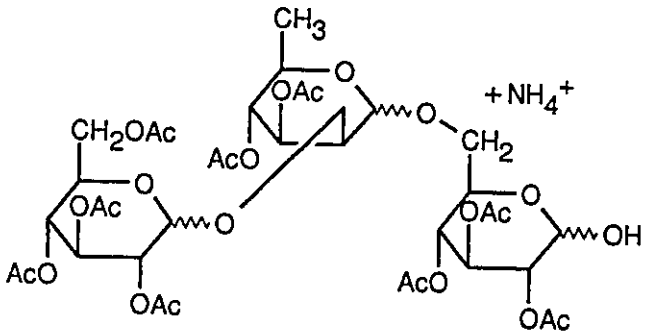
926	***p***	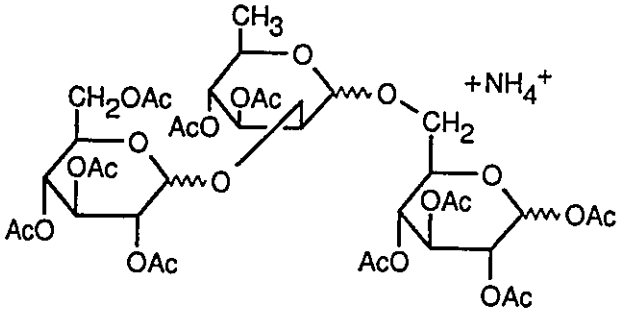

Table 5. continued

m/z	Designation	Possible Structure[a]
766	*q*	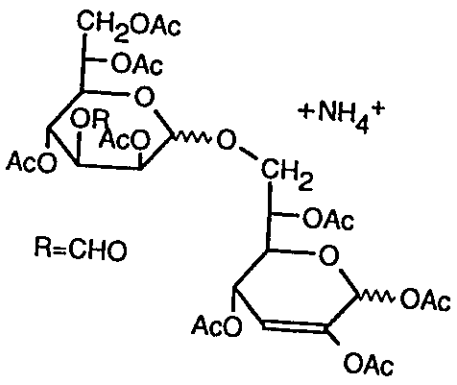
1063	*r*	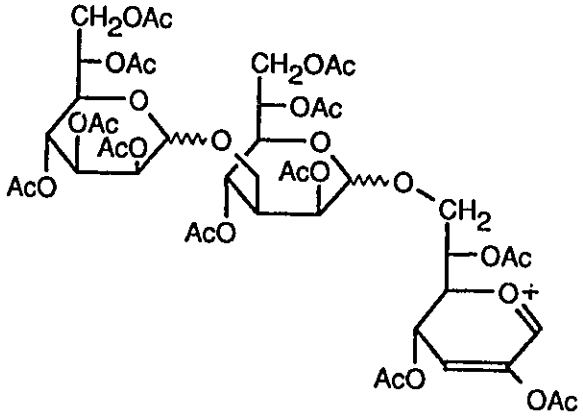
1783	*s*	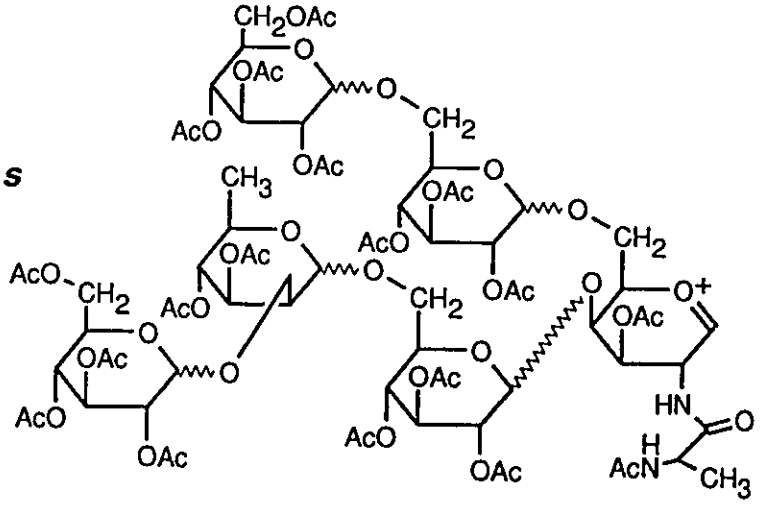

[a] position of linkages and any double bonds, OH's and formyl groups have been arbitrarily asigned.

that there is only one heptose between the GalNAla and the KDO. Therefore, the NH_3 DCI mass spectrum of the peracetylated dephosphorylated AK1012 core is consistent with structure 3 (Fig. 19).

The FAB mass spectrum of the peracetylated dephosphorylated AK1012 core (Fig. 22) exhibits an ion at *m/z* 401. This ion is again assigned structure ***b***. The ions at *m/z* 762, *m/z* 1182 and *m/z* 1468 cannot be interpreted in terms of the structures in Figure 19, although they are very close in mass to ions one might expect to observe (see Scheme 29) in the FAB spectrum of structure 3 (Fig. 19). The ions observed in the FAB spectrum of the AK1012 core were reproducible and apparently were not the result of a calibration error. At present the origin of these ions is uncertain; therefore the proposed structure for the AK1012 core must still be confirmed by other means.

The chemical analyses and the NH_3-DCI spectra suggest that the AK1012 core has structure 3 (Fig. 19). However, a number of structural features of the AK1012 core remain to be determined. These include the configuration of the linkages between the glycosyl units, the absolute configuration of the glycosyl units and the alanine, and which of the two glycosyl units is attached to the branched heptose at C-7 and at C-3. Application of ^{1}H and ^{13}C NMR techniques should provide further insight into the structure of the AK1012 core now that the basic framework of the molecule has been established.

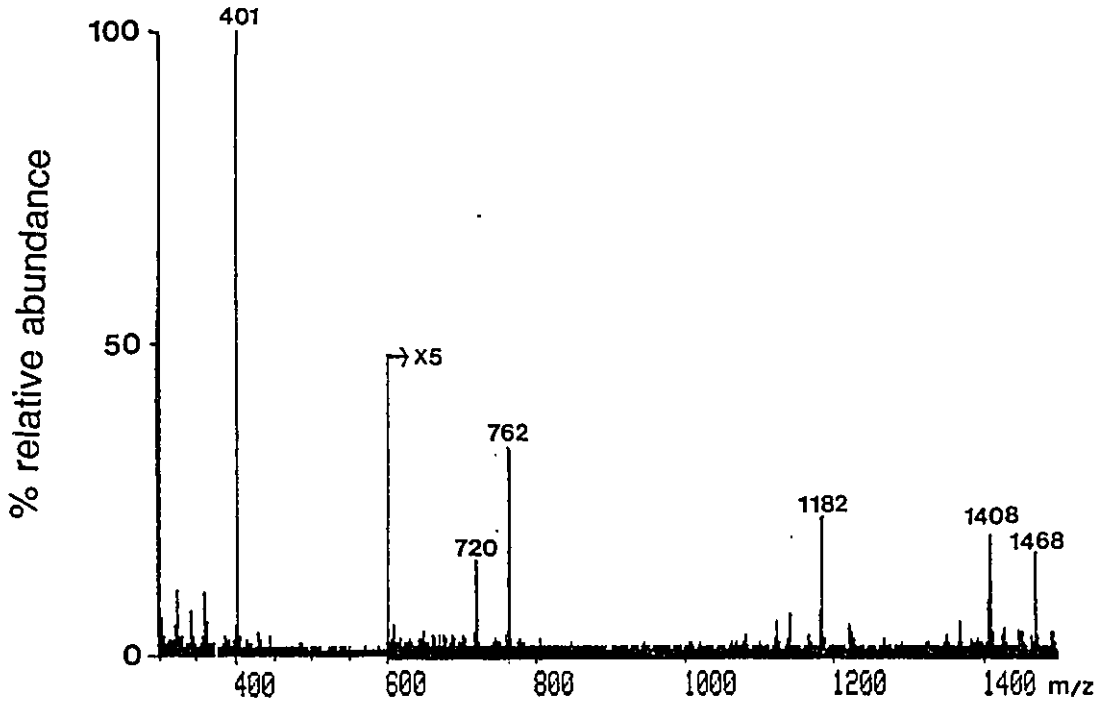

Figure 22. FAB mass spectrum of acetylated AK1012 core (the apparent absence of isotope peaks is a function of the printer resolution).

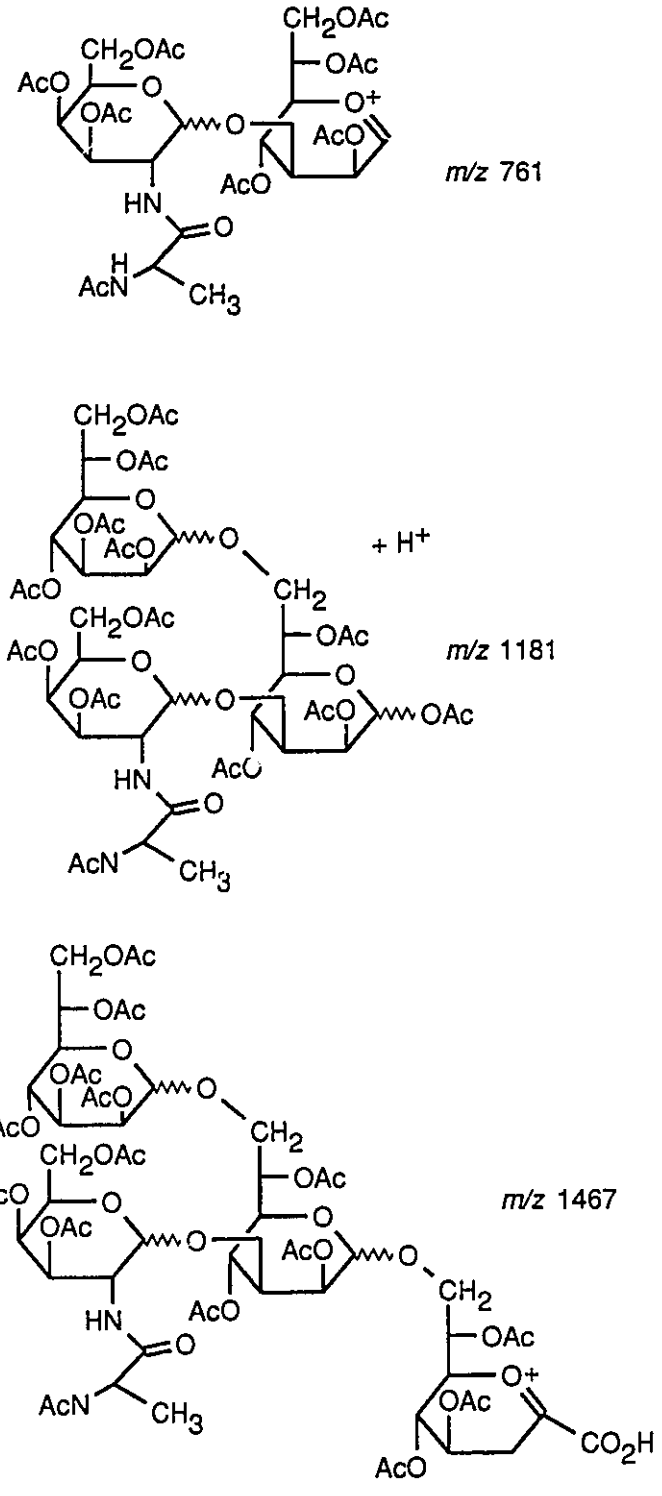

Scheme 29

4.7.2 Mass Spectrometry of the AK1401 Core

An NH_3-DCI MS spectrum of the peracetylated dephosphorylated AK1401 core (Fig. 23) exhibits an ion at *m/z* 331 that corresponds in mass to oxonium ion ***h*** and ions at *m/z* 366 and 408 that correspond in mass to the ammonium adduct ions ***i*** and ***j***, respectively. All of these ions are consistent with the presence of a terminal glucose in the AK1401 core.

The ion at *m/z* 561 corresponds to a disaccharide oxonium ion with structure ***k***, and the ion at *m/z* 596 corresponds to an ammonium adduct with structure ***i***. The rhamnose moiety was assigned to the reducing end in ions ***k*** and ***l*** because there are no ions in the spectrum that correspond to a terminal rhamnose and because the methylation analysis indicated that the rhamnose in the AK1401 core is 2-linked.

The ions at *m/z* 654 and *m/z* 696 are assigned structures ***m*** and ***n***, respectively. These ions are both consistent with a structure in which there is a non-reducing terminal glucose which is attached to another glucose. The ions at *m/z* 884 and *m/z* 926 correspond in mass to ions ***o*** and ***p***, respectively. These ions may be derived from any of structures 4-8 (Fig. 20), but not structure 9 (Fig. 20) because it does not contain a fragment with two glucoses and one rhamnose. No ions are observed which correspond to a tetrasaccharide fragment containing three glucoses and one rhamnose. Such an ion should be evident in the spectrum of the AK1401 core if any of structures 4-6 (Fig. 20) are correct.

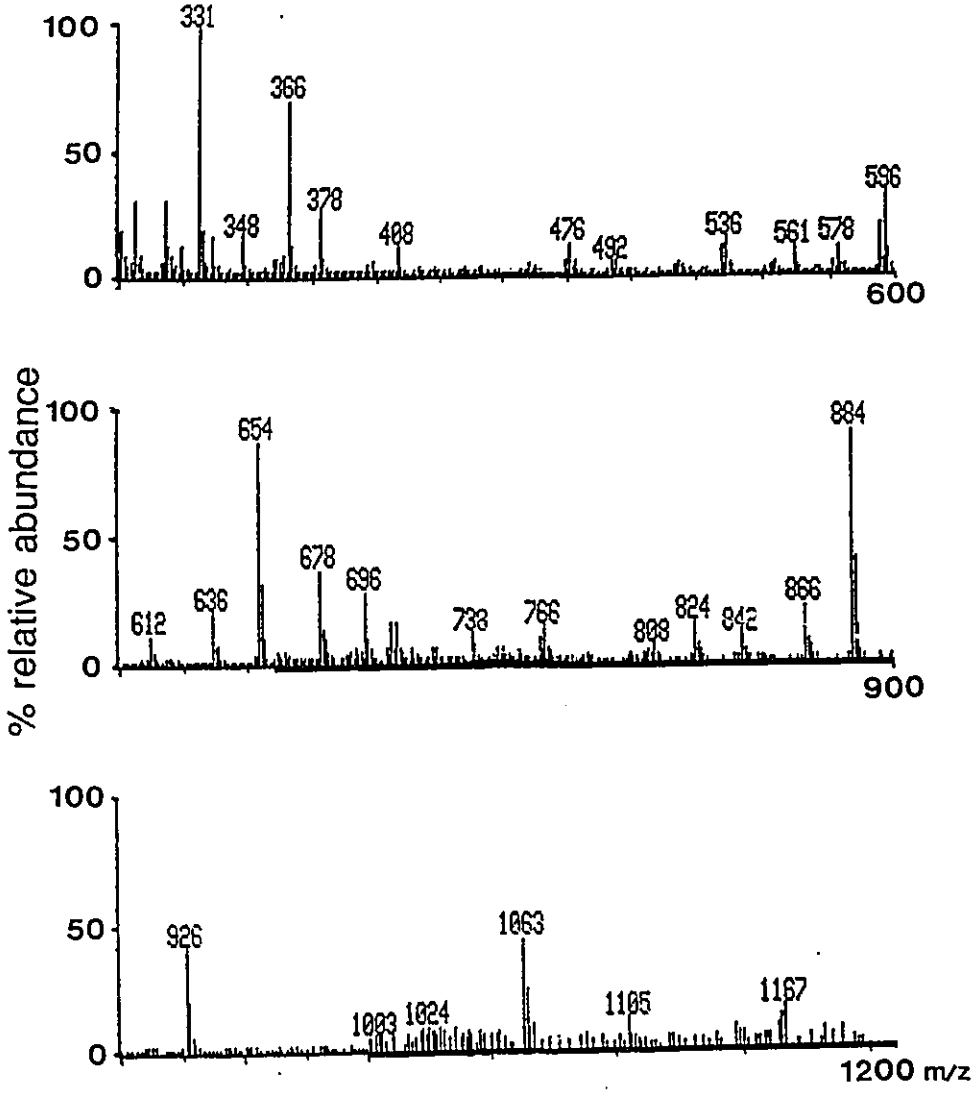

Figure 23. NH_3-DCI mass spectrum of acetylated AK1401 core.

The ion at *m/z* 766 is tentatively assigned structure ***q***. The ion was not sufficiently abundant to perform a MIKES experiment, which might have provided support for the assigned structure. The ion at *m/z* 1063 is assigned structure ***r***. This ion might be derived from a hep-hep-hep unit or from a hep-hep-KDO unit, in the original structure. The NH_3-DCI mass spectrum of the AK1401 core exhibits also an ion at *m/z* 1167. This ion is again assigned structure ***g***. The presence of ions ***r*** and ***g*** in the spectrum of the AK1401 core suggests that the inner region of this core has the same structure as the AK1012 core, namely Structure 3 (Fig. 19).

The peracetylated dephosphorylated AK1401 core was examined by FAB-MS also. Spectra were acquired over two mass ranges to simplify their acquisition. The low mass region of the spectrum is shown in Figure 24 and the high mass region of the spectrum is shown in Figure 25. The ion at *m/z* 1783 (Fig. 25) is assigned structure ***s*** based on the mass spectrometric evidence and on the chemical analysis. Ion ***s*** indicates that both branches of the outer core are attached to the galactosamine unit. This ion is still present in the spectrum after mild base hydrolysis, suggesting that the alanyl moiety is linked to the amine of the galactosamine unit.

If the core had structure 4,5, or 6 it might be expected to fragment as shown in Scheme 30 to afford ions at *m/z* 689 and *m/z* 731. No such ions are observed in the FAB spectra of the AK1401 core suggesting that the outer portion of the core does not include a tetrasaccharide containing three glucose units and one rhamnose unit. This result is in agreement with the results obtained from the

NH_3 DCI-MS analysis of the core and eliminates structures 4-6 (Fig. 20) as possible structures of the AK1401 core.

The other diagnostic ions in the FAB spectra of the AK1401 core may be derived from the *m/z* 1783 ion as outlined in Scheme 31. The ions at *m/z* 1223 and *m/z* 1265 can only be derived from a structure which has a non-reducing terminal glucose linked to a rhamnose unit. Of the remaining possible core structures (structures 7 and 8), only structure 8 has the arrangement of glucose and rhamnose described above. Thus, the results of the mass spectrometric analysis of the peracetylated dephosphorylated AK1401 core are consistent with a structure in which the inner core has the same sequence of monosaccharides as the AK1012 core, namely structure 3 (Fig. 19) and the outer portion of the AK1401 core has structure 8 (Fig. 20).

There are two other ions of note visible in the high mass FAB spectrum of the AK1401 core (Fig. 25). These ions appear at *m/z* 1034 and *m/z* 1670 and correspond in mass to the structures shown in Scheme 32. It is uncertain at this point whether the free amine results from loss of the alanyl moiety during mass spectrometric analysis, although this seems the most likely explanation. If the core had lacked the alanyl moiety prior to acetylation, the amine would have been acetylated. Similarly, if the alanyl moiety had been lost during acetylation then the amine should have been acetylated.

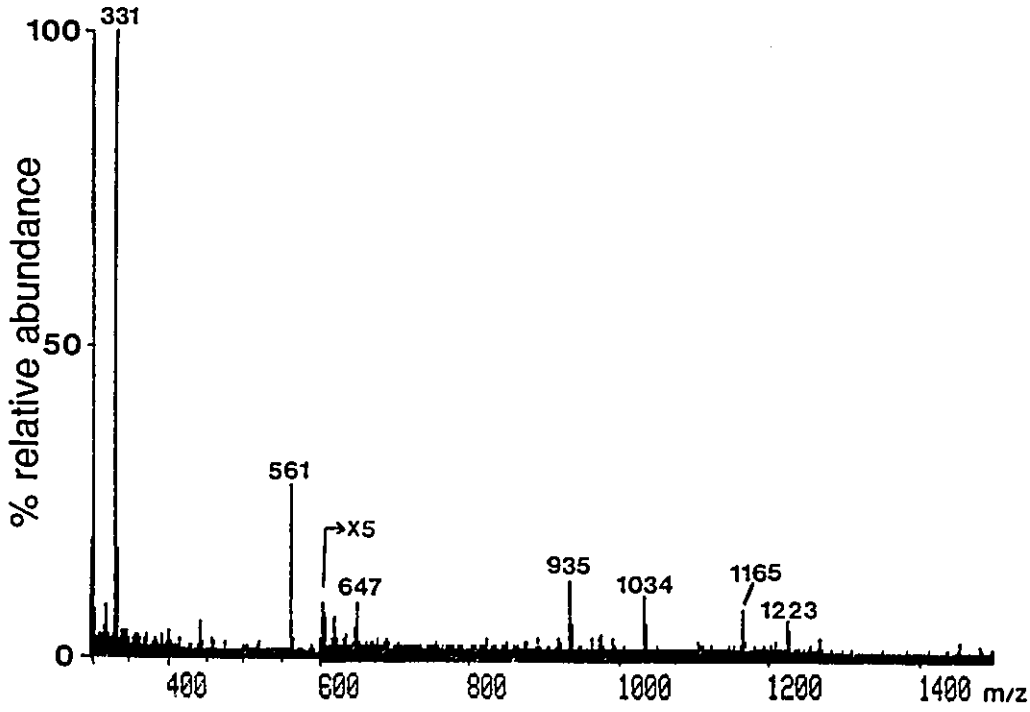

Figure 24. FAB mass spectrum of acetylated AK1401 core in the region *m/z* 300-*m/z* 1500.

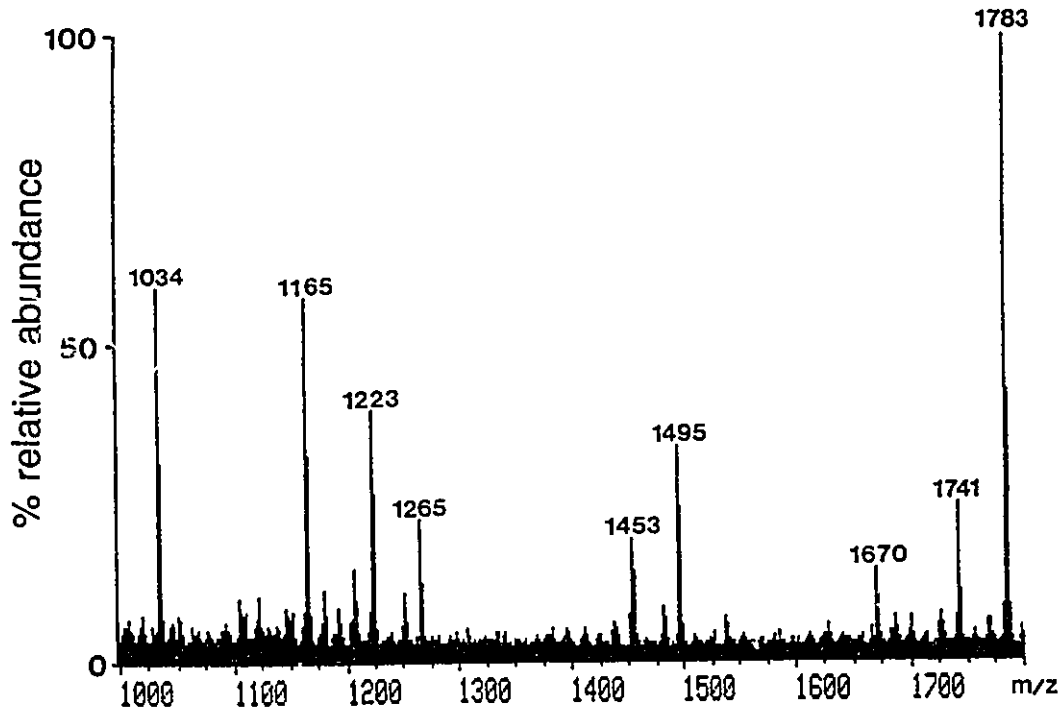

Figure 25. FAB mass spectrum of peracetylated AK1401 core in the region *m/z* 1000-*m/z* 1800.

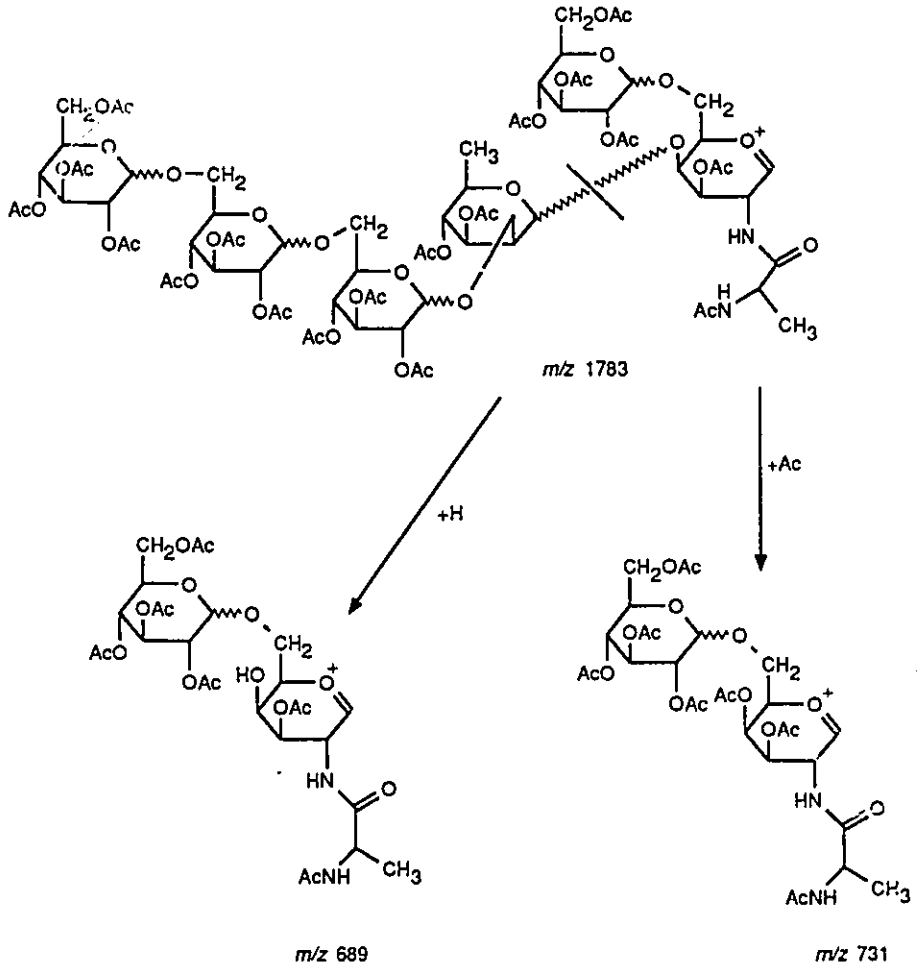

Scheme 30

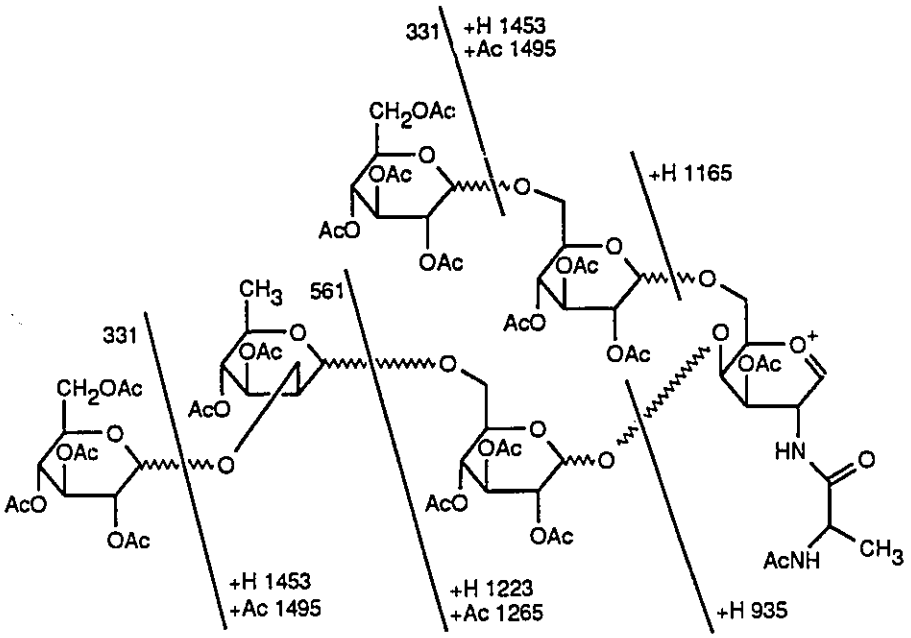
331
+H 1453
+Ac 1495
CH2OAc
OAc
AcO
OAc
+H 1165
CH3
561
331
CH2OAc
OAc
AcO
OAc
AcO
OAc
OAc
AcO
OAc
HN
O
AcNH
CH3
+H 1453
+Ac 1495
+H 1223
+Ac 1265
+H 935

Scheme 31

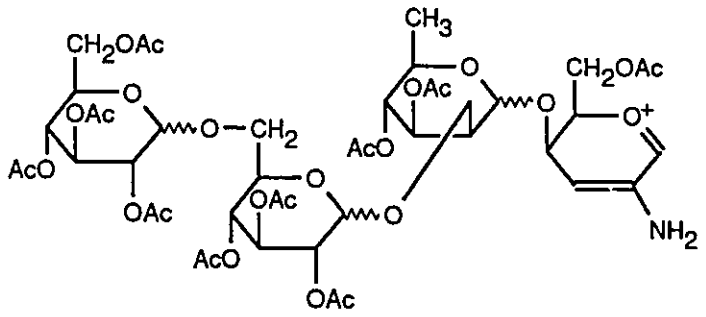

m/z 1034

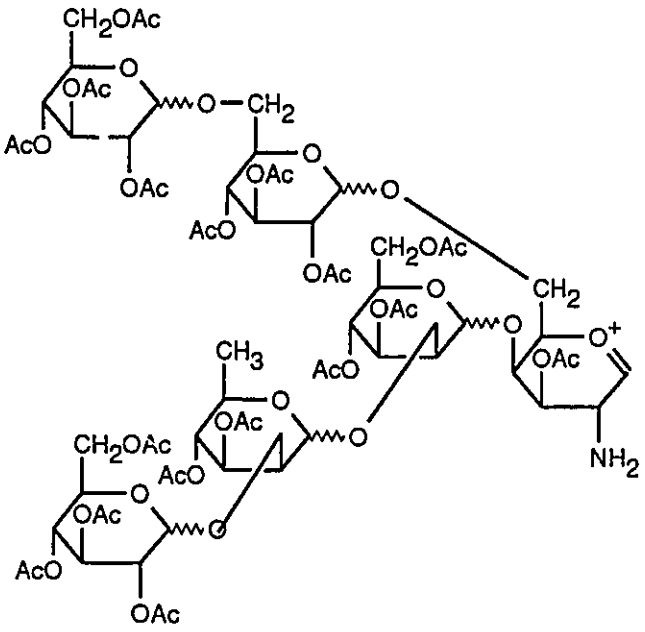

m/z 1670

Scheme 32

The proposed structure of the AK1401 core is similar to that proposed by Drewry *et al.*[59] for a related Pseudomonad (see Fig. 26). In their study, the core was characterized by a combination of chemical, enzymatic and mass spectrometric analyses. The chemical analyses included methylation analysis of the intact LPS and a number of oligosaccharides obtained by partial hydrolysis of the core. Enzymatic digests of the products of partial hydrolysis indicated the configuration of some of the linkages. The partial hydrolysis products were analyzed also by EI-MS of their trimethyl silyl ether derivatives. Based on their analyses, Drewry *et al.*[59] proposed the structure shown in Figure 26.

The aspects of the AK1012 core that remain uncertain are also uncertain in the case of the AK1401 core (see 4.7.1 p.134). In addition, the position of the linkages to the GalNAla residue have yet to be determined for the AK1401 core. A mild hydrolysis of the core might yield fragments amenable to methylation analysis or NMR analysis. Further work along these lines should lead to the structural elucidation of the AK1401 core.

4.8 Phosphate Analysis

Phosphorus-31 NMR spectra of the AK1012 and AK1401 cores (Fig. 27a and 27b) indicate that both cores contain phosphate. The splitting patterns of the signals in the ^{31}P NMR spectra could not be interpreted. The indistinct splitting patterns may be the result of overlapped signals caused by heterogeneity in the degree and position of phosphorylation of the cores. This heterogeneity may be

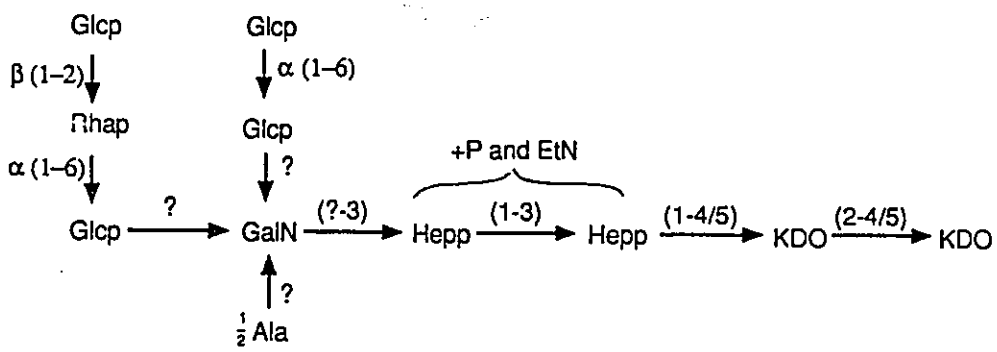

Where: Glcp is glucopyranose
Rhap is rhamnopyranose
Hepp is L-glycero-D-manno-heptopyranose
4/5 is 4 or 5
P is phosphate
EtN is ethanolamine

Figure 26. Proposed structure of P. aeruginosa N.C.T.C. 1999.[59]

natural or the result of degradation of the core in the course of its isolation. The signals at approximately +1 ppm have chemical shifts which suggest that they are due to phosphomonoester residues while those signals between approximately -5 and -12 ppm may be due to pyrophosphate residues.[93] The chemical shift of the signals at approximately -19 ppm is consistent with that of the middle phosphate residue in a triphosphate, suggesting that both cores contain at least some triphosphate.[93]

Two samples of the AK1012 core (15 mg each) were sent to Canadian Microanalytical Service Ltd., Delta, B.C. for phosphorus analysis. The analyses indicated that they contained 6.93 and 6.89 percent by weight of phosphorus. Given that the carbohydrate backbone of the AK1012 core shown in Figure 19 is correct, then the reported amount of phosphorus is consistent with the presence of approximately three phosphate residues per core. A similar analysis on the AK1401 core was not performed because of the large sample requirements.

The phosphates in the core interfere with the analyses performed on the cores and were therefore removed prior to the analyses discussed above. Nevertheless, a compositional analysis of the native cores proved informative. The results of the analyses are summarized in Table 6. The decrease in the relative abundance of the heptose in the native cores indicates that at least some of the heptoses are phosphorylated. A more precise location of the phosphate residues present in the cores might be made by means of ^{13}C-NMR. Those carbon atoms bearing a phosphate residue would be shifted down-field relative to their positions

in the spectra of the dephosphorylated cores. Such an experiment would necessitate assigning the ^{13}C spectra of the core oligosaccharides.

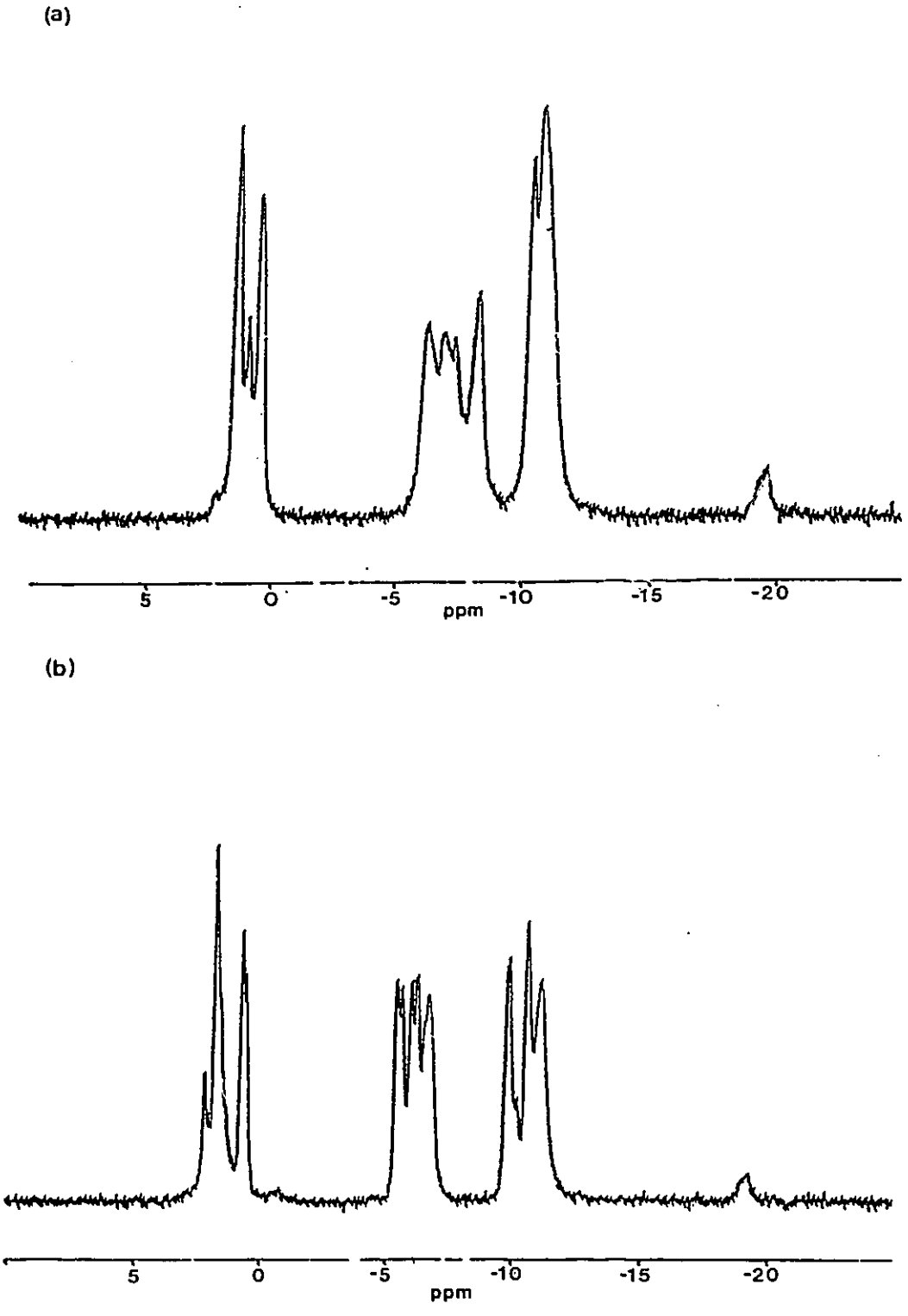

Figure 27. ^{31}P-NMR spectra of (a) native AK1401 core (b) native AK1012 core

Table 6. Comparison of the results from the compositional analyses of native and dephosphorylated AK1012 and AK1401 cores.

	AK1012		AK1401	
	Relative abundance		Relative abundance	
Component[a]	Dephos.[b]	Native	Dephos.	Native
rhamnitol	---	---	4.1	3.9
glucitol	---	---	16.2	16.0
heptitol	3.7	1.0	4.8	1.2
galactosaminitol	1.0	1.0	1.0	1.0

[a] Components were analyzed as their alditol peracetates.
[b] Dephos. = Dephosphorylated

CHAPTER 5

CONCLUSION

The ammonia (NH_3 and ND_3) DCI mass spectra of three peracetylated hexopyranoses (glucose, mannose and galactose) were acquired and examined. MIKE experiments were performed on the ammonium ion adducts and the oxonium ion observed at *m/z* 331 in the spectra of these monosaccharides. The peracetylated hexopyranoses were found to fragment by initial loss of the substituent at C-1 and subsequent losses of acetic acid and ketene. The MIKE spectra suggested that the losses of acetic acid and ketene proceed along the same pathway as that proposed previously for the same compounds under FAB conditions. Experiments on peracetylated glucopyranose using ND_3-DCI mass spectrometry suggest that an additional mode of fragmentation may involve the substitution of the acetate at C-1 by ammonia.

Three peracetylated gentiobioses were examined by NH_3-DCI MS and by MIKES experiments. Two of the octa-*O*-acetyl gentiobioses were labelled with trideuteroacetyl groups, one was labelled on the reducing end and the other was labelled on the non-reducing end. MIKE experiments on the $[M+NH_4]^+$ ions indicated that they fragment by loss of acetic acid and the elements of ammonium acetate, both of which are derived from the reducing end of the molecule. Additionally, the $[M+NH_4]^+$ ions fragment by fission of the glycosidic bond on the non-reducing side of the glycosidic oxygen to afford an oxonium derived from the non-reducing end of the disaccharide. The NH_3-DCI spectra of the labelled

disaccharides exhibited also ions that appear to be derived from a heterolytic cleavage of the $[M+NH_4]^+$, on the reducing side of the glycosidic oxygen. These ions are not derived from the $[M+NH_4]^+$ ion; however, their origin is still unknown. Ions which appear to result from loss of ketene from the $[M+NH_4]^+$ are also not derived from that ion. They appear to result from the random loss of the acetate groups of the disaccharides, possibly by a mechanism involving ammonolysis.

Another mode of fragmentation of the peracetylated disaccharides may formally be considered to involve fission of the glycosidic bonds, at either side of the glycosidic oxygen, with the attachment of H or CH_3CO to the glycosidic oxygen and subsequent complexation with ammonium. These ions are derived primarily from the non-reducing end of the disaccharides but are not derived direct from the $[M+NH_4]^+$ ion. The formation of the H transfer ions may involve a process other than heterolytic cleavage of a glycosidic bond; however, the nature of the process has not been determined. The mechanism for the formation of the acyl transfer ions is also unknown, although there is evidence that suggests that the transfer does not involve the addition of ketene to a fragment with a free hydroxyl. Another labelled compound is being synthesized and will be analyzed subsequently in the hope that it will provide further clues to the origin of the acyl transfer ions.

The peracetylated disaccharides undergo a fragmentation of the non-reducing ring to afford ions derived from the reducing end of the disaccharide containing a formyl group at the position of the linkage. These ring fragmentation ions are ammonium ion adducts which MIKE experiments have shown to undergo

fragmentation by loss of the elements of ammonium acetate. The resulting oxonium ions undergo further fragmentation by losses of acetic acid, formic acid and ketene. The ring fragmentation ions are not derived direct from the $[M+NH_4]^+$ ions. They may be produced by a mechanism involving reductive cleavage of the non-reducing ring.

Ring fragmentation ions containing a formyl group are produced also in DEI-MS of peracetylated hexopyranose disaccharides (except for the 1,1-linkage isomers). They appear at *m/z* 317 in the spectra of each of the (1→6)-, (1→4)-, (1→3)- and (1→2)-linked disaccharides and have isomeric structures in which the position of the formyl group reflects the position of the glycosidic linkage in the parent disaccharide. The MS spectra of these isomeric ions are distinct, thereby allowing the differentiation of the linkage isomers. The (1→6)-, (1→4)-, (1→3)- and (1→2)-linkage isomers of mannose disaccharides and the (1→6)- and (1→4)-linkage isomers of galactose disaccharides could be differentiated in the same manner. Additionally, this technique was successfully applied to the determination of the position of linkage between the glycosyl units in two flavonoid glycosides of known structure.

The structure of the core oligosaccharides derived from the lipopolysaccharides of two mutants of the bacterium Pseudomonas aeruginosa strain PAO1 were investigated. The composition of the cores was determined by GC and GC-MS analysis of the alditol peracetates derived from the oligosaccharides. Methylation analysis provided information on linkage positions

and ring sizes. Further structural information was obtained from the analysis of the products obtained from the selective degradation of the cores with $NaIO_4$ and subsequent reduction with $NaBD_4$. The information from these chemical analyses allowed a number of possible isomeric structures to be proposed for each of the cores. FAB and NH_3-DCI mass spectrometry of the dephosphorylated peracetylated cores was used to differentiate among the possible isomeric structures. The NH_3-DCI mass spectra exhibited ions which provided information that was in some instances complementary to the information provided by the FAB spectra; thus NH_3-DCI MS is useful in the analysis of the core oligosaccharides. The FAB mass spectra of the dephosphorylated peracetylated AK1012 core exhibited a number of anomalous ions that could not be interpreted in terms of the structure that was arrived at from the results of the other analyses. The origin of these ions is unknown and therefore the proposed structure of the AK1012 core must be viewed with caution. The results of the analyses described above suggest that the AK1012 core and the AK1401 core have the following structures:

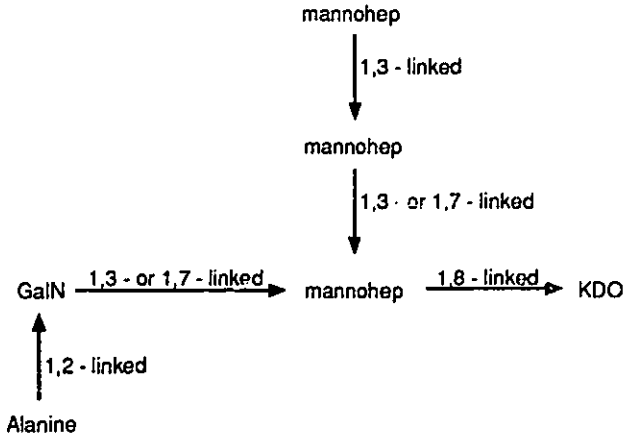

AK 1012

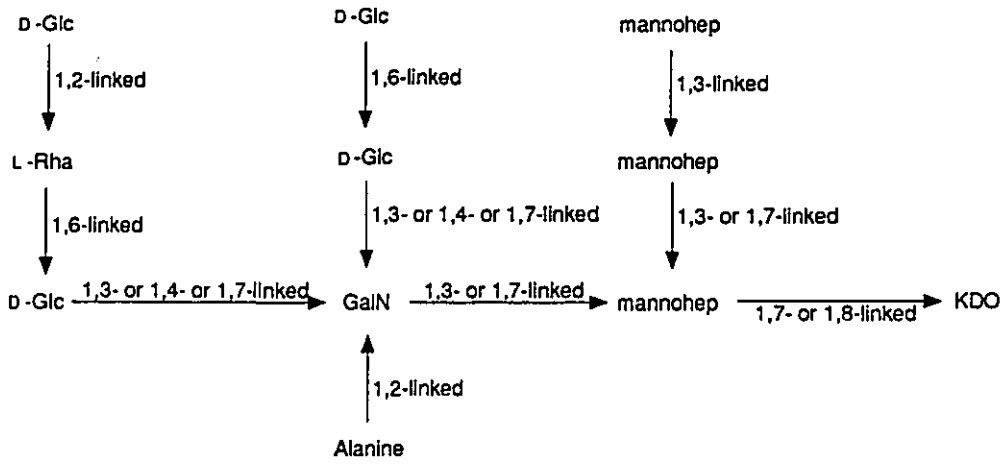

AK 1401
where mannohep = mannoheptopyranose

A number of aspects of the core structures remain to be determined. These include the absolute configuration of a number of the monosaccharides, the positions of the linkages to the galactosamine in the AK1401 core, the relative arrangement of the substituents of the branched heptose and the configuration of the glycosidic linkages. The absolute configuration may be determined by measuring the optical rotation of the monosaccharides. Elucidation of the remaining unknown aspects of the core structures may be achieved by the use of NMR methods.

REFERENCES

1. N.K. Kochetkov and O.S. Chizhov. Adv. Carbohydr. Chem. **21**, 39 (1966).
2. T. Radford and D.C. DeJongh. In *Biochemical Applications of Mass Spectrometry*. Ed. G.R. Waller. Wiley Interscience, New York, NY. p313, 1972.
3. T. Radford and D.C. DeJongh. In *Biochemical Applications of Mass Spectrometry*. 1st Supplementary Volume. Ed. G.R. Waller and O.C. Dermer. Wiley Interscience, New York, NY. p256, 1980.
4. A. Dell and G.W. Taylor. Mass Spectrom. Rev. **3**, 357 (1984).
5. V.N. Reinhold and S.A. Carr. Mass Spectrom. Rev. **2**, 153 (1983).
6. V.N. Reinhold. Methods in Enzymology. **138**, 59 (1987).
7. A. Dell. Adv. Carbohydr. Chem. Biochem. **45**, 19 (1987).
8. Y.A. Knirel. Crit. Rev. Microbiol. **17**, 273 (1990).
9. J.F. Stoddart. *Stereochemistry of Carbohydrates*. Wiley Interscience, New York, NY. 1971.
10. J.R. Chapman. In *Practical Organic Mass Spectrometry*. John Wiley and Sons Ltd., Chichester, [West Sussex]. 1985.
11. F.W. McLafferty. *Interpretation of Mass Spectra*. 3rd Edition, University Science Books. Mill Valley, CA. 1980.
12. M.S.B. Munson and F.H. Field. J. Am. Chem. Soc. **88**, 2621 (1966).

13. J.B. Westmore and M.M. Alauddin. Mass Spectrom. Rev. **5**, 381 (1986).

14. A.G. Harrison. *Chemical Ionization Mass Spectrometry.* CRC Press Inc. Boca Raton, FL., 1983.

15. M.A. Baldwin and F.W. McLafferty. Org. Mass Spectrom. **7**, 1353 (1973).

16. M. Barber, R.S. Bordoli, R.D. Sedgwick, and A.N. Tyler. J. Chem. Soc., Chem. Comm. 325 (1981).

17. L.D. Detter, O.W. Hand, R.G. Cooks, and R.A. Walton. Mass Spectrom. Rev. **7**, 465 (1988).

18. M. Barber, R.S. Bordoli, R.D. Sedgwick, and A.N. Tyler. Nature. **293**, 270 (1981).

19. E. Schröder, H. Münster, and H. Budzikiewicz. Org. Mass Spectrom. **21**, 707 (1986).

20. J.H. Beynon, R.G. Cooks, J.W. Amy, W.E. Baitinger, and T.Y. Ridley. Anal. Chem. **45**, 1023A (1973).

21. T. Ast, M.H. Bozorgzadeh, J.L. Wiebers, J.H. Beynon, and A.G. Brenton. Org. Mass Spectrom. **14**, 313 (1979).

22. K. Levsen and H. Schwarz. Angew. Chem. Int. Ed. **15**, 509 (1976).

23. K. Biemann, D.C. DeJongh, and H.K. Schnoes. J. Am. Chem. Soc. **85**, 1763 (1963).

24. T.C. Smale and E.S. Waight. J. Chem. Soc., Chem. Comm. 680 (1966).

25. K. Heyns and D. Müller. Tetrahedron Lett. **48**, 6061 (1966).

26. W.W. Binkley, R.C. Dougherty, D. Horton, and J.D. Wander. Carbohydr. Res. **17**, 127 (1971).

27. K.G. Das and B. Thayumanavan. Org. Mass Spectrom. **10**, 455 (1975).

28. C. Bosso, F. Taravel, J. Ulrich, and M. Vignon. Org. Mass Spectrom. **13**, 477 (1978).

29. T. Fujiwara and K. Arai. Carbohydr. Res. **87**, 11 (1980).

30. J. Guerrera and C.E. Weill. Carbohydr. Res. **27**, 471 (1973).

31. O.S. Chizhov, N.K. Kochetkov, N.N. Malysheva, A.I. Shiyonok, and V.L. Chashchin. Org. Mass Spectrom. **5**, 1157 (1971).

32. A.M. Hogg and T.L. Nagabhushan. Tetrahedron Lett. **47**, 4827 (1972).

33. D. Horton, J.D. Wander, and R.L. Foltz. Carbohydr. Res. **36**, 75 (1974).

34. S.-E. Sun, Y.-T. Long, X.-M. Wang, K.-W. Huang, R.-C. Li, and D.-P. Lu. Acta Chimica Sinica. **42**, 736 (1984).

35. R.C. Dougherty, J.D. Roberts, W.W. Binkley, O.S. Chizhov, V.I. Kadentsev, and A.A. Solov'yov. J. Org. Chem. **39**, 451 (1974).

36. H. Egge and J. Peter-Katalinić. Mass Spectrom. Rev. **6**, 331 (1987).

37. R. Guevremont and J.L.C. Wright. Rapid Commun. Mass Spectrom. **1**, 12 (1987).

38. R. Guevremont and J.L.C. Wright. Rapid Commun. Mass Spectrom. **2**, 47 (1988).

39. R. Guevremont, V.P. Pathak, and J.L.C. Wright. Org. Mass Spectrom. **25**, 101 (1990).

40. D.R. Mueller, B.M. Domon, W. Blum, F. Raschdorf, and W.J. Richter. Biomed. Environ. Mass Spectrom. **15**, 441 (1988).

41. E.G. de Jong, W. Heerma, J. Haverkamp, and J.P. Kamerling. Biomed. Mass Spectrom. **6**, 72 (1979).

42. E.G. de Jong, W. Heerma, and C.A.X.G.F. Sicherer. Biomed. Mass Spectrom. **6**, 242 (1979).

43. E.G. de Jong, W. Heerma, and G. Dijkstra. Adv. Mass Spectrom. **8B**, 1314 (1980).

44. E.G. de Jong, W. Heerma, and G. Dijkstra. Biomed. Mass Spectrom. **7**, 127 (1980).

45. J.W. Dallinga and W. Heerma. Biol. Mass Spectrom. **20**, 99 (1991).

46. D. Garozzo, M. Giuffrida, G. Impallomeni, A. Ballistreri, and G. Montaudo. Anal. Chem. **62**, 279 (1990).

47. A. Ballistreri, G. Montaudo, D. Garozzo, M. Giuffrida, and G. Impallomeni. Rapid Commun. Mass Spectrom. **3**, 302 (1989).

48. J.W. Dallinga and W. Heerma. Biomed. Environ. Mass Spectrom. **18**, 363 (1989).

49. J.W. Dallinga and W. Heerma. Biol. Mass Spectrom. **20**, 215 (1991).

50. B. Domon, D.R. Müller, and W.J. Richter. Org. Mass Spectrom. **24**, 357 (1989).

51. B. Domon, D.R. Müller, and W.J. Richter. Biomed. Environ. Mass Spectrom. **19**, 390 (1990).

52. B. Domon, D.R. Müller and W.J. Richter. Int. J. Mass Spectrom. Ion Processes. **100**, 301 (1990).

53. P.J. Vandemark and B.L. Datzing. *Microbes*. Benjamin and Cummings. Don Mills, Ont. 1987.

54. O. Lüderitz, K. Tanamoto, C. Galanos, O. Westphal, U. Zähringer, E. Th. Rietschel, S. Kusumoto, and T. Shiba. Am. Chem. Soc. Symposium Series. **231**, 21 (1983).

55. S.G. Wilkinson. Rev. Infect. Dis., **5**, S941 (1983).

56. V.A. Kulshin, U. Zähringer, B. Lindner, K-E. Jäger, B.A. Dmitriev, and E. Th. Rietschel. Eur. J. Biochem. **198**, 697 (1991).

57. S.G. Wilkinson, L. Galbraith, and G.A. Lightfoot. Eur. J. Biochem. **33**, 158 (1973).

58. S.G. Wilkinson and L. Galbraith. Eur. J. Biochem. **52**, 331 (1975).

59. D.T. Drewry, K.C. Symes, G.W. Gray, and S.G. Wilkinson. Biochem J. **149**, 93 (1975).

60. P.S.N. Rowe and P.M. Meadow. Eur. J. Biochem. **132**, 329 (1983).

61. A.M. Kropinski, L.C. Chan, and F.H. Milazzo. Can. J. Microbiol. **25**, 390 (1979).

62. M. Rivera, L.E. Bryan, R.E.W. Hancock, and E.J. McGroarty. J. Bacteriol. **170**, 512 (1988).

63. M. Rivera and E.J. McGroarty. J.Bacteriol. **171**, 2244 (1989).

64. Y.A. Knirel, E.V. Vinogradov, N.A. Kocharova, N.A. Paramonov, N.K. Kochetkov, B.A. Dmitriev, E.S. Stanislavsky, and B. Lanyi. Acta Microbiologica Hungarica. **35**, 3 (1988).

65. I.R. Chester, P.M. Meadow, and T.L. Pitt. J. Gen. Microbiol. **78**, 305 (1973).

66. E.S. Stanislavskii, B.A. Dmitriev, B. Lanyi, and I. Joo. Acta Microbiologica Hungarica. **32**, 3 (1985).

67. B. Lanyi and T. Bergan. Methods Microbiol. **10**, 92 (1978).

68. P.V. Liu, H. Matsumoto, H. Kusama, and T. Bergan. Int. J. Syst. Bacteriol. **33**, 256 (1983).

69. K.F. Jarrell Ph.D. thesis. Queens University, (1979).

70. T.L. Arsenault, D.W. Hughes, D.B. MacLean, W.A. Szarek, A.M. Kropinski, and J.S. Lam. Can. J. Chem. **69**, 1273 (1991).

71. A. Fox, S.L. Morgan, and J. Gilbart. In *Analysis of Carbohydrates by GLC and MS*. Ed. C.J. Biermann and G.D. McGinnis. CRC Press, Boca Raton, FL. p87, 1989.

72. H. Björndal, C.G. Hellerqvist, B. Lindberg, and S. Svensson. Angew. Chem. Int. Ed. **9**, 610 (1970).

73. B. Lindberg. Methods Enzymol. **28B**, 178 (1972).

74. P. Jansson, L. Kenne, H. Liedgren, B. Lindberg, and J. Lönngren. Chem. Comm. **8**, University of Stockholm, Sweden (1976).

75. S. Hakomori. J. Biochem. **55**, 205 (1964).

76. I. Ciucanu and F. Kerek. Carbohydr. Res. **131**, 209 (1984).

77. N.C. Carpita and E.M. Shea. In *Analysis of Carbohydrates by GLC and MS*. Ed. C.J. Biermann and G.D. McGinnis. CRC Press, Boca Raton, FL. pp157, 1989.

78. G.O. Aspinall. In *The Polysaccharides*. Vol. 1. Ed. G.O. Aspinall. Academic Press, New York, NY. p35 1982.

79. B. Lindberg, J. Lönngren, and S. Svensson. Adv. Carbohydr. Chem Biochem. **31**, 185 (1975).

80. K. Leontein, B. Lindberg, and J. Lönngren. Carbohydr. Res. **62**, 359 (1978).

81. L. Glaser and M.M. Burger. J. Biol. Chem. **239**, 3187 (1964).

82. J.C. Richards, M.B. Perry, and P.J. Kniskern. Can. J. Biochem. Cell Biol. **63**, 953 (1985).

83. A.I. Vogel. *A Text-Book of Practical Organic Chemistry*. Longmans. London, Eng. 1987.

84. P.Z. Allen. Methods Carbohydr. Chem. **1**, 372 (1962).

85. R.J. Weinkam and J. Gal. Org. Mass. Spectrom. **11**, 197 (1976).

86. D. Issachar and J. Yinon. Anal. Chem. **52**, 49 (1980).

87. A.G. Harrison and R.K.M.R. Kallury. Org. Mass Spectrom. **15**, 284 (1980).

88. R.H. Liu, I.A. Low, F.P. Smith, E.G. Piotrowski, and A.F. Hsu. Org. Mass Spectrom. **20**, 511 (1985).

89. K.G. Das, A.M. Reddy, M. Vairamani, K.P. Madhusudhanan, D. Fraise, and J.C. Tibet. Tetrahedron. **40**, 4085 (1985).

90. J.M. Peltier, R.W. Smith, D.B. MacLean, and W.A. Szarek. Carbohydr. Res. **207**, 1 (1990).

91. R.W. Kondrat and R.G. Cooks. Anal. Chem. **50**, 81A (1978).

92. unpublished results from this laboratory

93. S.G. Wilkinson. Biochem. J. **199**, 833 (1981).

APPENDIX I

Abbreviations

Ala	alanine
B	magnetic field strength
CA	collisional activation
CI	chemical ionization
CI-MS	chemical ionization mass spectrometry
DCI	desorption chemical ionization
DEI	desorption electron ionization
DMSO	dimethyl sulphoxide
e	charge on an electron
E	electric field strength
EI	electron ionization
EI-MS	electron ionization mass spectrometry
FAB	fast atom bombardment
FAB-MS	fast atom bombardment mass spectrometry
GalN	2-deoxy-2-amino galactose
Glc	glucose
GC	gas chromatography
GC-MS	gas chromatography mass spectrometry
hep	heptose
KDO	2-keto-3-deoxy-octulosonic acid

LPS	lipopolysaccharides
m	mass of the ion
m^*	observed mass of the metastable peak
m_1	mass of the metastable ion
m_2	mass of the ion produced on decomposition of the metastable ion
MIKES	mass-analysed ion kinetic energy scan
MS	mass spectrometry
MSD	mass selective detector
m/z	ratio of mass to charge
NH_3-CI	ammonia chemical ionization
NH_3-DCI	ammonia desorption chemical ionization
NMR	nuclear magnetic resonance
PA	proton affinity
PMAA	partially methylated alditol acetate
psig	pounds per square inch guage
r	radius of the ion path
Rha	rhamnose
TIC	total ion chromatogram
TLC	thin layer chromatography
TMS	tetramethylsilane
v	velocity of the ion
V	potential field strength

v/v	volume per volume
z	charge of the ion

APPENDIX II

GC-MS Spectra

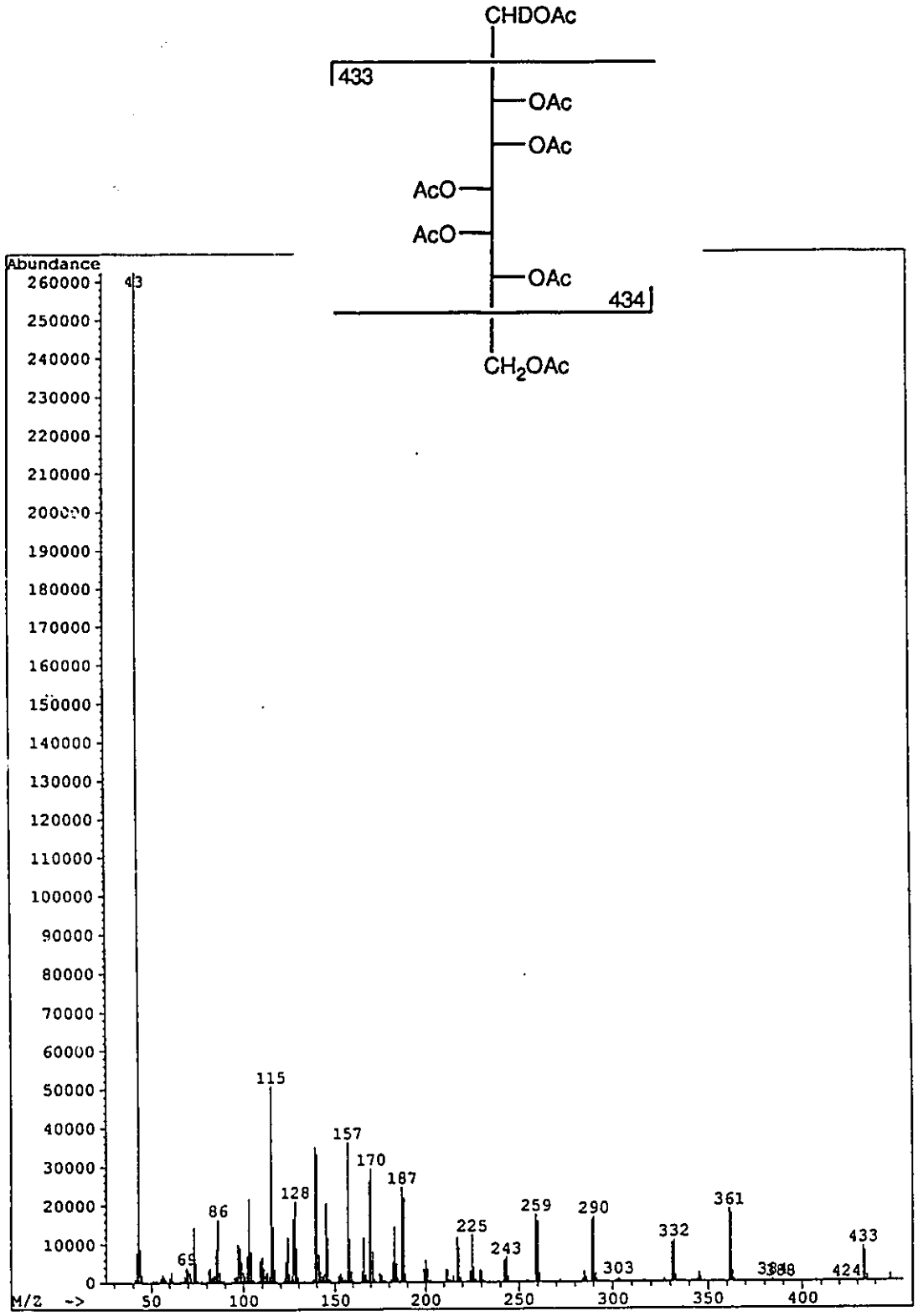
CHDOAc
433
OAc
OAc
AcO
AcO
OAc
434
CH2OAc
Abundance
260000
250000
240000
230000
220000
210000
200000
190000
180000
170000
160000
150000
140000
130000
120000
110000
100000
90000
80000
70000
60000
50000
40000
30000
20000
10000
0
M/Z ->
50
100
150
200
250
300
350
400
43
69
86
115
128
157
170
187
225
243
259
290
303
332
361
424
433

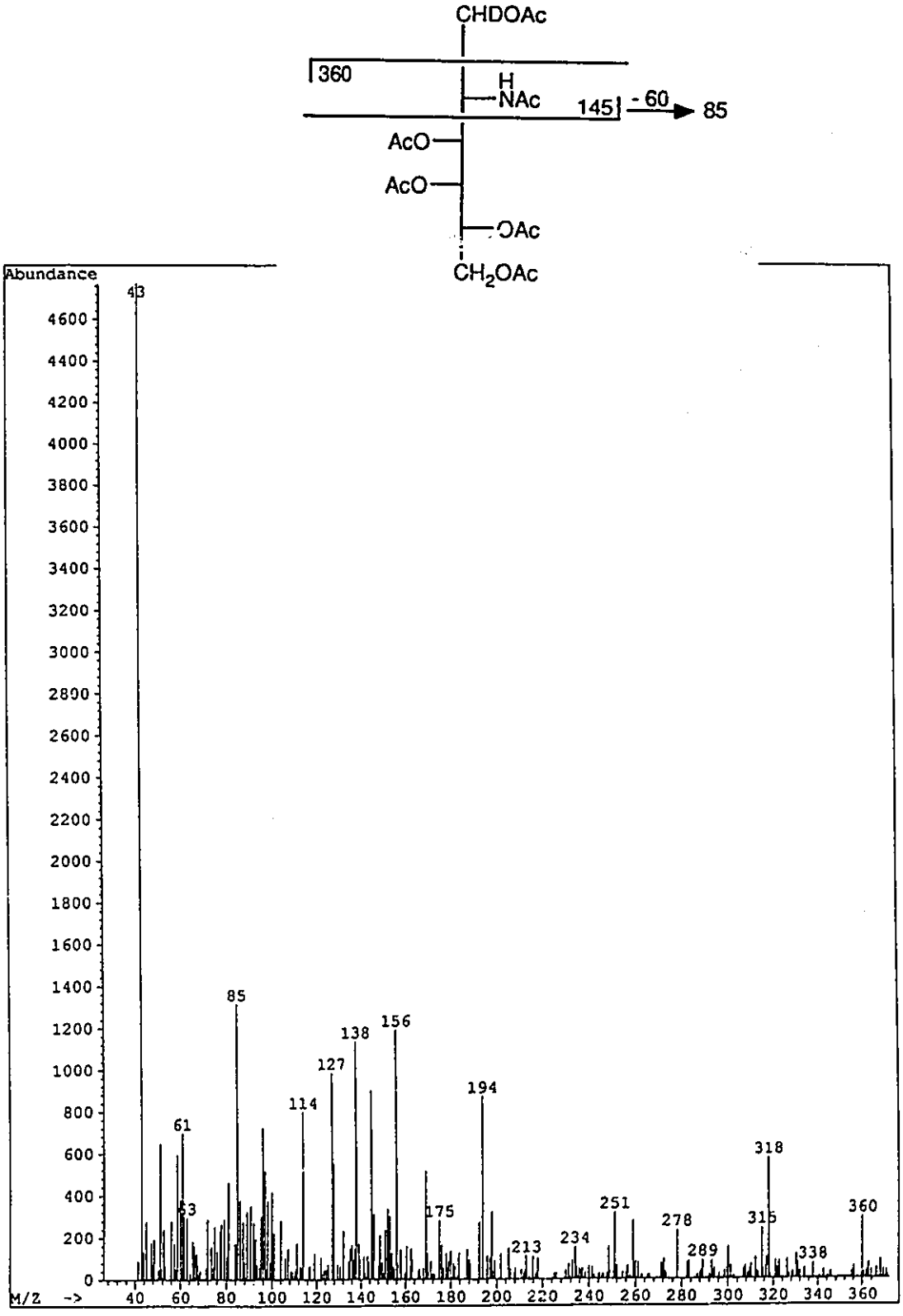
CHDOAc
360
H
NAc
145
- 60
85
AcO
AcO
OAc
CH2OAc
Abundance
43
4600
4400
4200
4000
3800
3600
3400
3200
3000
2800
2600
2400
2200
2000
1800
1600
1400
1200
1000
800
600
400
200
0
85
138
156
127
114
61
194
318
53
175
251
278
315
360
213
234
289
338
M/Z ->
40 60 80 100 120 140 160 180 200 220 240 260 280 300 320 340 360

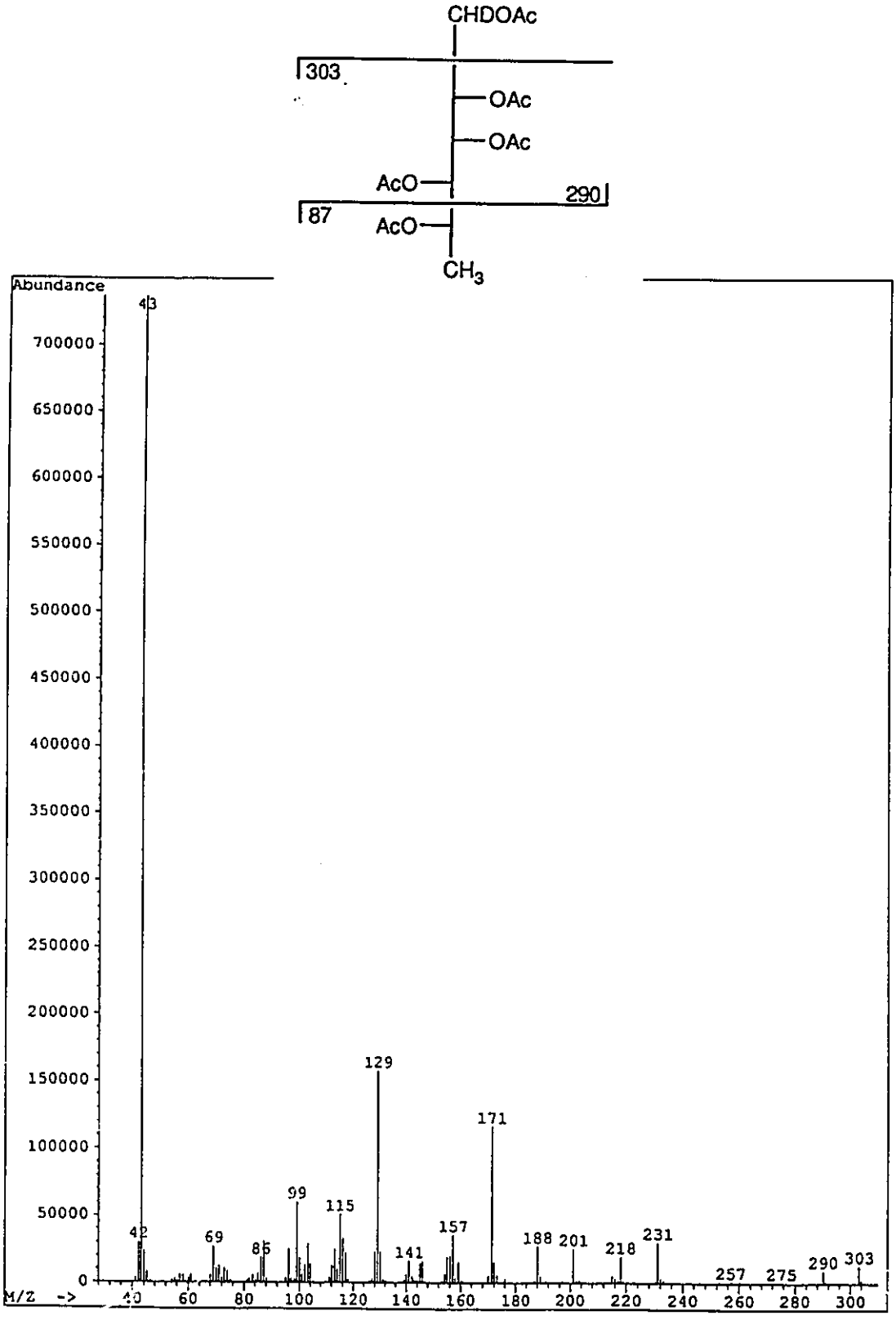
CHDOAc
303
OAc
OAc
AcO
290
87
AcO
CH3
Abundance
700000
650000
600000
550000
500000
450000
400000
350000
300000
250000
200000
150000
100000
50000
0
M/Z ->
43
42
69
85
99
115
129
141
157
171
188
201
218
231
257
275
290
303
40
60
80
100
120
140
160
180
200
220
240
260
280
300

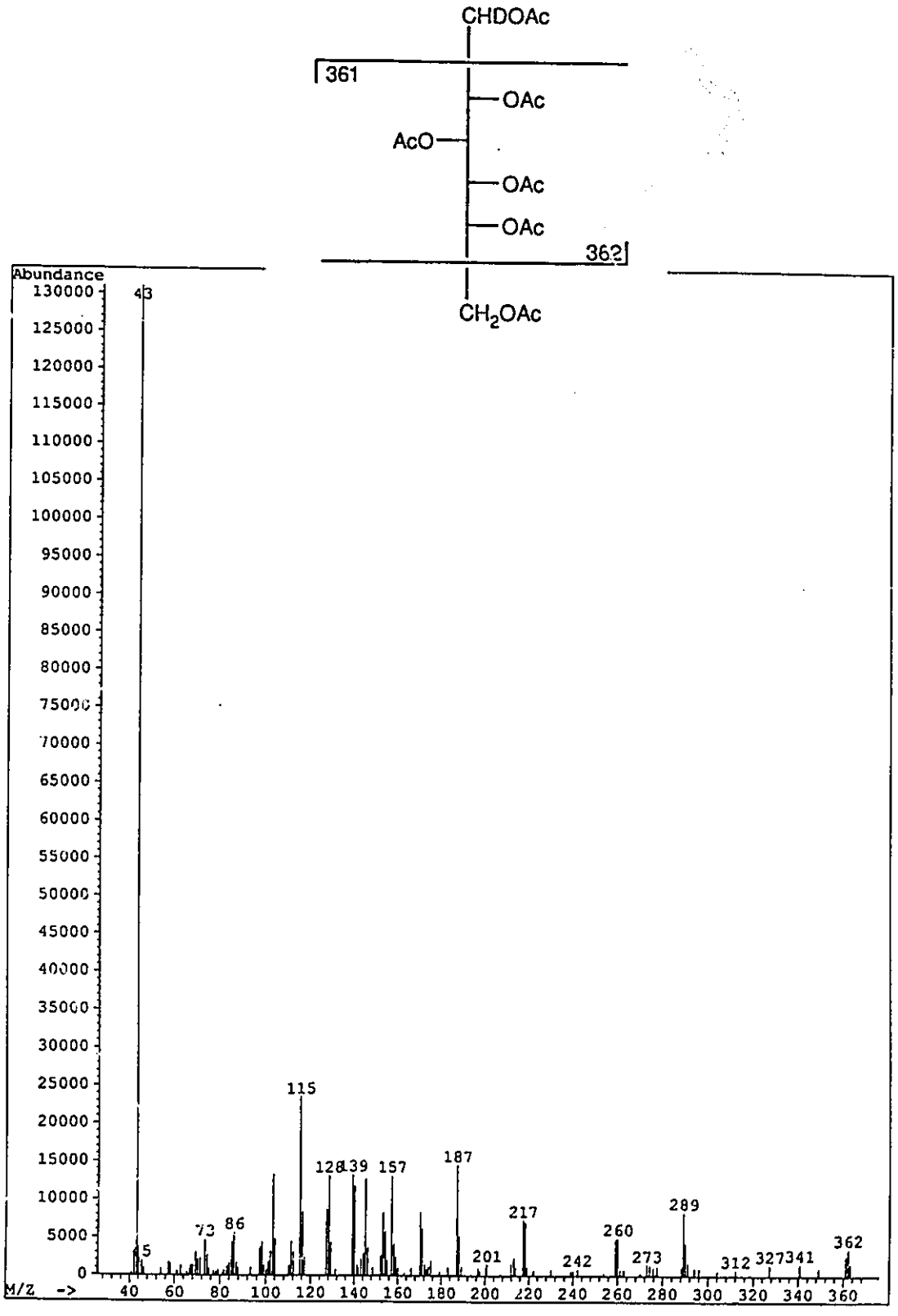
CHDOAc
361
OAc
AcO
OAc
OAc
362
CH2OAc
Abundance
130000
125000
120000
115000
110000
105000
100000
95000
90000
85000
80000
75000
70000
65000
60000
55000
50000
45000
40000
35000
30000
25000
20000
15000
10000
5000
0
M/Z ->
40 60 80 100 120 140 160 180 200 220 240 260 280 300 320 340 360
43
115
128
139
157
187
217
289
260
362
86
73
201
242
273
312
327
341

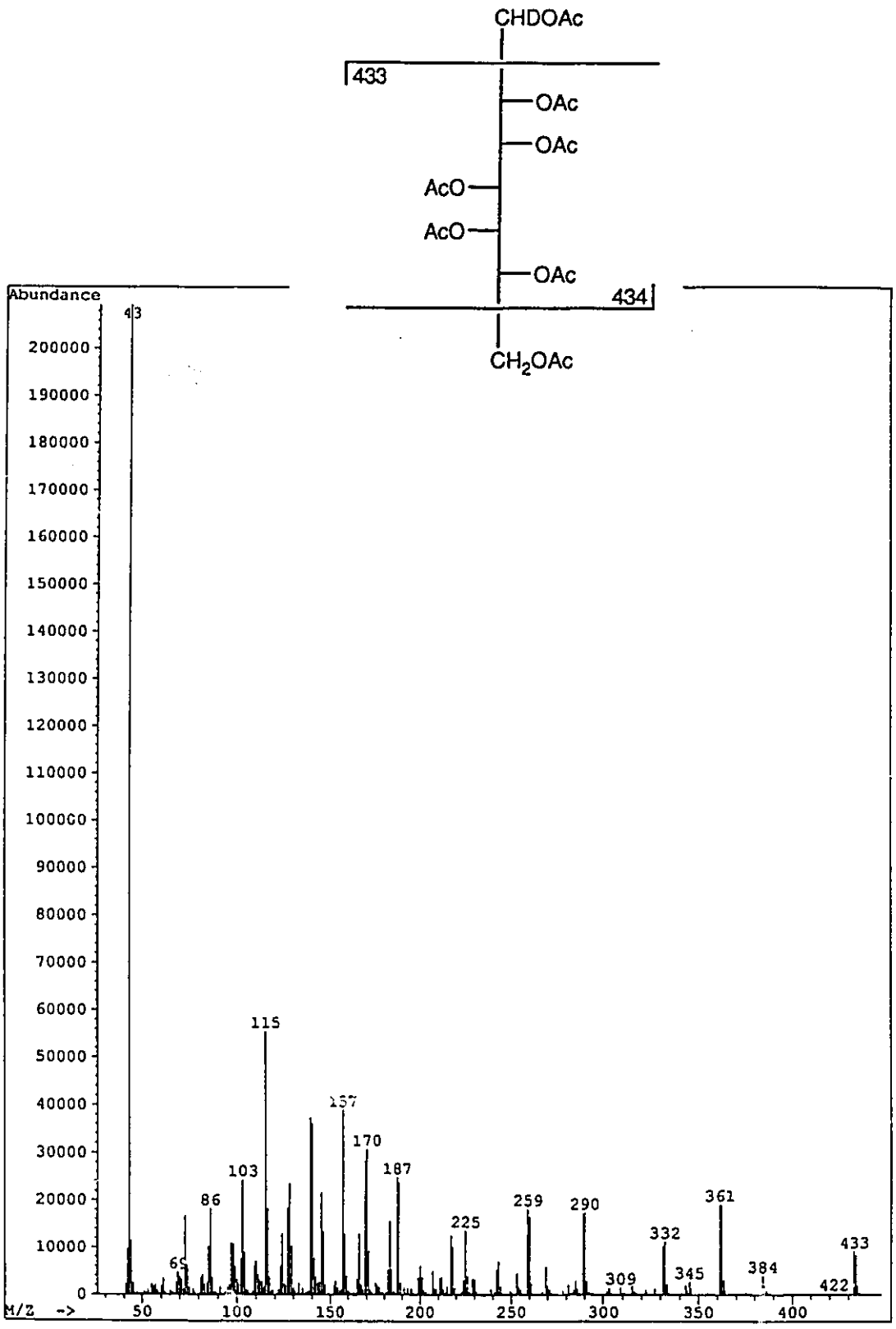
CHDOAc
433
OAc
OAc
AcO
AcO
OAc
434
CH2OAc
Abundance
M/Z ->
43
115
157
170
187
103
86
65
225
259
290
309
332
345
361
384
422
433

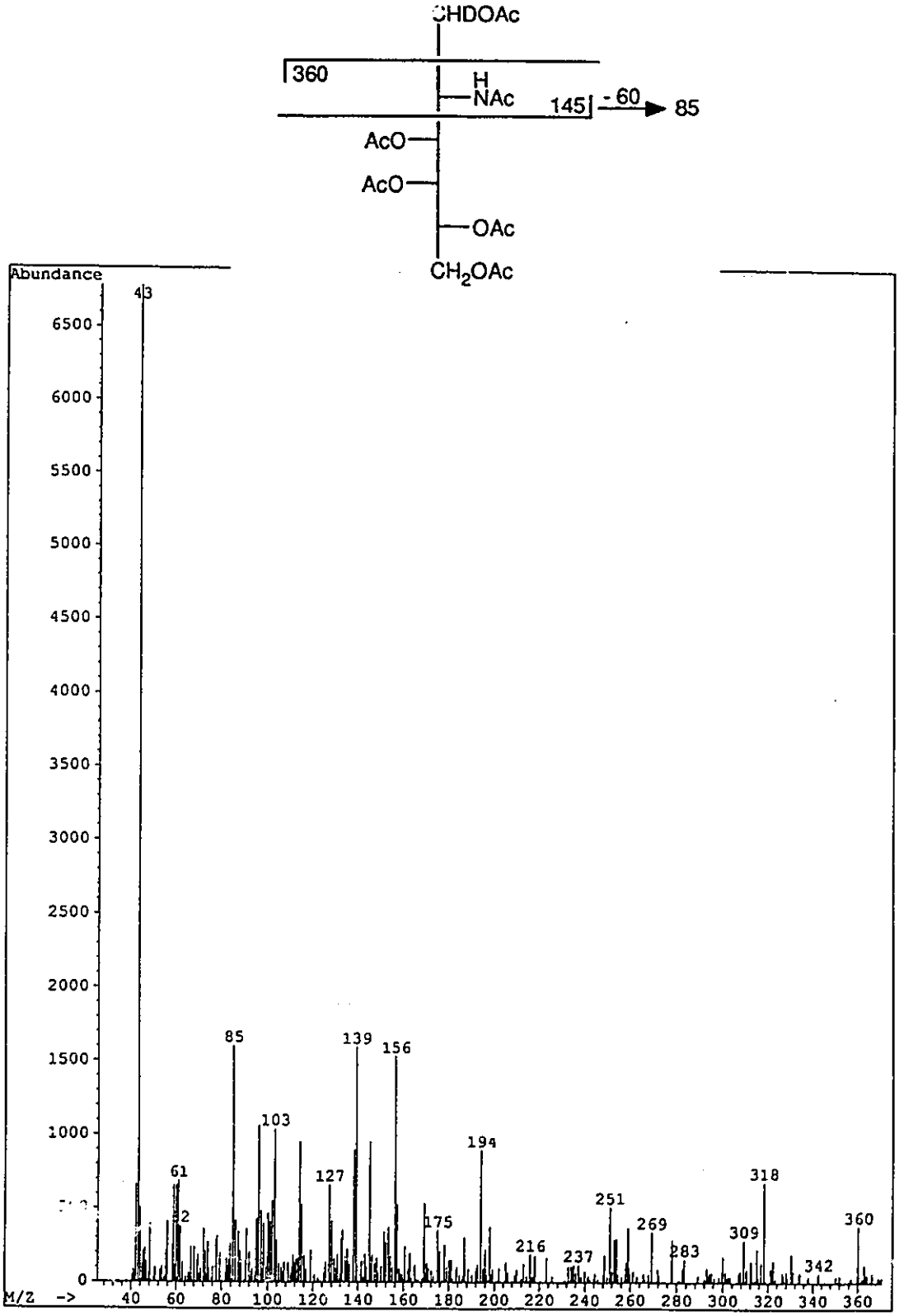
CHDOAc
360
H
NAc
145
-60
85
AcO
AcO
OAc
CH2OAc
Abundance
43
6500
6000
5500
5000
4500
4000
3500
3000
2500
2000
1500
1000
0
85
139
156
103
194
61
127
318
251
269
175
309
360
216
237
283
342
M/Z ->
40 60 80 100 120 140 160 180 200 220 240 260 280 300 320 340 360

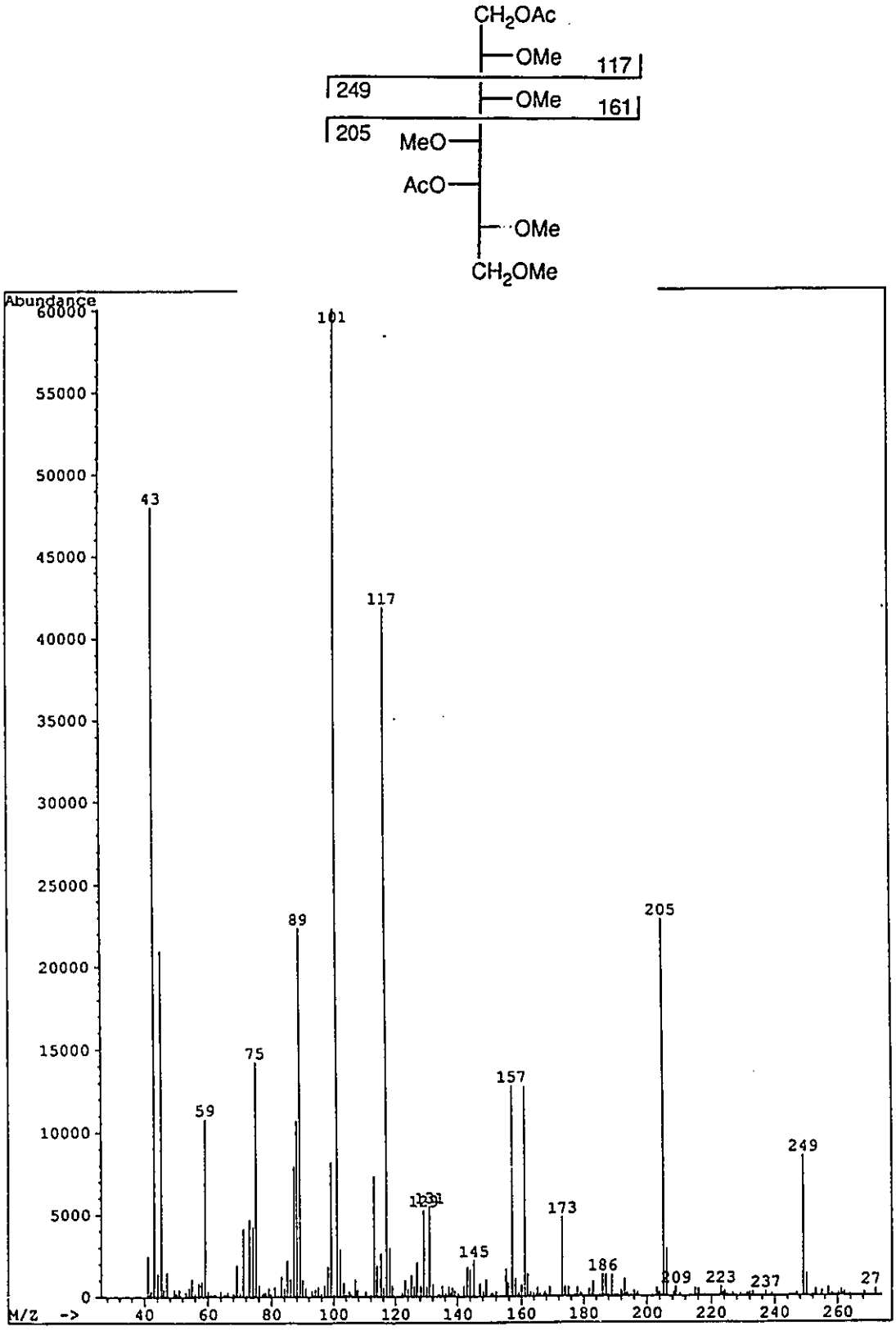
CH2OAc
OMe
117
249
OMe
161
205
MeO
AcO
OMe
CH2OMe
Abundance
60000
55000
50000
45000
40000
35000
30000
25000
20000
15000
10000
5000
0
M/Z ->
40
60
80
100
120
140
160
180
200
220
240
260
101
43
117
89
205
75
157
59
249
173
145
186
209
223
237
27

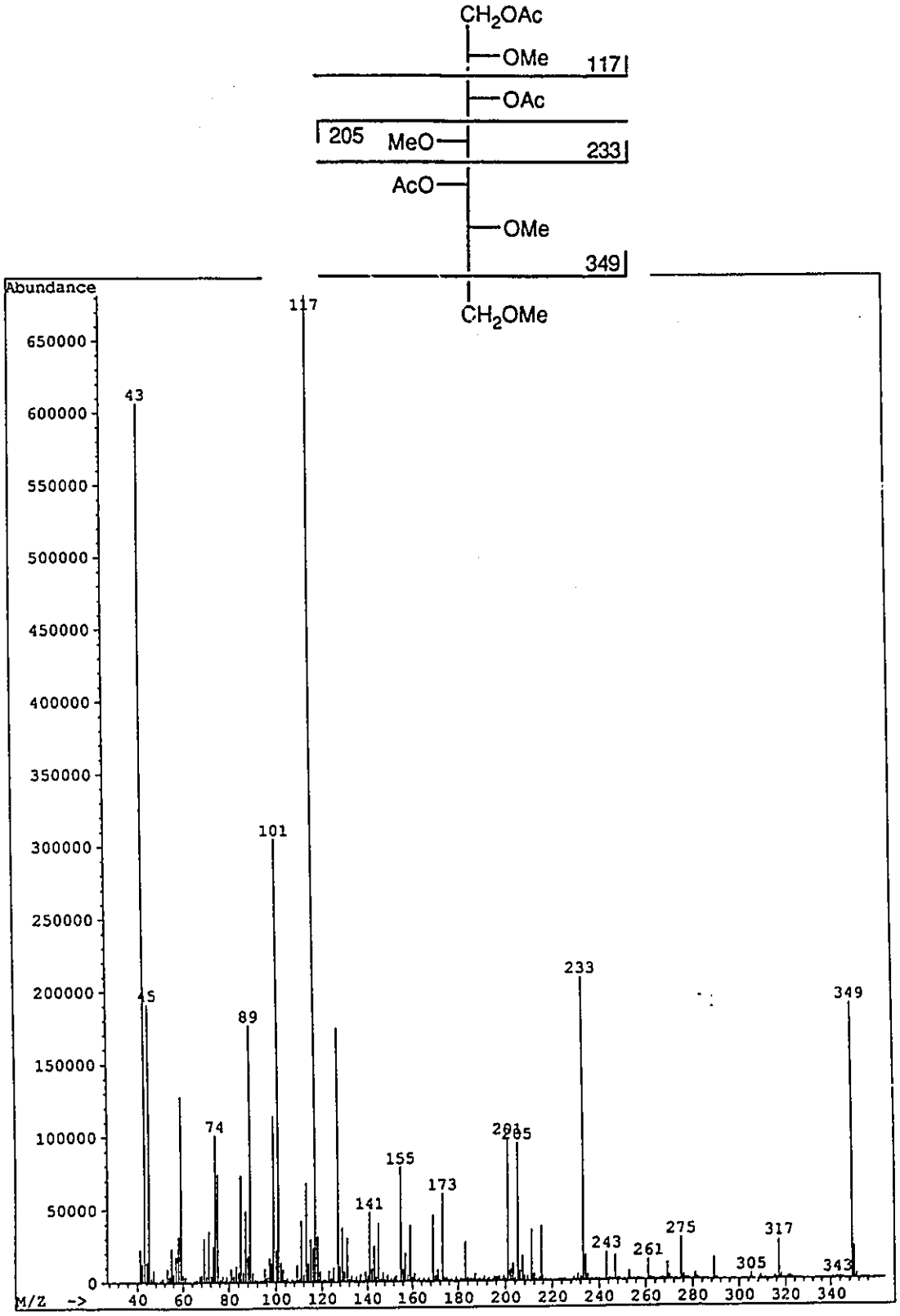
CH2OAc
OMe
117
OAc
205
MeO
233
AcO
OMe
349
CH2OMe
Abundance
650000
600000
550000
500000
450000
400000
350000
300000
250000
200000
150000
100000
50000
0
M/Z ->
40 60 80 100 120 140 160 180 200 220 240 260 280 300 320 340
43
45
74
89
101
117
141
155
173
203
205
233
243
261
275
305
317
343
349

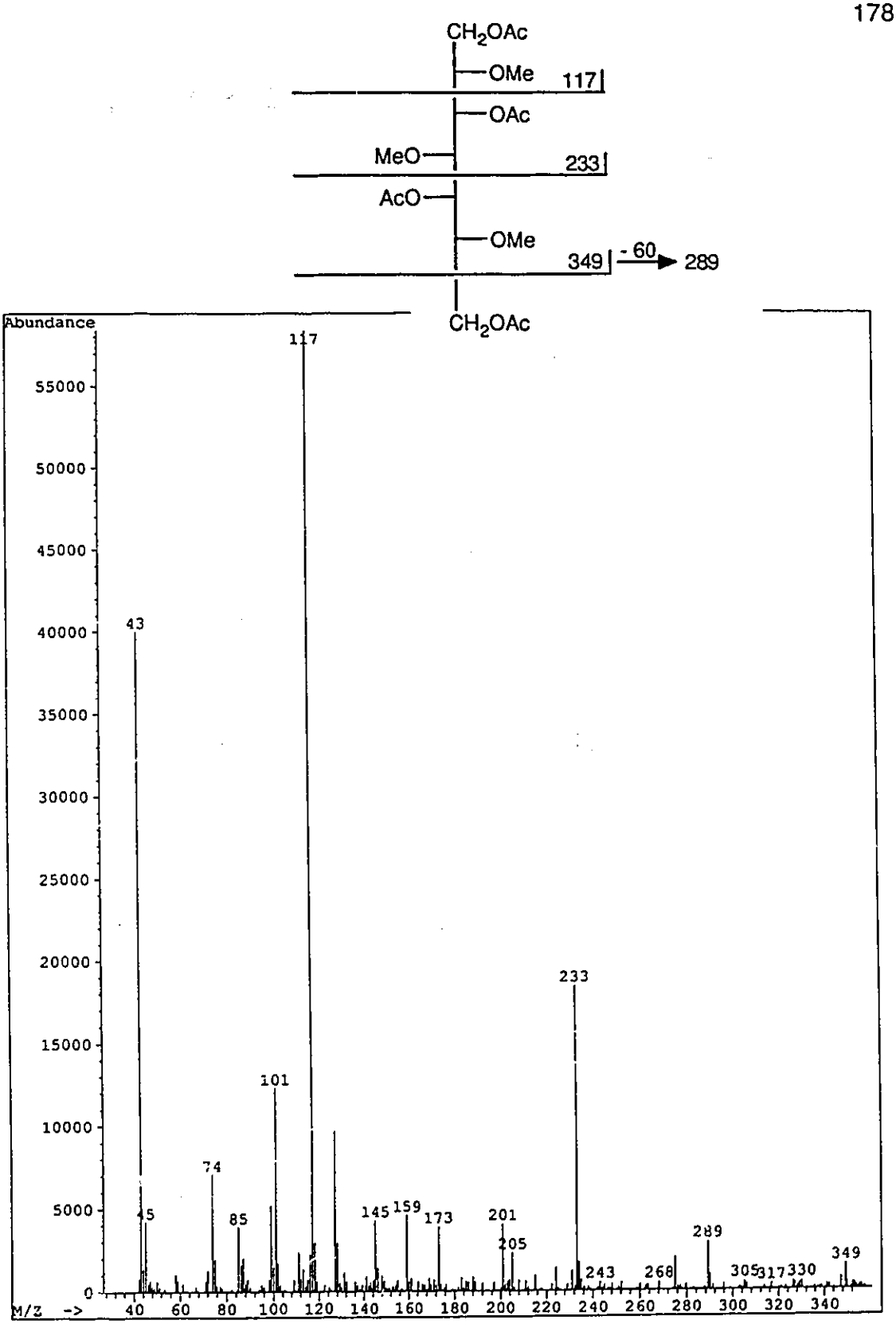
CH2OAc
OMe
117
OAc
MeO
233
AcO
OMe
349
- 60
289
CH2OAc
Abundance
55000
50000
45000
40000
35000
30000
25000
20000
15000
10000
5000
0
M/Z ->
40 60 80 100 120 140 160 180 200 220 240 260 280 300 320 340
117
43
101
74
85
45
145
159
173
201
205
233
243
268
289
305
317
330
349

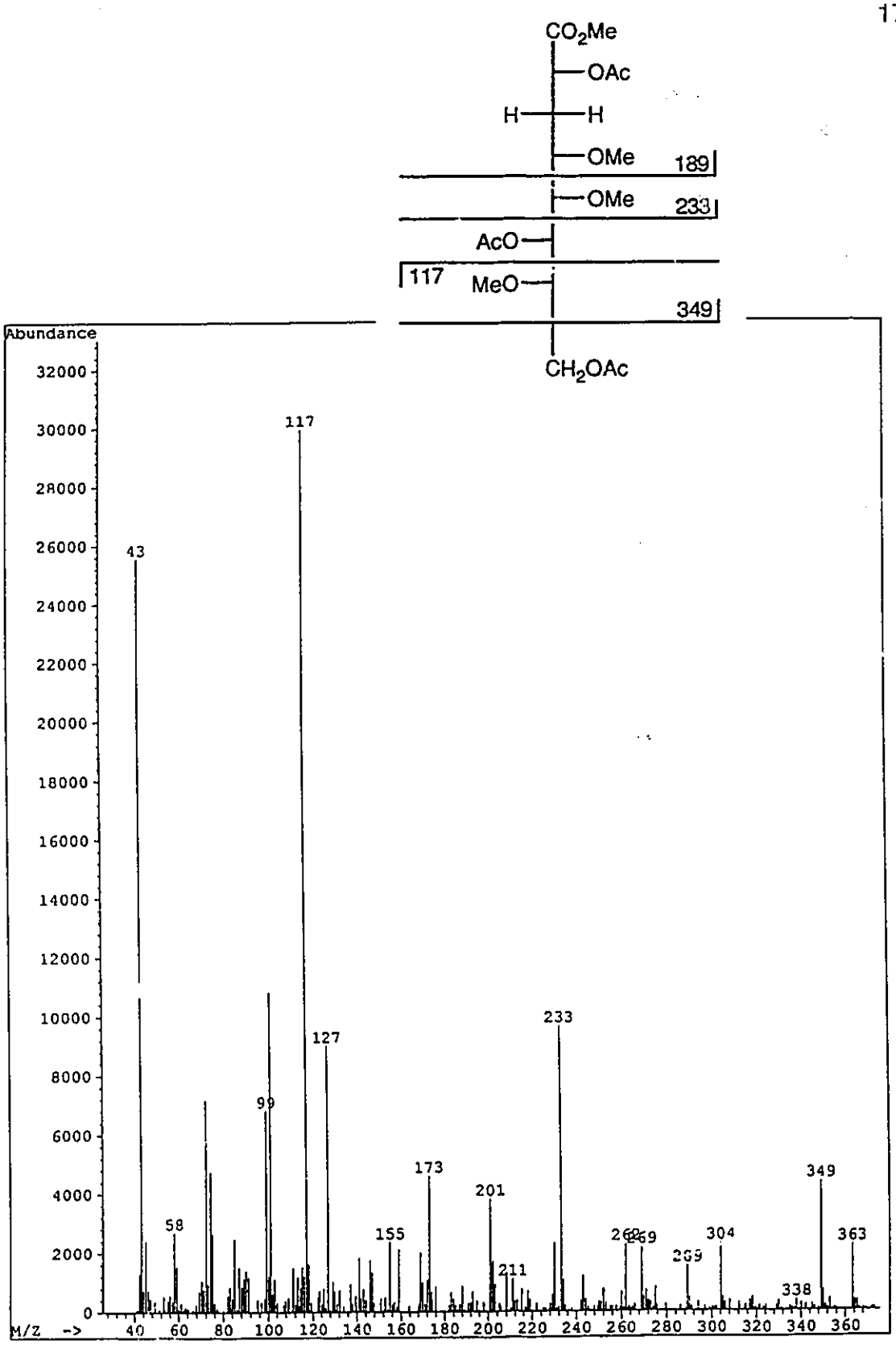
CO2Me
OAc
H
H
OMe
189
OMe
233
AcO
117
MeO
349
CH2OAc
Abundance
32000
30000
28000
26000
24000
22000
20000
18000
16000
14000
12000
10000
8000
6000
4000
2000
0
M/Z ->
40 60 80 100 120 140 160 180 200 220 240 260 280 300 320 340 360
117
43
99
127
233
173
201
58
155
211
304
363
349
338

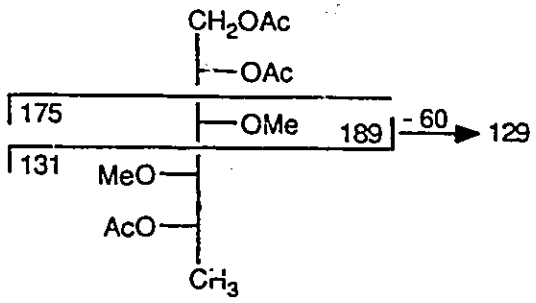
CH2OAc
OAc
175
OMe
189
- 60
129
131
MeO
AcO
CH3

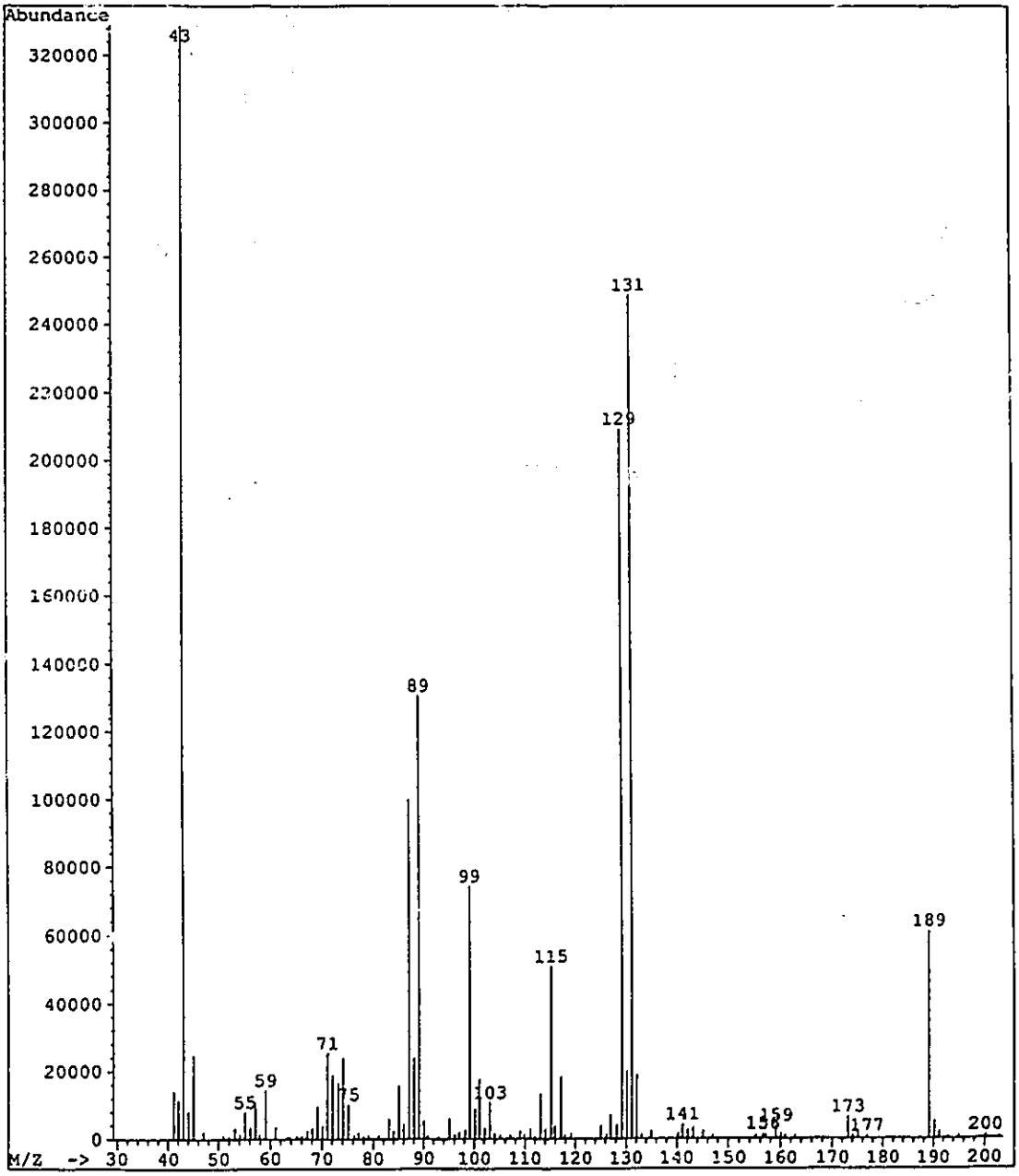
Abundance
320000
300000
280000
260000
240000
220000
200000
180000
160000
140000
120000
100000
80000
60000
40000
20000
0
M/Z ->
30 40 50 60 70 80 90 100 110 120 130 140 150 160 170 180 190 200
43
131
129
89
99
189
115
71
59
55
75
103
141
159
173
177
200

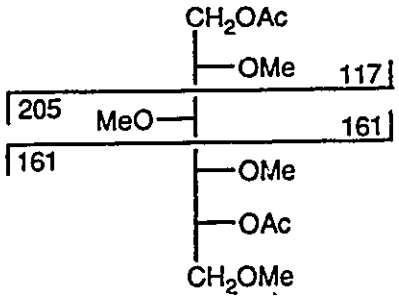
CH2OAc
OMe
117
205
MeO
161
161
OMe
OAc
CH2OMe

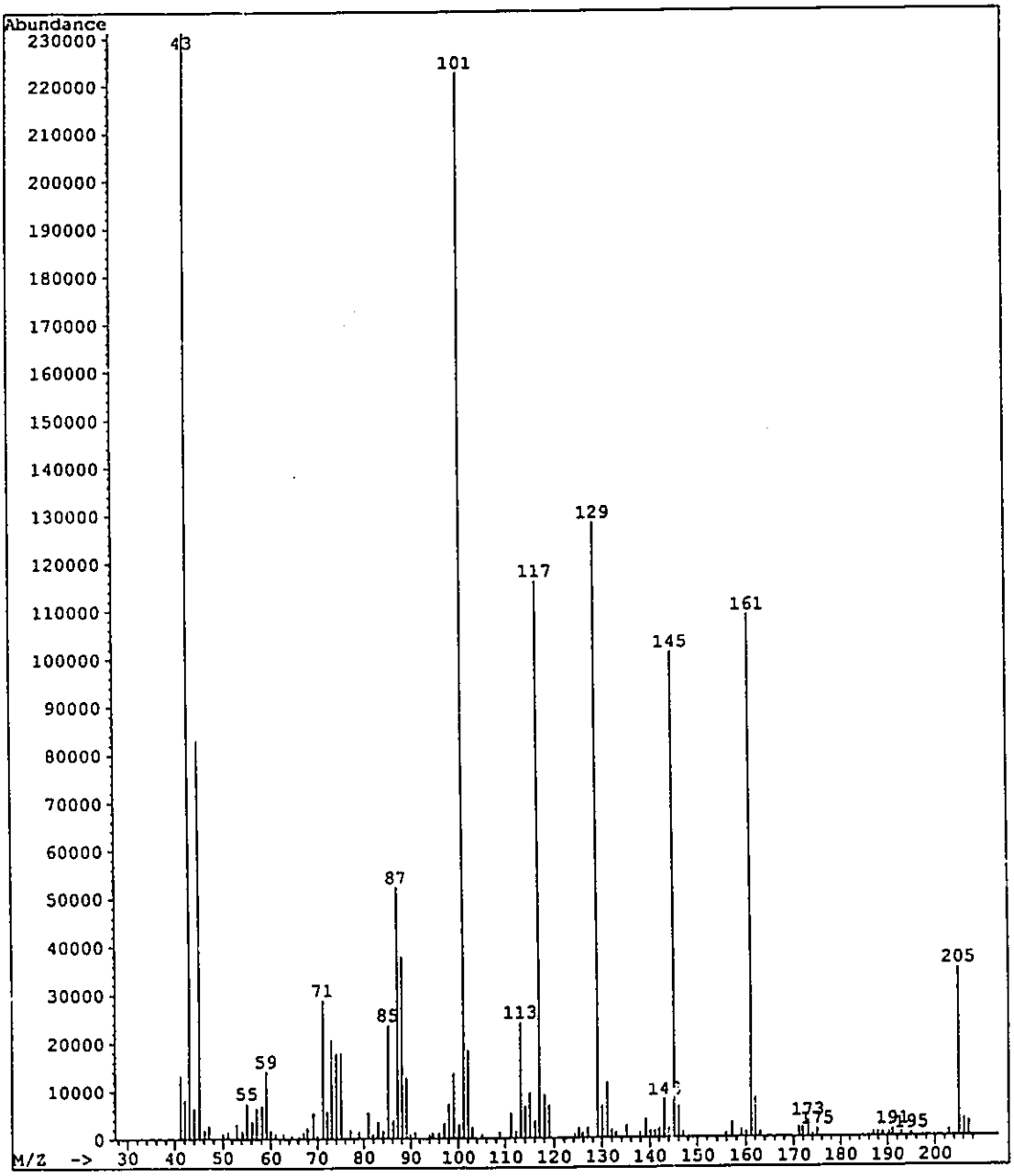
Abundance
230000
220000
210000
200000
190000
180000
170000
160000
150000
140000
130000
120000
110000
100000
90000
80000
70000
60000
50000
40000
30000
20000
10000
0
M/Z ->
30 40 50 60 70 80 90 100 110 120 130 140 150 160 170 180 190 200
43
101
129
117
161
145
87
205
71
85
113
59
55
173
175
191
195

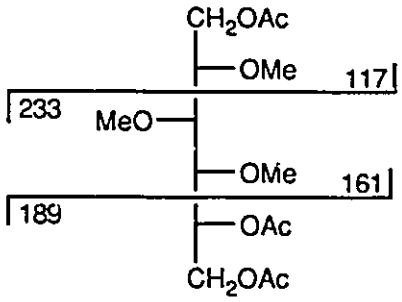
CH2OAc
OMe
117
233
MeO
OMe
161
189
OAc
CH2OAc

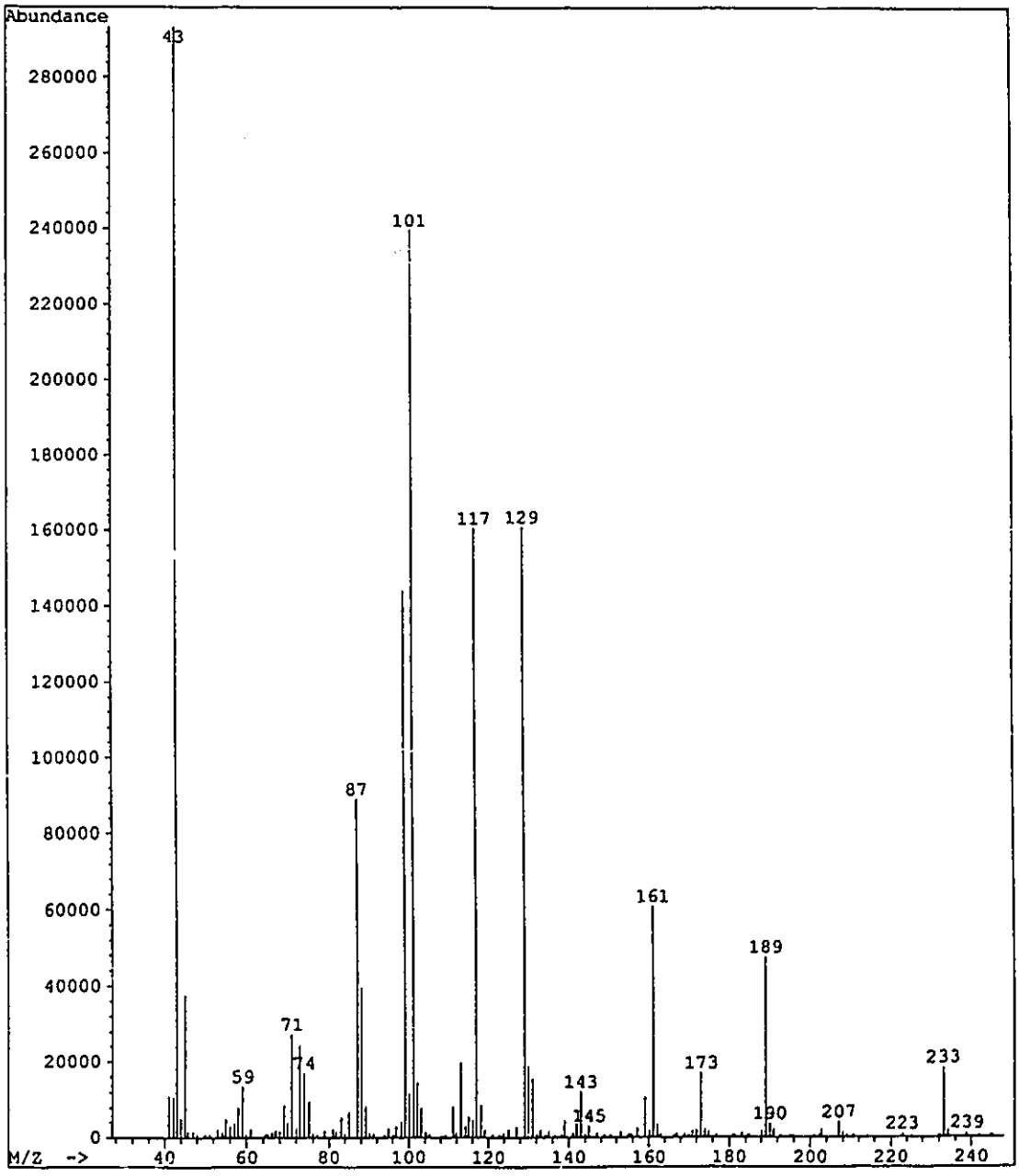
Abundance
280000
260000
240000
220000
200000
180000
160000
140000
120000
100000
80000
60000
40000
20000
0
M/Z ->
40
60
80
100
120
140
160
180
200
220
240
43
101
117
129
87
161
189
71
74
59
143
145
173
233
130
207
223
239

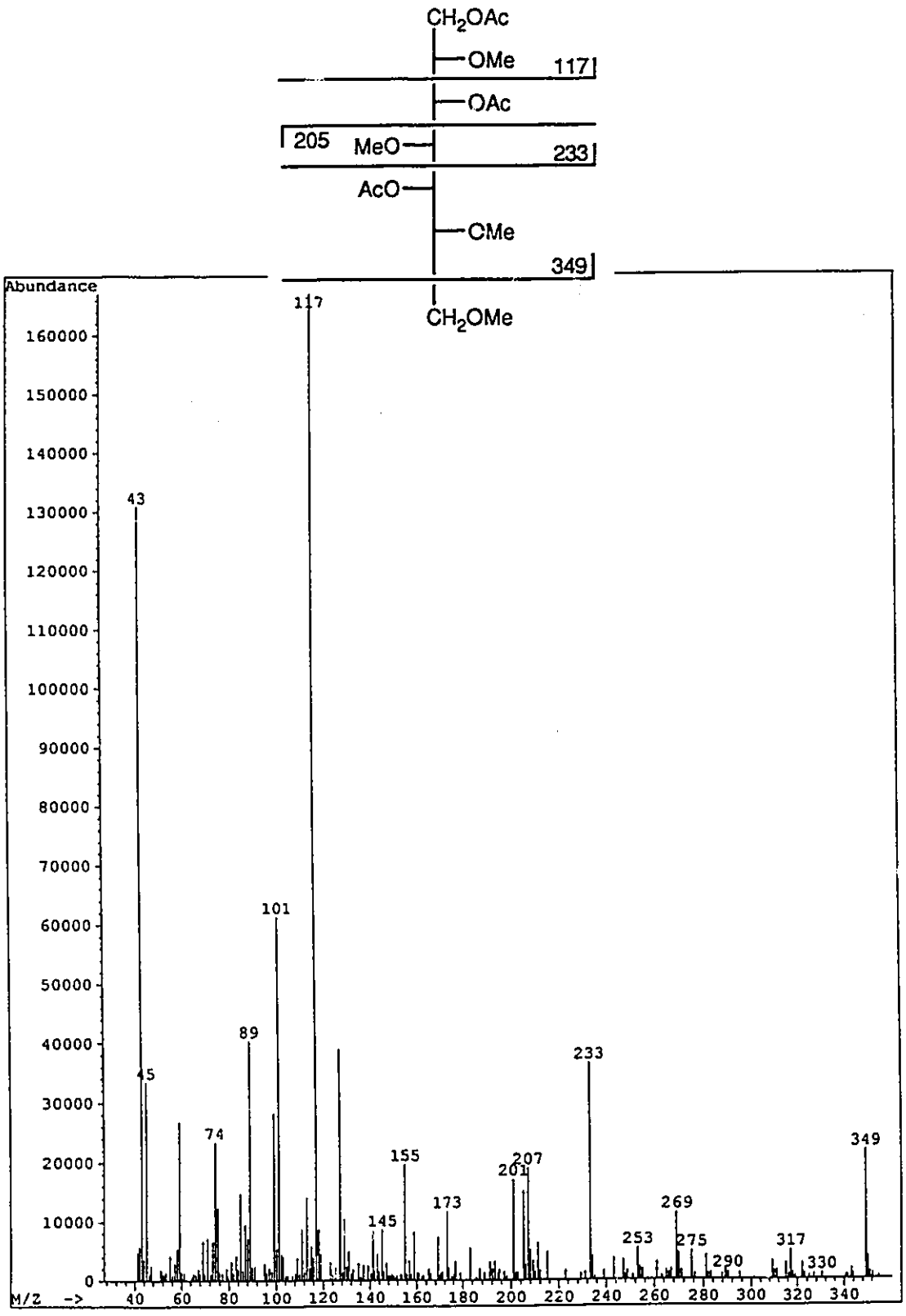
CH2OAc
OMe
117
OAc
205
MeO
233
AcO
CMe
349
CH2OMe
Abundance
160000
150000
140000
130000
120000
110000
100000
90000
80000
70000
60000
50000
40000
30000
20000
10000
0
M/Z ->
40
60
80
100
120
140
160
180
200
220
240
260
280
300
320
340
117
43
101
89
45
74
233
155
207
201
173
145
269
253
275
290
317
330
349

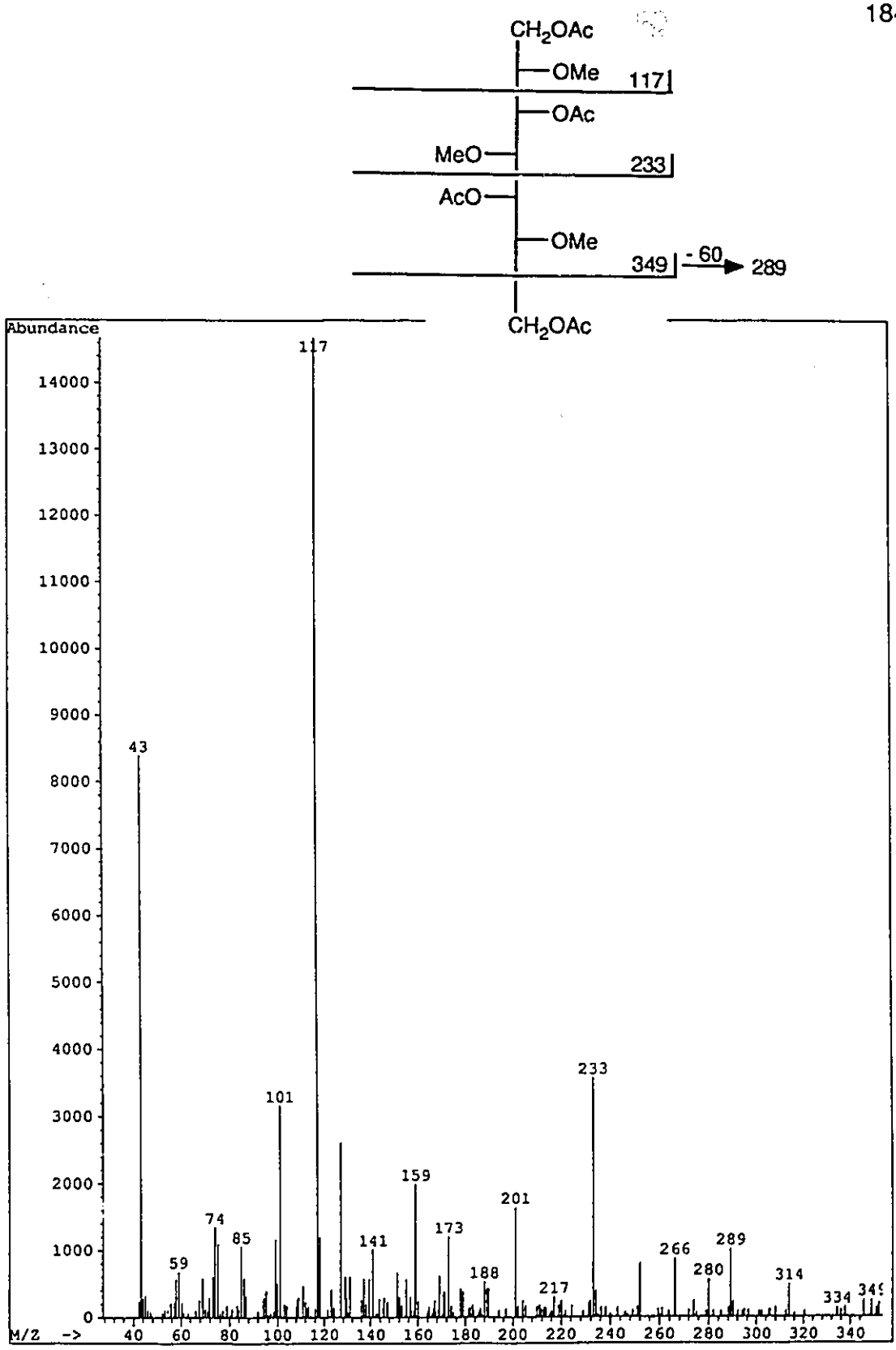
CH2OAc
OMe
117
OAc
MeO
233
AcO
OMe
349
- 60
289
CH2OAc
Abundance
14000
13000
12000
11000
10000
9000
8000
7000
6000
5000
4000
3000
2000
1000
0
M/Z ->
40
60
80
100
120
140
160
180
200
220
240
260
280
300
320
340
117
43
101
233
159
201
74
85
173
141
59
188
217
266
289
280
314
334

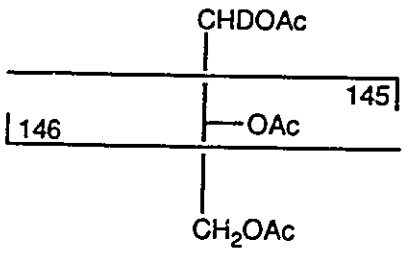
CHDOAc
145
146
OAc
CH2OAc

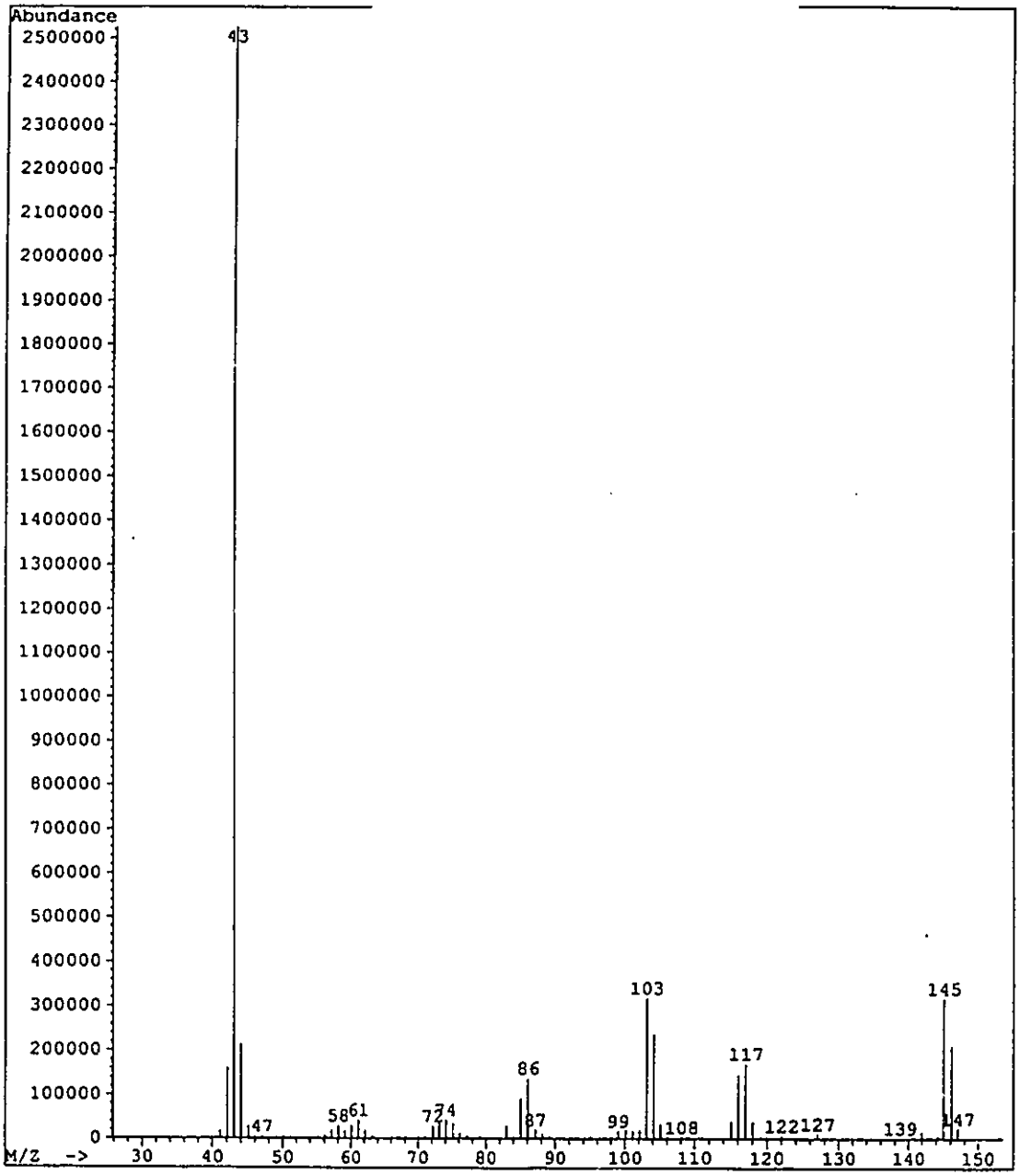
Abundance
2500000
2400000
2300000
2200000
2100000
2000000
1900000
1800000
1700000
1600000
1500000
1400000
1300000
1200000
1100000
1000000
900000
800000
700000
600000
500000
400000
300000
200000
100000
0
M/Z ->
30
40
50
60
70
80
90
100
110
120
130
140
150
43
47
58
61
73
74
86
87
99
103
108
117
122
127
139
145
147

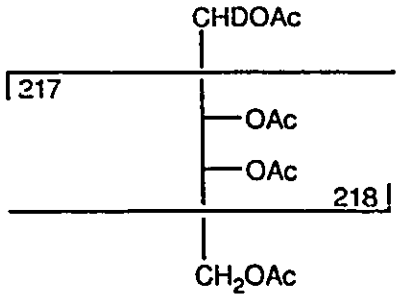
CHDOAc
217
OAc
OAc
218
CH2OAc

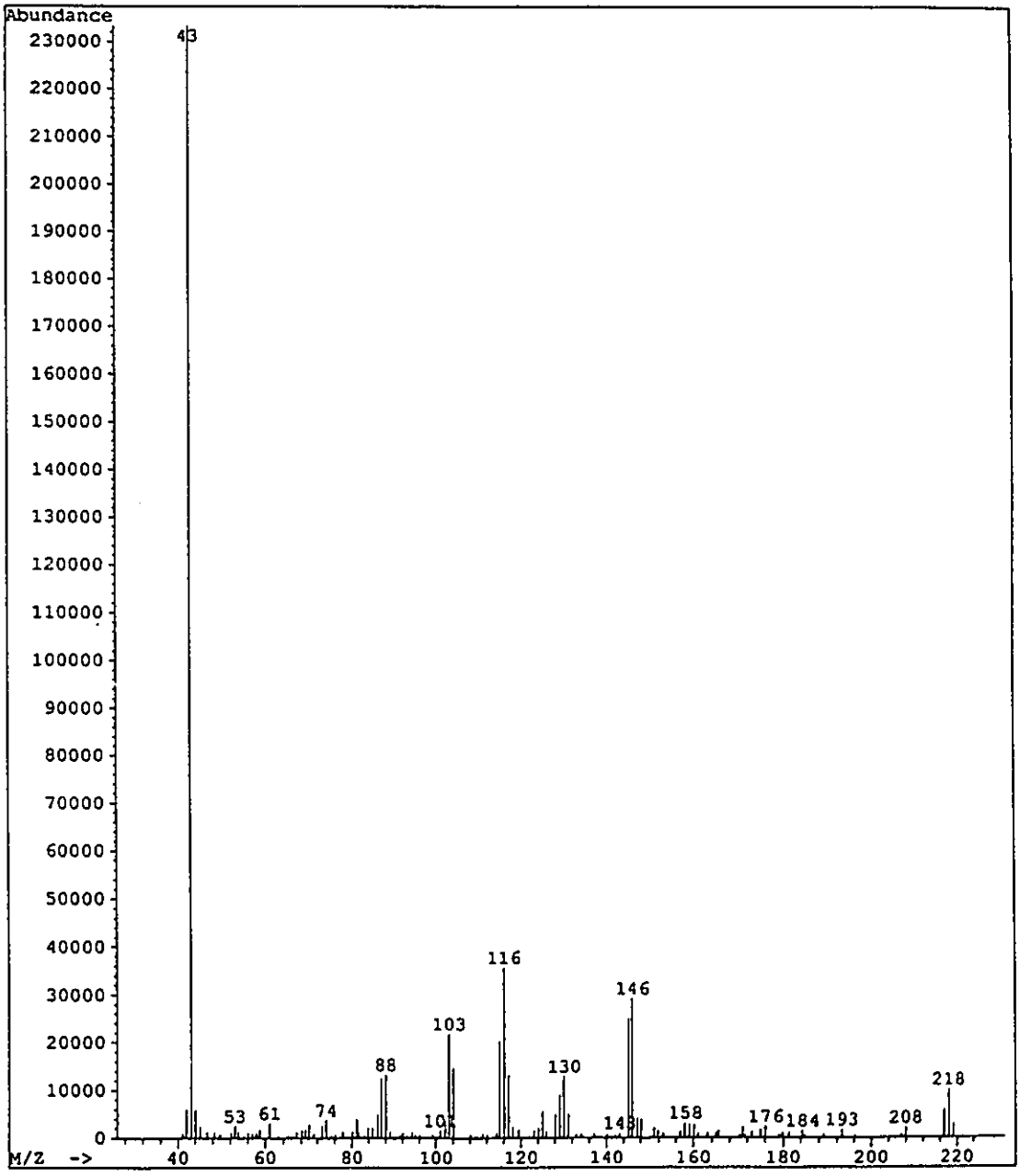
Abundance
230000
220000
210000
200000
190000
180000
170000
160000
150000
140000
130000
120000
110000
100000
90000
80000
70000
60000
50000
40000
30000
20000
10000
0
M/Z ->
40
60
80
100
120
140
160
180
200
220
43
53
61
74
88
103
116
130
146
158
176
184
193
208
218

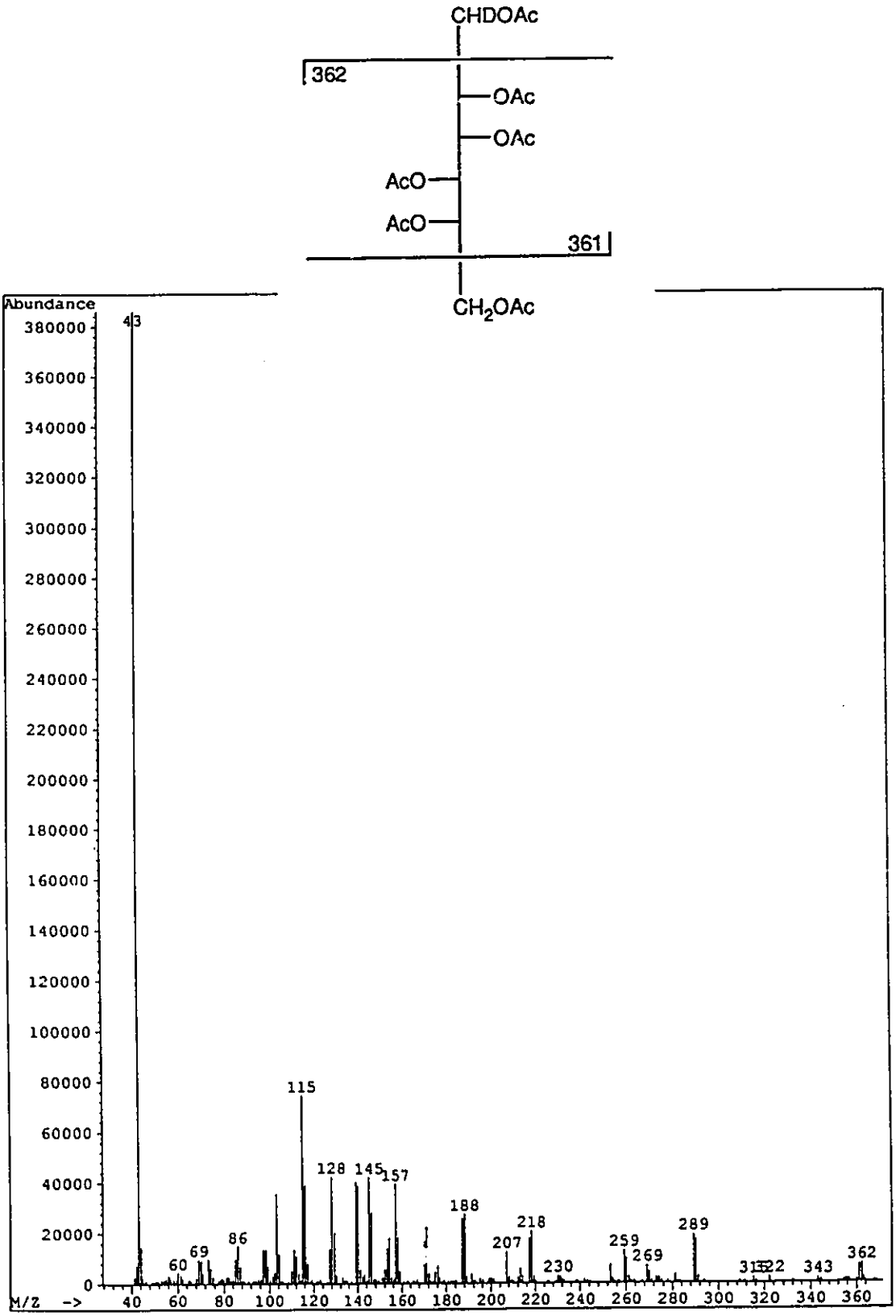
CHDOAc
362
OAc
OAc
AcO
AcO
361
CH2OAc
Abundance
380000
360000
340000
320000
300000
280000
260000
240000
220000
200000
180000
160000
140000
120000
100000
80000
60000
40000
20000
0
M/Z ->
40 60 80 100 120 140 160 180 200 220 240 260 280 300 320 340 360
43
115
128
145
157
188
218
207
230
259
269
289
343
362
60
69
86

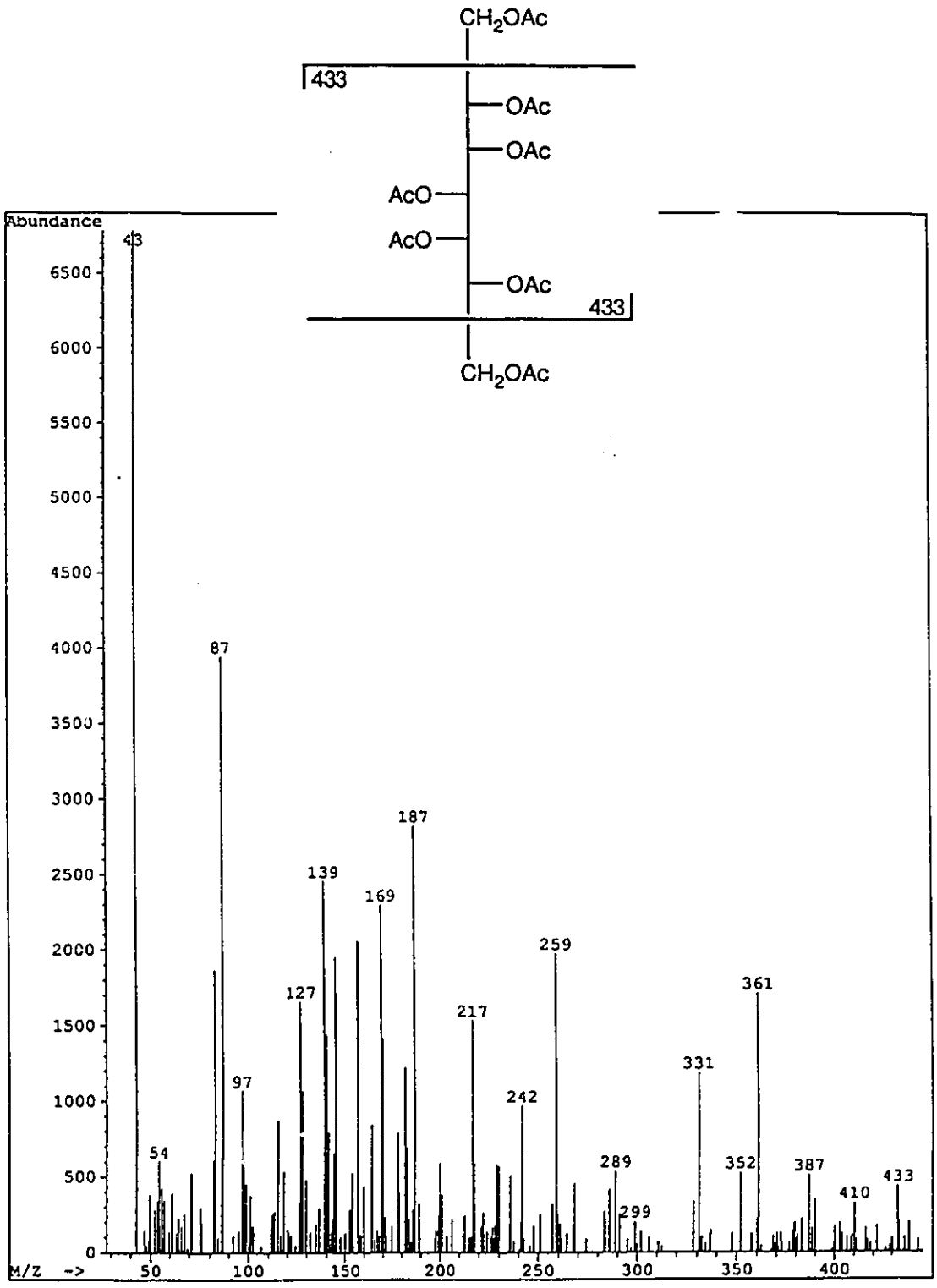
CH2OAc
433
OAc
OAc
AcO
AcO
OAc
433
CH2OAc
Abundance
M/Z ->
43
87
54
97
127
139
169
187
217
242
259
289
299
331
352
361
387
410
433

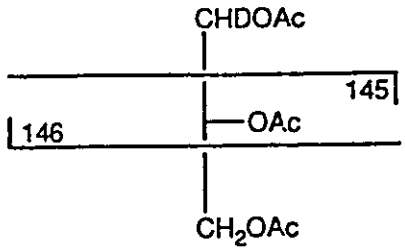
CHDOAc
145
146
OAc
CH2OAc

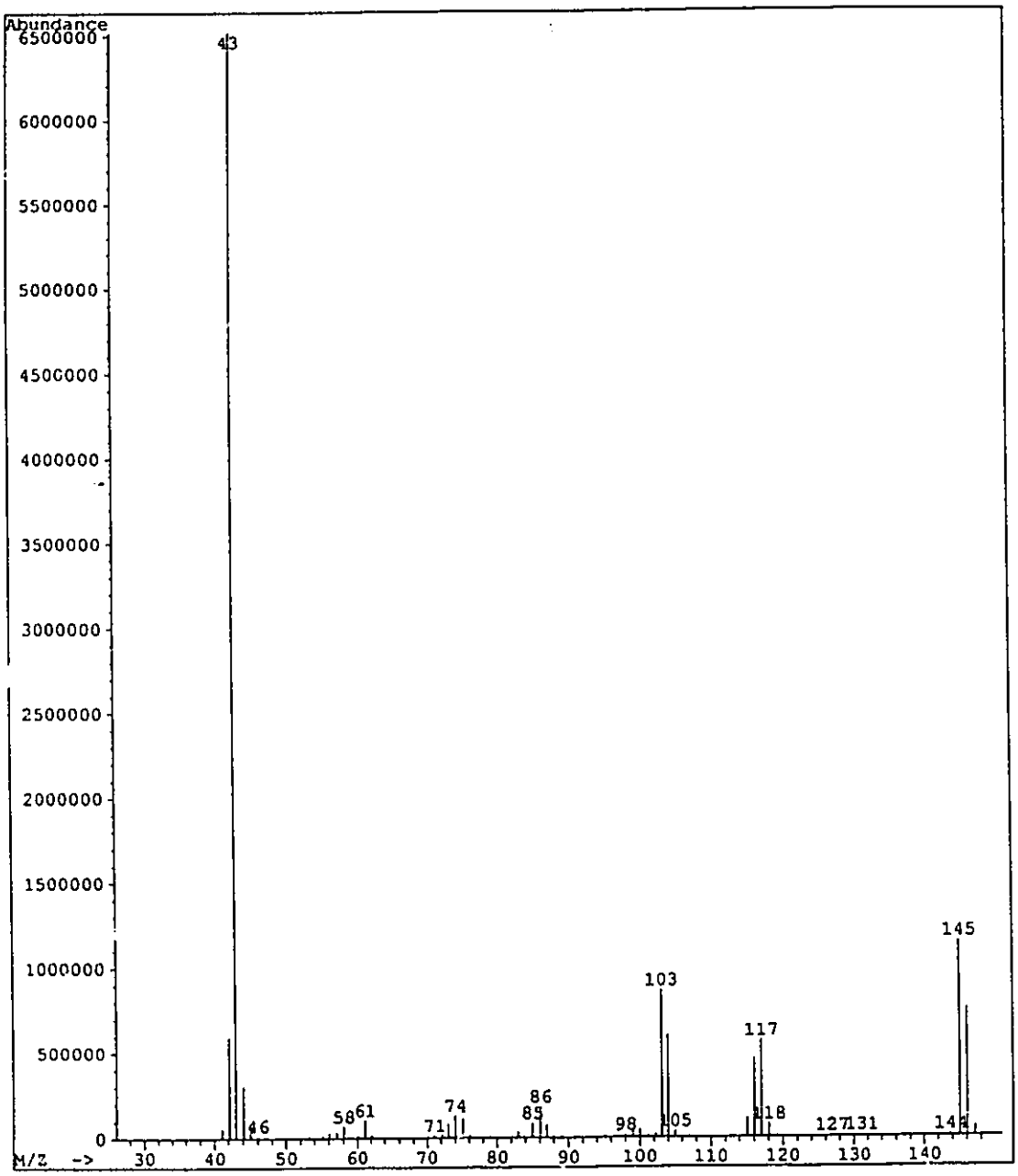
Abundance
6500000
6000000
5500000
5000000
4500000
4000000
3500000
3000000
2500000
2000000
1500000
1000000
500000
0
M/Z ->
30
40
50
60
70
80
90
100
110
120
130
140
43
46
58
61
71
74
85
86
98
103
105
117
118
127
131
145

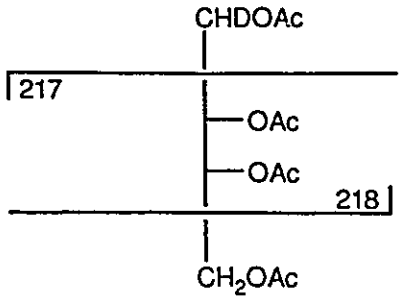
CHDOAc
217
OAc
OAc
218
CH2OAc

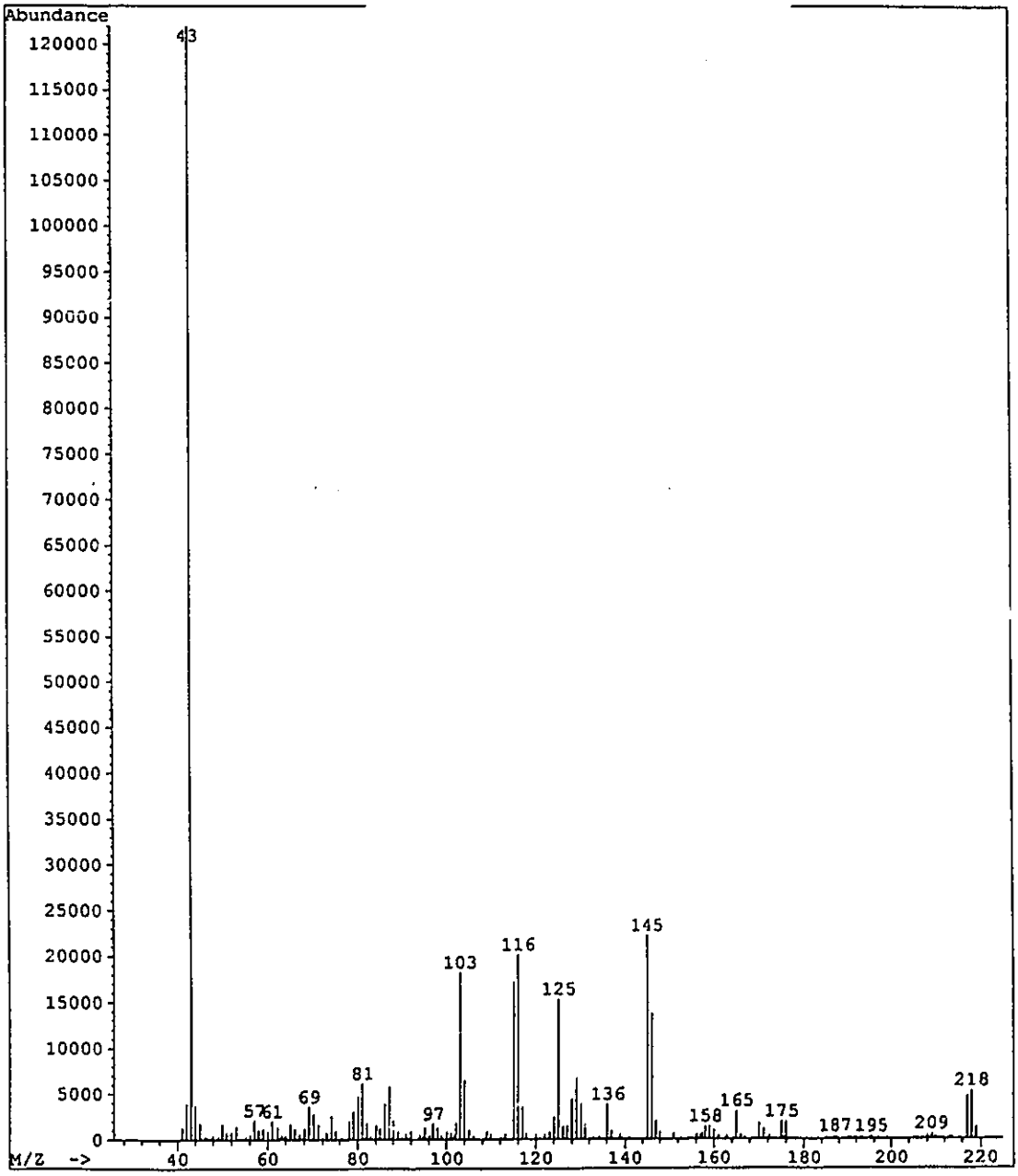
Abundance
120000
115000
110000
105000
100000
95000
90000
85000
80000
75000
70000
65000
60000
55000
50000
45000
40000
35000
30000
25000
20000
15000
10000
5000
0
M/Z ->
40
60
80
100
120
140
160
180
200
220
43
57
61
69
81
97
103
116
125
136
145
158
165
175
187
195
209
218

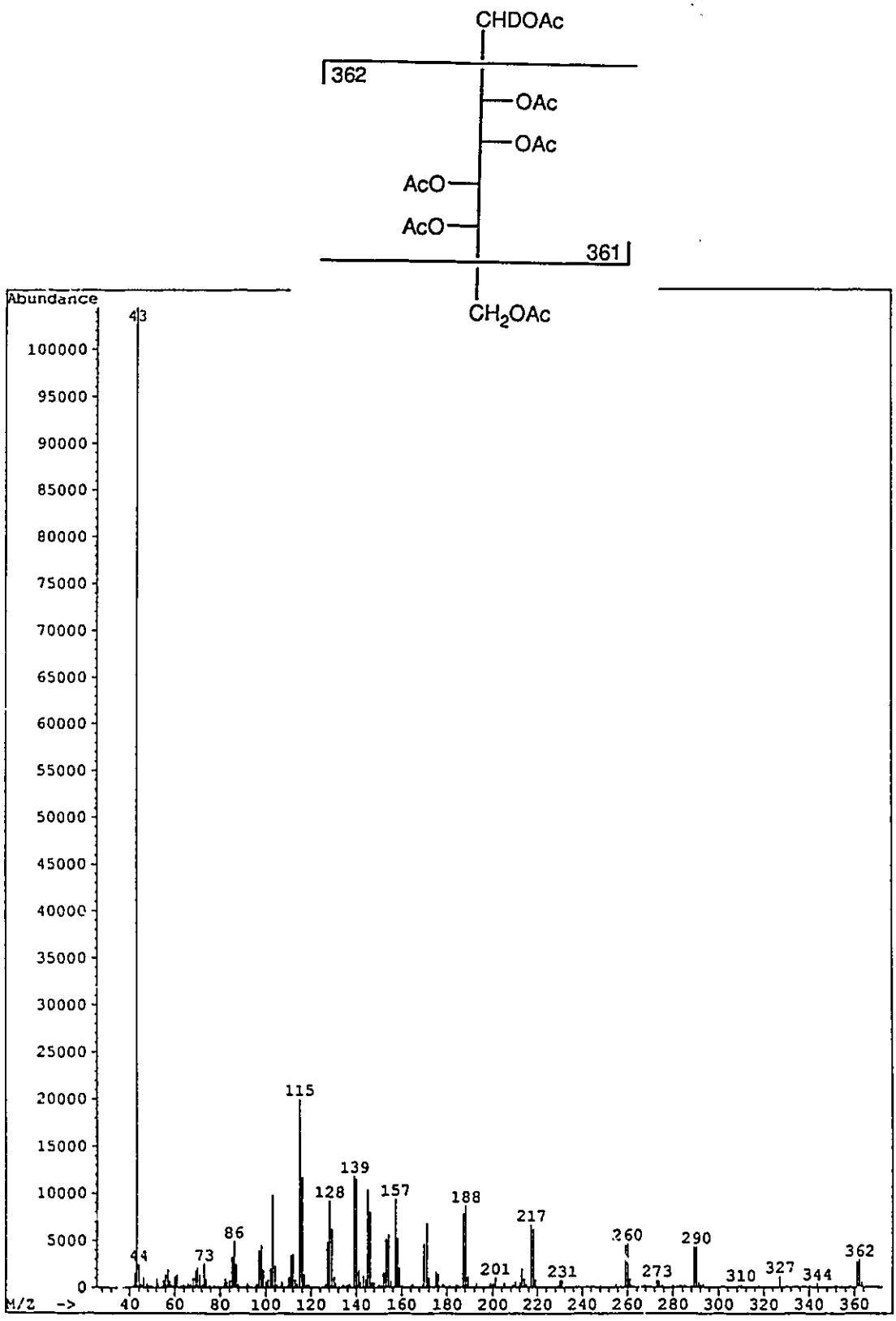
CHDOAc
362
OAc
OAc
AcO
AcO
361
CH2OAc
Abundance
M/Z ->
43
115
139
128
157
188
217
86
260
290
362
44
73
201
231
273
310
327
344

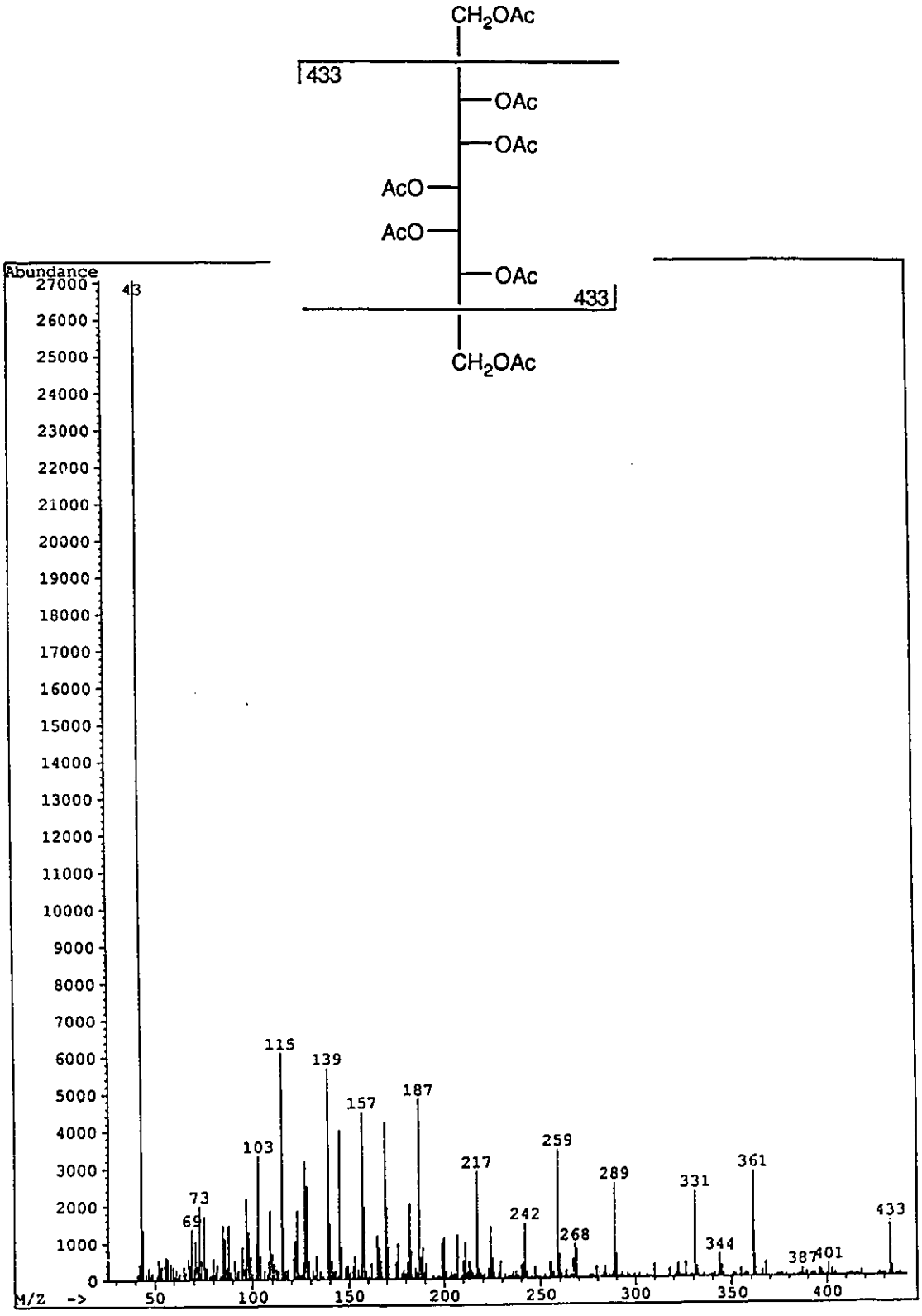
CH2OAc
433
OAc
OAc
AcO
AcO
OAc
433
CH2OAc
Abundance
M/Z ->
43
115
139
157
187
103
217
259
289
331
361
73
69
242
268
344
387
401
433

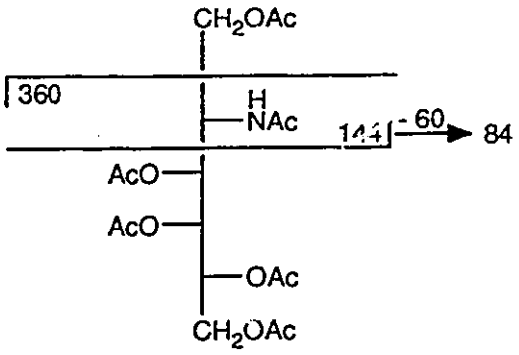
CH2OAc
360
H
NAc
144
- 60
84
AcO
AcO
OAc
CH2OAc

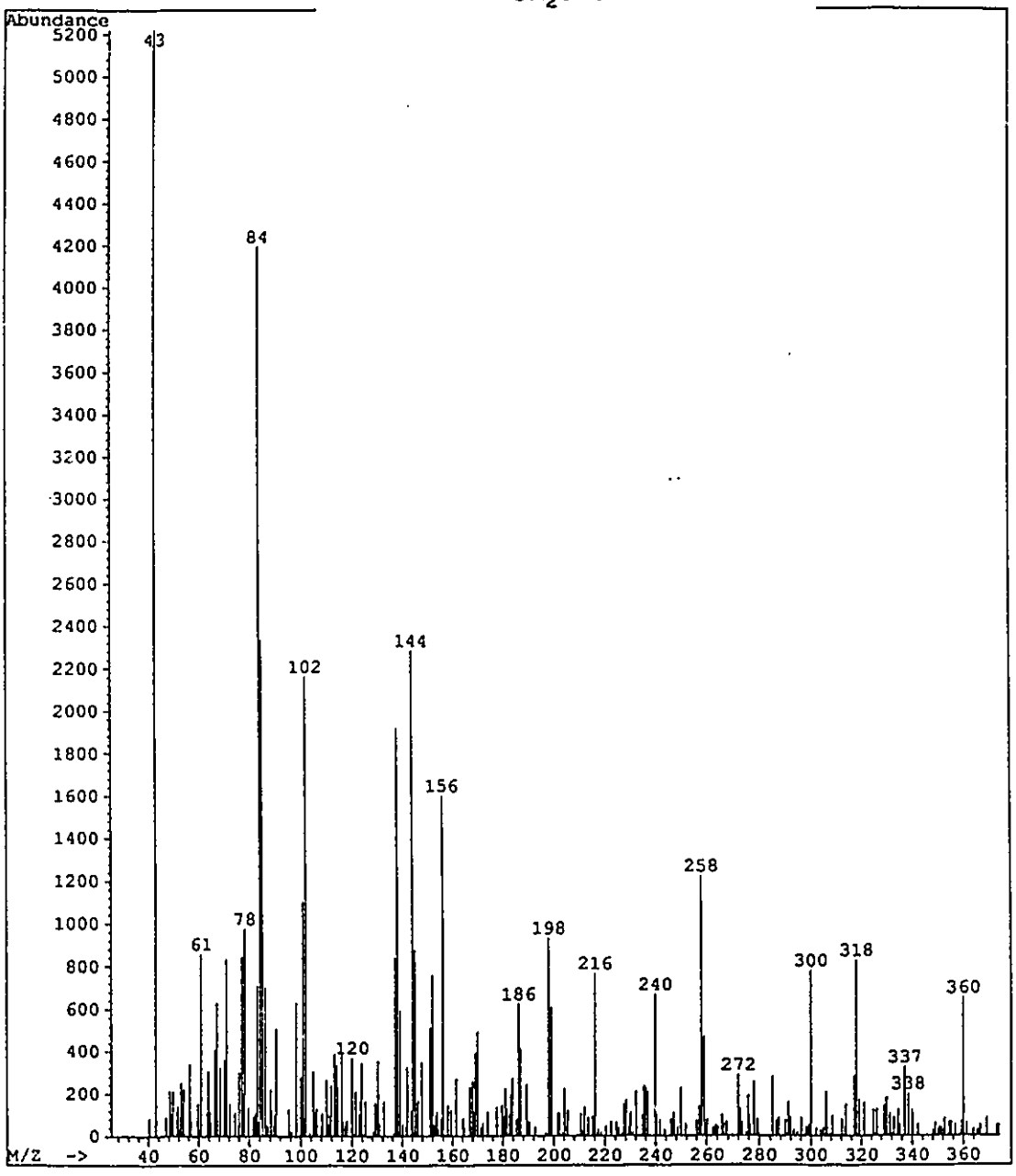
Abundance
5200
5000
4800
4600
4400
4200
4000
3800
3600
3400
3200
3000
2800
2600
2400
2200
2000
1800
1600
1400
1200
1000
800
600
400
200
0
M/Z ->
40
60
80
100
120
140
160
180
200
220
240
260
280
300
320
340
360
43
84
102
144
156
61
78
198
216
240
258
300
318
360
186
120
272
337
338